THE MECHANISM OF CASPASE-8-MEDIATED GENE EXPRESSION AND ITS INTEGRAL ROLE IN HOST DEFENSE

Alexandra Anne DeLaney

A DISSERTATION

in

Cell and Molecular Biology

Presented to the Faculties of the University of Pennsylvania

in

Partial Fulfillment of the Requirements for the

Degree of Doctor of Philosophy

2019

Supervisor of Dissertation

_____

Igor E. Brodsky, Ph.D.

Associate Professor, Pathobiology, University of Pennsylvania School of Veterinary Medicine

Graduate Group Chairperson

_____

Daniel S. Kessler, Ph.D.

Associate Professor of Cell and Developmental Biology

Dissertation Committee

Mitchell A. Lazar, M.D., Ph.D., Willard And Rhoda Ware Professor In Diabetes And Metabolic Diseases, University of Pennsylvania Perelman School of Medicine.

Rahul M. Kohli, MD., Ph.D., Assistant Professor of Medicine, University of Pennsylvania Perelman School of Medicine.

Jorge Henao-Mejia, M.D., Ph.D., Assistant Professor of Pathology and Laboratory Medicine, University of Pennsylvania Perelman School of Medicine.

Michael J. May, Ph.D., Associate Professor, Department of Biomedical Sciences, University of Pennsylvania School of Veterinary Medicine.

Sunny Shin, Ph.D., Associate Professor of Microbiology, University of Pennsylvania Perelman School of Medicine.

THE MECHANISM OF CASPASE-8-MEDIATED GENE EXPRESSION AND ITS INTEGRAL ROLE IN HOST DEFENSE

ACKNOWLEDGEMENTS

The process of getting a Ph.D. is truly a collaborative effort. There are countless people in the Perelman School of Medicine, School of Veterinary Medicine, Institute for Immunology, Center for Public Health Initiatives, Microbiology Department, and Biomedical Sciences Department who have provided critical reagents and feedback to make this project possible.

I would like to begin by thanking my thesis committee: Drs. Mitchell Lazar, Jorge Henao-Mejia, Sunny Shin, Rahul Kohli, and Michael May. They have provided hours of their time to the advancement of this project, and I would not have been able to complete my research without their thoughtful feedback and support.

Thank you to my thesis advisor Dr. Igor E. Brodsky for your support and advice these last four years. I aspire to the level of scientific knowledge that you possess, and I am so grateful to you for taking the time to nurture my own scientific development. You have created an intellectually rigorous and rewarding laboratory environment, and I know I am a better person and scientist because of it.

My lab mates have contributed countless hours of their time to this project. They have listened to the same talk over and over to prepare me for every presentation I have ever given, and spent hours helping with experiments. Drs. Meghan Wynosky-Dolfi and Elisabet Bjanes have been a constant source of support and their feedback has been essential to the success of this project. Thank you to Drs. Daniel Grubaugh, Daniel

Sorobetea and soon to be Dr. Dr. Daniel Akuma for being the best Daniels around. Thank you to former lab members Drs. Naomi H. Philip and Lance W. Peterson; their foundational studies led to the development of this project. Thank you to all of the former and current Brodsky Lab members for creating such a wonderful environment to do science. I would also like to thank the entire Shin Lab, particularly Dr. Jess Doerner, for their feedback and advice during our joint lab meetings.

The Hunter Lab has been very gracious in inducting me into the world of parasitology. The pathogens we study in the Brodsky Lab do not have a nucleus so *T. gondii* was a whole new world. I would specifically like to highlight all of the work that Dr. David Christian put into the intellectual development of this project. He provided reagents, mice, and hours of his time to make this work possible—I am incredibly grateful to him. Thank you to Dr. Anthony Phan, Lindsey Shallberg, and Joe Clark for all of your help fixing the Fortessa, providing parasites, and teaching me how to use the Hill Pavilion confocal.

Thank you to my wonderful IGG friends: Drs. Chris Ecker, Caroline Bartman, as well as Sarah Sneed, Scarlett Yang, and Megan Clark for making me feel like an immunologist.

Thank you to my cohort as well as the CAMB and MVP offices for their awesome support. I feel incredibly privileged to be a part of such an intellectually diverse community that produces wonderful science.

Thank you to Dr. Walter K. Mowel for making sure my dog was well fed and loved while I was traveling. More importantly, thank you for all of the advice and time you have given to this project. I am excited to see you excel during your postdoctoral fellowship and to see what you accomplish during your very promising career in science.

Thank you to my family: my father, Steve DeLaney: stepmother, Lori DeLaney; and my in-laws, Susan and Steve Reischl who made me feel like part of the family the first day we ever met. I know sometimes it is hard to understand what I am doing or why I am doing it, but I want you to know that your unconditional love has made all of my accomplishments possible. I look to you all every day as a source of inspiration and strength, so thank you for all that you do.

Last but certainly not least I would like to thank my wonderful life-partner/husband Patrick K. Reischl, J.D. This project is as much his achievement as it is mine. He has been nothing, but supportive of my career. In fact, he got a 179 on the LSAT so he could come to Penn Law and spend the last three years of my Ph.D. with me (and also so he could get a law degree). He has given me his love, time, and support during a very challenging journey and has made my transition to law school possible. He has spent his time helping me study for the LSAT—I did not get a 179—and apply to law schools. I like to believe that he is a big reason that I will be matriculating at Penn Law in the fall of this year. He is truly a magical human being, and I am so excited to see him excel in his judicial clerkships and wherever his career takes him after that.

ATTRIBUTIONS

Some work in this thesis appears in the following publication:

DeLaney AA et al. Caspase-8 promotes c-Rel dependent inflammatory cytokine expression and resistance against *Toxoplasma gondii*. *PNAS.* June 11, 2019 116 (24) 11926-11935.

Experimental help was provided for some experiments:

Experiments in **Chapter 4** were performed in collaboration with Dr. Walter K. Mowel.

Drs. Elisabet Bjanes and Meghan Wynosky-Dolfi helped with PEC, mLN, and blood isolations as well as bacterial plating. Data from mouse harvests they helped with are in: **Fig 5.1**, **Fig 5.2**, **Fig 5.3**, **Fig 5.5**, **Fig 5.6**, **Fig 6.2**, **Fig 6.3**, **Fig 6.5**, **Fig 6.6**, **Fig 6.7**, and **Fig 6.8**.

Drs. Jess Doerner and Daniel Sorobetea performed the injections for the bone marrow chimeras that appear in **Fig. 5.6**.

Dr. Corbett Berry performed all RNAseq analysis (**Fig 2.1** and **Fig 2.2**).

Megan Clark sorted the immortalized macrophages that appear in **Fig 3.5B** and **Fig 3.5C**.

Andrew Hart participated in the early *T. gondii* experiments monitoring mice for survival (**Fig 5.1A**).

The caspase-8 non-cleavable mouse described throughout this thesis was generated in collaboration with the Henao-Mejia Lab.

Ripk3$^{-/-}$*Casp8*$^{-/-}$ and *Mlkl*$^{-/-}$*Fadd*$^{-/-}$ mice were provided by Dr. Doug Green (St. Jude Children's Research Hospital).

Ripk3$^{-/-}$ mice were provided by Dr. Vishva Dixit (Genentech).

Il12b$^{-/-}$ mice were provided by Dr. David Christian in the Hunter Lab.

Rel$^{-/-}$ mice were generated and provided by Dr. Hsiou-chi Liou (Perelman School of Medicine).

ABSTRACT

THE MECHANISM OF CASPASE-8-MEDIATED GENE EXPRESSION AND ITS INTEGRAL ROLE IN HOST DEFENSE

Alexandra Anne DeLaney

Igor E. Brodsky, Ph.D.

Caspase-8 is a key integrator of cell survival and cell death decisions during infection and inflammation. Additionally, caspase-8 has an important, but less understood, role in cell-intrinsic inflammatory gene expression. Macrophages lacking caspase-8 have defective inflammatory cytokine expression in response to bacterial infection or TLR stimulation. How caspase-8 regulates cytokine gene expression, and whether caspase-8-mediated gene regulation has a physiological role during infection remains poorly defined. In this thesis we demonstrate that both caspase-8 enzymatic activity and scaffolding functions play a role in control of inflammatory cytokine gene expression. Caspase-8 enzymatic activity mediates IKK phosphorylation and nuclear translocation of the NF-κB family member c-Rel to promote maximal expression of *Il1b* and *Il12b.* Overexpression of c-Rel was sufficient to restore expression of IL-12 and IL-1β in caspase-8-deficient cells. Moreover, the cytokine regulatory function of caspase-8 promoted host survival during infection by the intracellular parasite *Toxoplasma gondii.* Caspase-8-deficient mice displayed acute mortality during *T. gondii* infection and a defect in intracellular IL-12 production by DCs. Exogenous IL-12 promoted complete survival of caspase-8-deficient mice during acute toxoplasmosis. Our findings provide new insight into how caspase-8 controls inflammatory gene expression and, for the first time, identify a critical role for caspase-8 in host defense against a eukaryotic pathogen.

TABLE OF CONTENTS

ACKNOWLEDGEMENTS ..... **iii**

ATTRIBUTIONS ..... **vi**

ABSTRACT ..... **vii**

CHAPTER 1: INTRODUCTION **1**

1.1 INNATE IMMUNE SENSING 1
1.1.1 Overview of Toll-like-receptor activation and gene transcription. 3
1.1.2 Overview of NF-κB-dependent gene regulation in macrophages. 4
1.1.3 Overview of caspase-8 biology. 6
1.1.4 Caspase-8 mediates cytokine secretion. 8
1.2 ROLE OF APOPTOSIS AND CYTOKINE SECRETION IN HOST DEFENSE 10
1.2.1. Caspase-8 deficiency leads to embryonic lethality. 11
1.2.2 Role of caspase-8 in host survival during acute *Toxoplasma gondii* infection. 12
1.2.3 Caspase-8 mediates host survival in response to *Yersinia pseudotuberculosis*. 13
1.2.4 Caspase-8 deficiency in humans leads to acute susceptibility to microbial infection. 14
1.3 SUMMARY 16
1.4 FIGURES 18
Fig 1.1 Schematic of signal transduction induced in response to TLR stimulation 18
Fig 1.2 Schematic of NF-κB and IκB protein structure 19
Fig 1.3 Schematic of proteins involved in death receptor signaling and the signal transduction cascade that mediates apoptosis and programmed necrosis 20
Fig 1.4. Model of IL-12-mediated clearance of *Toxoplasma gondii* infection. 21
Fig 1.5 Schematic of *Yersinia pseudotuberculosis*-induced apoptosis in macrophages. 22

CHAPTER 2: CASPASE-8 REGULATES TLR-INDUCED MACROPHAGE GENE EXPRESSION THROUGH THE NF-KB FAMILY MEMBER C-REL **23**

2.1 ABSTRACT 23
2.2 INTRODUCTION 24
2.3 RESULTS 29
2.3.1 Caspase-8 regulates hundreds of inflammatory genes in response to TLR stimulation that are enriched for NF-κB binding motifs. 29
2.3.2 Caspase-8 promotes IKK phosphorylation in response to TLR stimulation. 30
2.3.3 Caspase-8 promotes IκBε degradation in response to TLR4 stimulation. 31
2.3.4 Caspase-8 promotes c-Rel nuclear translocation in response to TLR4 and TLR9 stimulation. 32
2.3.5 Caspase-8 promotes c-Rel recruitment to the promoters of caspase-8-dependent genes. 33

2.3.6 c-Rel regulates several caspase-8-dependent genes in response to TLR stimulation. 33
2.3.7 c-Rel expression restores IL-12p40 and pro-IL-1β expression in caspase-8-deficient macrophages. 34
2.3.8 Caspase-8 is coupled to TLR activation through the adaptor protein FADD. 36
2.4 DISCUSSION 37
2.5 FIGURES 40
Fig 2.1. Caspase-8 regulates hundreds of genes in response to TLR stimulation. 40
Fig 2.2 Caspase-8 regulates inflammatory genes that are enriched for NF-κB binding motifs. 42
Fig 2.3 IKK phosphorylation is caspase-8-dependent in response to TLR stimulation. 43
Fig 2.4 TLR4-induced IκBε degradation is impaired in the absence of caspase-8. 45
Fig 2.5 Caspase-8 promotes c-Rel translocation independently of p65. 46
Fig 2.6 Caspase-8 promotes c-Rel recruitment to the promoters of caspase-8-dependent genes. 48
Fig 2.7 c-Rel regulates both IL-12p40 and pro-IL-1β expression in response to TLR activation. 49
Fig 2.8 hc-Rel-IRES-GFP is expressed robustly in primary macrophages. 51
Fig 2.9 hc-Rel expression restores both IL-12p40 and pro-IL-1β production in the absence of caspase-8. 52
Fig 2.10 In the absence of caspase-8 hc-Rel expression restores both IL-12p40 and pro-IL-1β to levels observed in *Ripk3*$^{-/-}$ cells. 54
Fig 2.11 FADD promotes inflammatory gene expression and IKK phosphorylation in response to TLR activation. 55
Fig 2.12 Graphical abstract and future directions: Caspase-8 promotes *Il12b* and *Il1b* expression through c-Rel. 57

CHAPTER 3: CASPASE-8 ENZYMATIC ACTIVITY PROMOTES INFLAMMATORY GENE EXPRESSION IN MACROPHAGES. 58

3.1 ABSTRACT 58
3.2 INTRODUCTION 59
3.3. RESULTS 61
3.3.1 TLR stimulation promotes caspase-8 catalytic activity. 61
3.3.2 Caspase-8 enzymatic activity promotes inflammatory gene expression and IKK phosphorylation. 61
3.3.3 Caspase-8 enzymatic activity promotes *Il12b* transcription and IL-12p40 secretion. 63
3.3.4 Caspase-8 enzymatic activity promotes c-Rel nuclear translocation. 64
3.3.5 Caspase-8 enzymatic activity promotes cytokine secretion. 64
3.3.6 Caspase-8 non-apoptotic activity mediates inflammatory cytokine expression and IKK phosphorylation. 65
3.4 DISCUSSION 67
3.5 FIGURES 70
Fig 3.1 TLR stimulation promotes caspase-8 catalytic activity. 70

Fig 3.2 Caspase-8 enzymatic activity regulates activation of the IKK complex.. 71
Fig 3.3 Caspase-8 enzymatic activity mediates *Il12b* expression in response to TLR activation. 72
Fig 3.4 Caspase-8 enzymatic activity contributes to c-Rel nuclear translocation in response to TLR signaling. 73
Fig 3.5 Caspase-8 enzymatic activity and scaffolding promote inflammatory cytokine secretion. 75
Fig 3.6 Non-cleavable caspase-8 promotes inflammatory gene expression and IKK phosphorylation in response to TLR stimulation. 76
Fig 3.7 Graphical abstract and future directions: Caspase-8 enzymatic activity and scaffolding mediate inflammatory gene expression. 78

CHAPTER 4: SELECTIVE ABLATION OF CASPASE-8 APOPTOTIC ACTIVITY PROTECTS THYMOCYTES FROM FAS-MEDIATED CELL DEATH AND LEADS TO THE ACCUMULATION OF MYELOID CELLS. 79

4.1 ABSTRACT 79
4.2 INTRODUCTION 81
4.3 RESULTS 84
4.3.1 *Ripk3*$^{-/-}$*Casp8*$^{DA/DA}$ mice display a lymphoproliferative disease that is divergent from that of *Ripk3*$^{-/-}$*Casp8*$^{-/-}$ mice. 84
4.3.2 Ablation of capsase-8 apoptotic activity mediates splenomegaly that is characterized by both myeloid and lymphocyte infiltration. 85
4.3.3 Ablation of the apoptotic activity of caspase-8 correlates with innate immune population expansion in secondary lymphoid organs. 85
4.3.4 Caspase-8 apoptosis is dispensable for T cell development in the thymus. 87
4.4 DISCUSSION 88
4.5 FIGURES 92
Fig 4.1 RIPK3-null *Casp8*$^{DA/DA}$ mice are expected to be deficient in cell death pathways. 92
Fig 4.2 Ablation of capsase-8 apoptotic activity mediates splenomegaly. 93
Fig 4.3 Non-cleavable capsase-8 protects mice from CD3^{+}B220^{+} cell accumulation. 94
Fig 4.4 RIPK3-null *Casp8*$^{DA/DA}$ mice have disrupted splenic architecture and increased immune cell infiltrate. 95
Fig 4.5 RIPK3-null *Casp8*$^{DA/DA}$ mice have expanded populations of myeloid cells in secondary lymphoid organs. 96
Fig 4.6 Representative gating strategy for the characterization of both innate and adaptive immune populations in RIPK3-null *Casp8*$^{DA/DA}$ mice. 98
Fig 4.7 RIPK3-null *Casp8*$^{DA/DA}$ mice have normal T cell development and are partially protected from Fas-dependent apoptosis. 100

CHAPTER 5: CASPASE-8 PROMOTES HOST SURVIVAL DURING ACUTE *TOXOPLASMA GONDII* INFECTION. 101

5.1 ABSTRACT 101
5.2 INTRODUCTION 102
5.3.1 Caspase-8-deficient animals are acutely susceptible to *T. gondii* infection. . 104
5.3.2 IL-12 rescues caspase-8-deficient animals during acute *T. gondii* infection. 105

5.3.3 IL-12 rescues c-Rel-deficient animals during acute *T. gondii* infection. 105
5.3.4 Expression of non-cleavable caspase-8 reduced host mortality during acute *T. gondii* infection. 106
5.3.5 Ablation of caspase-8 in hematopoietic cells results in increased parasite burdens and a defect in monocyte infiltration. 107
5.4 DISCUSSION 108
5.5 FIGURES 111
Fig 5.1 Caspase-8 promotes survival during acute *T. gondii* infection. 111
Fig 5.2. Caspase-8 promotes IL-12 production by DCs during acute *T. gondii* infection. 113
Fig 5.3. Exogenous IL-12 rescues caspase-8-deficient animals during acute *T. gondii* infection. 115
Fig 5.4. Exogenous IL-12 rescues c-Rel-deficient animals during acute *T. gondii* infection. 117
Fig 5.5. Non-cleavable caspase-8 promotes host survival during acute *T. gondii* infection. 118
Fig 5.6. Caspase-8 deficiency in hematopoietic cells leads to increased parasite burdens and impaired monocyte infiltration during *T. gondii* infection. 119
Fig 5.7. Graphical abstract: Caspase-8 promotes secretion of IL-12 in response to *T. gondii* infection. 120
Fig 5.8. Future directions: Potential *in vitro* mechanism of caspase-8-dependent *Il12b* expression in DCs during *T. gondii* infection. 121

CHAPTER 6: NON-CLEAVABLE CASPASE-8 MEDIATES HOST SURVIVAL DURING INFECTION WITH THE GRAM-NEGATIVE BACTERIAL PATHOGEN *YERSINIA PSEUDOTUBERCULOSIS*. 122

6.1 ABSTRACT 122
6.2 INTRODUCTION 124
6.3 RESULTS 127
6.3.1. Non-cleavable caspase-8 promotes host survival during oral infection with *Yersinia pseudotuberculosis*. 127
6.3.2. Non-cleavable caspase-8 expression correlates with reduced bacterial burdens during oral infection with *Yersinia pseudotuberculosis*. 128
6.3.3. Systemic IL-12p40 is produced independently of caspase-8 expression. 129
6.3.4 Cell-intrinsic IL-12p40 expression occurs independently of caspase-8 expression. 129
6.4 DISCUSSION 132
6.5 FIGURES 135
Fig 6.1. Non-cleavable caspase-8 promotes host survival during oral infection with *Yersinia pseudotuberculosis*. 135
Fig 6.2. Non-cleavable caspase-8 expression correlates with reduced bacterial burdens during oral infection with *Yersinia pseudotuberculosis*. 136
Fig 6.3. Systemic IL-12p40 is produced independently of caspase-8 expression. 137
Fig 6.4. Flow-cytometry gating strategy for innate immune populations during oral infection with *Yersinia pseudotuberculosis*. 138

Fig 6.5 Monocyte IL-12p40 expression is independent of caspase-8. 139
Fig 6.6. Neutrophil IL-12p40 expression is independent of caspase-8. 140
Fig 6.7 RIPK3-null mice expressing non-cleavable caspase-8 have higher levels of monocyte infiltration during *Yersinia pseudotuberculosis* infection. .. 141
Fig 6.8 RIPK3-null mice expressing non-cleavable caspase-8 have higher neutrophil numbers at steady-state..... 143
Fig 6.9. Graphical abstract and future directions: Caspase-8 promotes host survival during oral infection with *Yersinia pseudotuberculosis* independently if its cytokine regulatory or apoptotic functions. 145

CHAPTER 7: DISCUSSION AND FUTURE DIRECTIONS..... 146

7.1 SUMMARY OF FINDINGS 146
7.2 KEY FINDINGS OF THIS WORK..... 148
7.2.1 Distinct regulation of the NF-κB family members p65 and c-Rel is mediated, in part, through caspase-8..... 148
7.2.2 Caspase-8 regulates inflammatory gene expression through both its enzymatic and non-enzymatic activity..... 150
7.2.3 Caspase-8 regulates cell cycle gene expression in response to multiple TLRs. 152
7.2.4 Caspase-8-dependent apoptosis, and RIPK3-mediated programmed necrosis may regulate steady-state numbers of myeloid cells. 154
7.2.5. Caspase-8 mediates host survival during infection with *Toxoplasma gondii*. 157
7.2.6 Caspase-8 may play a role in intestinal epithelial cell homeostasis at steady-state and during infection. 159
7.3 CONCLUDING REMARKS 161

CHAPTER 8: MATERIALS AND METHODS 162

8.1 EXPERIMENTAL MODEL AND SUBJECT DETAILS 162
8.1.1 Mice 162
8.1.2. *Toxoplasma gondii*..... 162
8.1.3. *Yersinia pseudotuberculosis* 163
8.2 METHOD DETAILS..... 164
8.2.1 Bone marrow chimeras 164
8.2.2 BMDM electoporation and hc-Rel plasmid..... 164
8.2.3 Caspase-8 activity assay 164
8.2.4 Cell culture..... 165
8.2.5 ChIP-qPCR 165
8.2.6 Confocal Microscopy..... 166
8.2.7 Cytospins 167
8.2.8 ELISA (*in vitro*)..... 167
8.2.9 ELISA (*in vivo*)..... 167
8.2.10 FasL stimulation of thymocytes and thymocyte characterization..... 167
8.2.11 Flow cytometry (*in vitro*)..... 168
8.2.12 Flow cytometry (*in vivo*)..... 169
8.2.13 RNA-seq 169
8.2.14 RT-qPCR 170

8.2.15 Western Blots 171
8.3 QUANTIFICATION AND STATISTICAL ANALYSIS 173
8.4 APPENDIX 174
REFERENCES 175

CHAPTER 1: Introduction

1.1 Innate immune sensing

The innate immune system is the first line of defense in the host response to insult or injury from the environment. Often this injury is triggered by attack from microbes such as bacteria, viruses, protozoan parasites, or prions. After a breach of physical barrier sites such as the skin, the innate immune system must (1) recognize this diverse group of microbes as a threat to the host, (2) activate inflammatory mediators to promote microbe clearance and host survival, and ultimately (3) trigger the adaptive immune response to promote long-term protection.

For many years, addressing the way innate immune cells recognized such a diverse group of organisms in the absence of antigen specificity was an open question in the field of immunology. It was not until Dr. Charles Janeway proposed the Pattern Recognition framework—in which he hypothesized that innate immune cells recognize conserved microbial products known as Pathogen-Associated Molecular Patterns (PAMPs) through Pattern Recognition Receptors (PRRs) expressed on their surface—that immunologists had a comprehensive framework explaining *how* this process might occur in the host [1]. While Dr. Janeway's prediction was not demonstrated experimentally until the mid 1990s [2-4], it has become a foundational pillar for our understanding of the ways in which host innate immune cells distinguish self from non-self. Subsequent groups have gone on to characterize a wide variety of PRRs that are expressed on the cell surface, intracellular membranes, and the cytoplasm [5, 6, 7, 8]. Moreover, we now know that PRRs are not restricted to innate immune cells, such as macrophages or dendritic cells, but are expressed on a variety of other immune cell types [9] as well as non-immune cells such as fibroblasts

[10] and epithelial cells [11-13]. PRR stimulation promotes functional alterations in these cell types that are critical for both immune activation and host homeostasis [14-16].

Recently our appreciation for the robust colonization of mammalian hosts by non-self-microbes, such as the billions of bacteria and viruses in our intestinal tract [17], has raised a conceptual problem for the understanding of how PRR activation and inflammation target pathogenic microbes specifically. Under homeostatic conditions the host gut is not constitutively inflamed [18]. In fact it is hypothesized that commensal microbes conferred an evolutionary fitness advantage for our ancestors, allowing them to efficiently acquire nutrients and prevent colonization by pathobionts [19-21]. In exchange our guts provide a replicative niche for these commensals. How can we reconcile this with the knowledge that the PAMPs expressed by these commensal microbes are indistinguishable from pathogens? How does the host specifically promote clearance of pathogens while preserving beneficial microbes? One solution lies in the properties of the inflammatory networks activated in response to PRR stimulation. These networks are not on/off switches, rather they are regulated by a variety of intracellular factors that can dampen [22, 23] or heighten [24] the inflammatory signal. We are continually expanding the list of host factors that allow cells to fine-tune the inflammatory response. The aim of this thesis is to address the contribution of the cysteine protease caspase-8 to the regulation of inflammation in response to PRR activation, and to build upon our current understanding of the intracellular mechanisms that regulate activation in response to microbial products originating from both commensal and pathogenic organisms.

1.1.1 Overview of Toll-like-receptor activation and gene transcription.

Toll-like receptors (TLRs) are a subset of PRRs that act as sensors for microbial products [2, 3, 25, 26]. TLRs can be expressed on the cell surface (TLR1, TLR2, TLR4, TLR5 [27], TLR6, and TLR10) or on endosomal membranes (TLR3 [28], TLR7 [29], TLR8, TLR9 [30], TLR11 [31], TLR12, and TLR13) [32]. Broadly, cell surface TLRs recognize microbial membrane components [33], and endosomal TLRs recognize microbial nucleic acids [34]. Activation of TLRs via the detection of PAMPs leads to the recruitment of the adapter proteins MyD88 (Myeloid differentiation primary response 88) and TRIF (TIR-domain-containing adapter-inducing interferon-β) [35-37].These adapter proteins mediate the induction of intracellular signaling cascades that ultimately activate the transcription factors NF-κB (nuclear factor kappa-light-chain-enhancer of activated B cells), AP-1(Activator protein 1) and IRF3 (Interferon regulatory factor 3) [38, 39, 40]. These transcription factors in turn promote upregulation of inflammatory molecules that directly or indirectly promote killing of microbes [41-44](**Figure 1.1**). The roles of MyD88 and TRIF are non-redundant as *Myd88*$^{-/-}$ and *Trif*$^{-/-}$ mice are differentially susceptible to infection with bacteria [45, 46] and viruses [35], respectively. TLR4, which recognizes a component of the cell wall of gram-negative bacteria known as lipopolysaccharide (LPS), is unique in that it is the only TLR that signals through both MyD88 and TRIF—MyD88 when TLR4 is expressed at the plasma membrane and TRIF after TLR4 endocytosis [47, 48]. Although TLRs signal through a common set of adaptor proteins (TLR4 and TLR3 through TRIF and TLR4 along with all other TLRs through MyD88), it has been recently appreciated that the magnitude and breadth of this response is not uniform across all TLR-stimuli [49]. This appreciation for the divergent activation of transcriptional responses

downstream of TLR stimulation has led to a body of work aimed at determining how signals from these common adaptors and transcription factors lead to unique gene expression patterns [50-52]. While significant progress has been made in defining the regulatory mechanisms by which common TLR-inputs are integrated into divergent gene expression outputs, these studies are by no means exhaustive, creating a gap in our knowledge surrounding one of the most fundamental aspects of the innate immune system.

1.1.2 Overview of NF-κB-dependent gene regulation in macrophages.

TLR-mediated activation of NF-κB induces the upregulation of pro-inflammatory mediators and antimicrobial peptides to promote killing of microbes [53-55]. NF-κB transcription factors are a family of five proteins that form active homo- and heterodimers to mediate gene expression [56](**Figure 1.2**). They are constitutively expressed in macrophages, and held in the cytoplasm by negative regulators from the IκB family; these negative regulators are degraded in response to TLR activation via the 26S proteasome [57, 58](**Figure 1.2**). Degradation of IκB proteins allows NF-κB dimers to translocate to the nucleus and induce the expression of their target genes. NF-κB signaling is often used as a classic example of a negative feedback loop in biology, as the genes encoding inhibitory IκB proteins are among the many transcriptional targets for NF-κB dimers [59]. This provides an elegant mechanism to prevent chronic induction of inflammatory mediators triggered by TLR activation.

In macrophages NF-κB gene targets can be categorized into primary and secondary response genes [60] that are thought to be organized by lineage determining factors expressed during macrophage development [61, 62]. As the name implies, primary

response genes are poised for rapid transcription due to their (1) open chromatin state, (2) limited occupation by nucleosomes, (3) independence from SWI/SNF-mediated chromatin modification, and (4) poised RNA polymerase II at their promoters [63-65]. However, secondary response genes require chromatin remodeling [66, 67] and RNA polymerase II recruitment to initiate transcription. Macrophage chromatin organization creates a temporal hierarchy for inflammatory gene expression through the division of gene accessibility to transcription factors such as NF-κB proteins [68, 69]. In macrophages the TLR4 agonist, LPS, is one of the most potent activators of NF-κB-dependent gene transcription, which is thought to be primarily dependent on the activity of p65 [70]. However, seminal work has shown that a less well-characterized NF-κB protein, c-Rel, is specifically required for the transcription of the secondary response gene *Il12b* [71], which encodes the IL-12p40 subunit of IL-12p70 and IL-23, two cytokines essential for host defense against a variety of pathogens [72-74]. Data from our lab as well as others has shown a requirement for the cysteine protease caspase-8 in cytokine production in response to LPS and other TLR ligands such as Poly I:C (TLR3) and CpG (TLR9) [75-78]. Uniformly the gene we found to be most differentially affected by the absence of caspase-8 was *Il12b* [75]. Caspase-8 affects *Il12b* transcription downstream of both TLR3, which is TRIF-dependent, and TLR9, which is MyD88-dependent. This suggests that in macrophages caspase-8 may serve as signaling node that enhances the magnitude of inflammatory cytokine expression in response to all TLRs regardless of their respective adaptor proteins. In **Chapter 2** we identify the diversity of caspase-8-dependent genes induced in response to TLR4 and TLR9 activation.

1.1.3 Overview of caspase-8 biology.

Caspase-8 belongs to a family of pro-enzymes, termed caspases, which are activated by homodimerization and auto-processing [79-81]. Caspase-8 consists of tandem N-terminus death effector domains (DED) [82] that promote homotypic interactions between other DED-containing proteins, and a C-terminus catalytic domain that is auto-processed during homodimerization to form the p20 and p10 subunits of the apoptotic formation of caspase-8 (**Figure 1.3A**). Upon activation of death receptors, such as TNFR (Tumor necrosis factor receptor) or Fas/CD95, the adaptor protein TRADD (Tumor necrosis factor receptor type 1-associated death domain protein) is recruited via homotypic interaction between its death domain and that of the death receptor [83, 84] **(Figures 1.3B** and **1.3C)**. TRADD then recruits FADD (FAS associated death domain), which contains both a death domain and death effector domain, thereby allowing for the recruitment of RIPK1 (Receptor-interacting serine/threonine-protein kinase 1) and caspase-8, respectively [85]. These proteins assemble to form the death inducing signaling complex (DISC) [86] then are rapidly endocytosed to form a cytoplasmic supramolecular complex known as Complex II [87]. Complex II serves as a platform for apoptotic signaling [87, 88] (**Figure 1.3C**). Under pro-survival conditions, such as TNF stimulation, some death-inducing proteins remain at the plasma membrane and promote activation of NF-κB and MAPK through TRADD-mediated recruitment of TRAF2 (TNFR associated factor 2) (**Figures 1.1** and **1.3C**) [89-94]. Under these pro-survival conditions, the expression of a catalytically inactive homolog of caspase-8, cFLIP (cellular FLICE like inhibitory protein), prevents caspase-8 auto-processing, thereby inhibiting caspase-8 apoptotic activity [91, 95, 96]. TLR or TNFR stimulation coupled to chemical- or pathogen-mediated blockade of

gene transcription results in activation of Complex II, and a decrease in cFLIP expression [97-101]. These two signals promote the auto-processing of caspase-8 monomers and cleavage of downstream substrates to induce cell-extrinsic apoptosis **(Figure 1.3C)** [102, 103].

Recently, it has also been appreciated that caspase-8 constitutively represses another form of cell death known as programmed necrosis [104, 105]. Both the non-apoptotic and apoptotic conformations of caspase-8 represses RIPK3- (Receptor-interacting serine/threonine protein-kinase 3) mediated programmed necrosis through the constitutive cleavage of the lysine 63 deubiquitinase CYLD [106, 107]. CYLD cleaves K63 ubiquitin on RIPK1 promoting its dissociation from Complex II and promoting association with RIPK3 via homotypic interactions in their RHIM (RIP homotypic interaction motif) domains [108]. This interaction in turn leads to the phosphorylation of MLKL (Mixed lineage kinase domain like pseudokinase), oligomerization and plasma membrane disruption (**Figure 1.3C**) [109]. Previously, caspase-8-deficient animals were not viable because of the requirement for caspase-8-mediated repression of necrosis during embryonic development. The generation of *Ripk3*$^{-/-}$*Casp8*$^{-/-}$ mice [104, 105] has provided a genetic tool to investigate the role of caspase-8 in inflammatory gene regulation without the confounding role of programmed necrosis. Using *Ripk3*$^{-/-}$*Casp8*$^{-/-}$ mice as a tool, our lab, as well as other labs, have shown a role for caspase-8 in inflammatory cytokine production apart from its role in apoptosis and programmed necrosis [75-78, 110, 111].

1.1.4 Caspase-8 mediates cytokine secretion.

The enzymatic properties of caspase-8 that mediate cytokine secretion have yet to be elucidated. Caspase-8 likely has both scaffolding and enzymatic functions within the cell, but the relative contributions of scaffolding and enzymatic activity to gene expression has not been directly tested in response to TLR stimulation. Early it was reported that the pro-domains of caspase-8 were sufficient to mediate NF-κB signaling [78]. Recently, caspase-8 scaffolding has been implicated in TRAIL (TNF related apoptosis inducing ligand)-induced inflammatory gene expression in HeLa cells [112]. However, we previously observed that treatment of RIPK3-deficient macrophages with a caspase-8-specific inhibitor reduced inflammatory cytokine production during TLR stimulation [75]. To address this potential discrepancy, and to mechanistically dissect the contribution of caspase-8 to macrophage inflammatory gene expression, we examined the roles of both caspase-8 scaffolding and enzymatic activities in regulation of NF-κB signaling. One approach we took to address this question was to generate a mouse expressing a catalytically active, non-cleavable form of caspase-8 in which the linker region between the p20 and p10 subunits is mutated from an aspartic acid to an alanine, inhibiting auto-processing and stabilization of the apoptotic conformation of caspase-8 while preserving protein expression and its cytokine regulatory function (**Figure 1.3A**) [80, 113]. These mice will be referred to as *Casp8*$^{DA/DA}$. We have previously shown that bone marrow derived macrophages (BMDMs) from these mice are resistant to apoptosis induced via infection with the gram-negative bacterial pathogen *Yersinia pseudotuberculosis* (*Yp*) [75]. *Yp* is a potent activator of caspase-8-dependent apoptosis in macrophages [97, 100, 114], but *Casp8*$^{DA/DA}$ BMDMs do not undergo apoptosis, and maintain their ability to secrete

inflammatory cytokines when stimulated with TLR ligands [75]. A combination of chemical inhibition of caspase-8 activity, genetic ablation of caspase-8, and specific mutation of caspase-8 apoptotic activity have allowed us to investigate both the mechanism by which caspase-8 regulates inflammatory gene expression (**Chapter 2**) in response to TLR stimulation, and the enzymatic requirements of caspase-8 in this context (**Chapter 3**).

1.2 Role of apoptosis and cytokine secretion in host defense

The hallmarks of inflammation—redness, swelling with heat, and pain—were first described by the Roman physician Cornelius Celsus in the first century A.D. [115]. Subsequent discoveries identified the soluble factors, which we now refer to as cytokines, that mediated some of the observed characteristics of inflammation, resulting in the identification of TNF in 1975 and IFN in 1978 [116-118]. Cytokines are defined as "soluble factor[s] produced by one cell and acting on another cell, in order to bring about a change in the function of the target cell" [119]. This broad definition encompasses an array of functions within the host of which signaling during inflammation is but one. The protective effect of cytokines has been appreciated since the observation that endotoxin-induced TNF was cytotoxic to tumor cells [116]. Moreover, in the early 80s Cantell and others began purifying bulk IFN preps from human donor cells stimulated with Sendai Virus for human clinical trials [120]. However, prolonged secretion of cytokines can also have detrimental effects, and chronic inflammation mediated by cytokines has been implicated in diseases such as diabetes, rheumatoid arthritis, Crohn's disease, and plaque psoriasis [121-124]. As such there is considerable interest in identifying the mechanisms by which the host immune system secretes inflammatory mediators to promote acute clearance of pathogens, but controls long-term release to prevent tissue damage and host mortality.

A second line of defense in control of microbial infection is programmed cell death, which allows the host to destroy the infected cell, control pathogen spread, and promote the release of danger-associated molecular patterns (DAMPs) that signal to bystander cells. Both caspase-8 enzymatic activity and scaffolding are implicated in many of these programmed cell death pathways. Caspase-8 plays a role in host defense during pyroptosis

[77, 125, 126], programmed necrosis [127], and apoptosis [128] during both viral and bacterial infection. Apoptosis is unique in that under developmental and homeostatic conditions it is largely thought to be immunologically silent [129]. However, there are contexts in which apoptosis can be inflammatory [130, 131], particularly when it is coupled to infection [98, 132]. In investigating the role of apoptosis in host defense we discovered that the caspase-8 serves as a bridge between the regulation of cell death and cytokine production in response to PAMP stimulation [75]. Given the role of both cell death and cytokine production in host defense during infection we sought to determine the relative contributions of both caspase-8-mediated cytokine secretion and caspase-8-mediated cell death in this context.

1.2.1. Caspase-8 deficiency leads to embryonic lethality.

Caspase-8 negatively regulates programmed necrosis through the constitutive cleavage of the lysine 63 deubiquitinase CYLD [133]. For this reason, the single ablation of caspase-8 results in lethality ten days into embryonic development. Dual ablation of caspase-8 and RIPK3, a mediator of programmed necrosis, yield viable mice with normal development [104, 105]. However, beginning at 6 weeks *Ripk3*$^{-/-}$*Casp8*$^{-/-}$ mice display lymphadenopathy and splenomegaly that is attributed to the accumulation of lymphocytes, specifically a CD4^{-}CD8^{-}CD3^{+}B220^{+} adaptive population of T cells [105]. Conditional deletion of caspase-8 using the Cre/LoxP system in specific cell lineages leads to activation of programed necrosis upon cell stimulation [107, 134]. Therefore, *Ripk3*$^{-/-}$*Casp8*$^{-/-}$ mice are currently the best tool to study caspase-8-mediated apoptosis and cytokine secretion during host defense *in vivo.* Recently, we have also generated a mouse, *Casp8*$^{DA/DA}$,

sufficient for the cytokine regulatory function of caspase-8, but not its apoptotic activity (**Section 1.1.4**) [75]. These mice were also bred to *Ripk3*$^{-/-}$ mice to create *Ripk3*$^{-/-}$ *Casp8*$^{DA/DA}$ mice. *Ripk3*$^{-/-}$*Casp8*$^{DA/DA}$ mice should not be able to undergo apoptosis or programmed necrosis, but should be able to produce caspase-8-dependent inflammatory cytokines. We have performed preliminary characterizations of the developmental phenotype of these mice that will be described in **Chapter 4** as well as infections with *Toxoplasma gondii* and *Yersinia pseudotuberculosis* that are discussed in **Chapters 5** and **6**, respectively.

1.2.2 Role of caspase-8 in host survival during acute *Toxoplasma gondii* infection.

The protozoan parasite *T. gondii* infects warm-blooded animals via ingestion of oocysts shed in the feces of the parasites' obligate hosts: members of Felidae family (domestic cats) [135]. The CDC estimates that 40 million adults, adolescents, and children are infected at any given time in the U.S., and that *Toxoplasma spp*. are the leading cause of foodborne-related deaths [136]. Early work investigating the mechanisms of immune protection against *T. gondii*-infection identified the cytokine IL-12p70 as a key mediator of host defense [137]. C57BL/6 mice clear infection with the attenuated Prugniaud (Pru) strain of *T. gondii* within 30 days, and this clearance is dependent on the early production of IL-12p70 [138]. IL-12p70 secreted by conventional dendritic cells (cDCs) promotes early release of NK cell IFNγ as well as a CD4 and CD8 T cell recruitment [139]. These events lead to myeloid- and T-mediated killing of infected cells [140-143].

Interestingly, the cytokine that is most affected by the loss of caspase-8 is IL-12p40 [75], but to our knowledge no one had identified a role for caspase-8 in protection against

T. gondii. Caspase-8-mediated apoptosis is not thought to play a role in host defense during *T. gondii* infection as the parasite actively suppresses apoptotic signaling [144, 145]. For these two reasons we hypothesized that caspase-8-mediated cytokine production—not cell death—is required for survival during acute *T. gondii* infection. The results from these studies are described in **Chapter 5**.

1.2.3 Caspase-8 mediates host survival in response to *Yersinia pseudotuberculosis.*

Previous work from our lab as well as others has shown that caspase-8 plays a cell-intrinsic role in cytokine production in response to gram-negative bacterial infections [75-77, 100, 110, 146] and fungal infections [147]. These data suggest that caspase-8-dependent cytokine production may promote antimicrobial host defense independently of its apoptotic activity. One potent activator of caspase-8-dependent apoptosis and cytokine production is *Yersinia pseudotuberculosis*, a gram-negative bacterial pathogen that causes self-limiting gastroenteritis in humans [148, 149], but in mice mimics infection with the related species *Yersinia pestis*, the causative agent of plague [150-152]. *Yersinia pestis* is still endemic in the United States, with a mortality rate between 30-90% when left untreated [153], making it not only a model to dissect the dual functions of caspase-8 in host defense, but also a pathogen of broad public health relevance. *Yersinia pseudotuberculosis* expresses seven effector proteins known as *Yersinia* outer proteins (Yops) that are injected into target cells through a needle like structure known as the Type III secretion system [154, 155]. One of these effectors, YopJ, blocks MAPK and NF-κB signaling, leading to the activation of caspase-8-mediated apoptosis (**Figure 1.5**) [154]. Injection of YopJ occurs within the first hour of infection and results in irreversible cell death within 4 hours *in vitro*

[132, 156]. We have previously shown that sublethally irradiated C57BL/6 mice reconstituted with *Ripk3*$^{-/-}$*Casp8*$^{-/-}$ bone marrow infected orally with *Yersinia pseudotuberculosis* have a cell-intrinsic defect in cytokine secretion, and an acute survival defect [114]. However, these data do not address whether caspase-8-mediated apoptosis or caspase-8-mediated cytokine production promote host survival in this context. Therefore, we sought to determine the relative contributions of both caspase-8-mediated cell death and inflammatory cytokine production to host survival during infection with *Yersinia pseudotuberculosis* (**Chapter 6)**.

1.2.4 Caspase-8 deficiency in humans leads to acute susceptibility to microbial infection.

A majority of the mechanistic research interrogating the apoptotic- and immune signaling-functions of caspase-8 have been performed using mice and mouse cells. However, there are humans with a caspase-8 deficiency. These patients were identified in 2001 as a brother and sister whose asymptomatic parents possessed a heterozygous mutation that rendered caspase-8 catalytically inactive and the protein unstable [157]. The clinical history of these patients revealed ongoing, acute susceptibility to microbial infections, suggesting that caspase-8-induced control of cell death contributes to antimicrobial defense [157]. However, B, NK, and T cells from these patients had defects in activation, which was attributed to impaired NF-κB signaling mediated through caspase-8 [78, 157-159]. These data raised the possibility that these patients' susceptibility to microbial infection may involve caspase-8-mediated control of immune cell activation in lieu of caspase-8-mediated cell death.

Subsequent studies investigating the role of caspase-8 in T cell activation in mice using the dual ablation of caspase-8 and RIPK3 showed no defects in T cell activation or defects in T cell expansion after infection with LCMV Armstrong (Lymphocytic Choriomeningitis virus) or MHV (Mouse Herpes virus) [134, 160]. One explanation of this discrepancy is that there are human- and mouse-specific signaling mechanisms that dictate the differential impact of caspase-8 on immune cell activation. It also possible that this difference can be attributed to the expression of the caspase-8 homolog caspase-10 in humans and not rodents [161]. In fact, redundancy between caspase-8 and caspase-10 in humans was offered as an explanation for the ability of humans to survive embryonic development without functional caspase-8 [157]. However, we are optimistic that our investigations of caspase-8 in inflammatory gene expression and host defense will provide some basis for further investigations into caspase-8-specific functions in human immune cells.

1.3 Summary

Caspase-8 is uniquely poised at the interface of cell death and cytokine production—two essential biological processes that mediate host defense. Understanding both (1) the mechanism of caspase-8 dependent cytokine production and (2) the relative contributions of caspase-8-mediated cell death and cytokine secretion to host survival will allow us to elucidate how host immune cells are able to switch between expression of pro-inflammatory mediators and cell death during infection. The aim of this project was to begin to resolve two conceptual and scientific gaps in the field of caspase-8 biology, thereby expanding our understanding of the intimate integration of inflammation and cell death.

One gap in knowledge was the structural requirements of caspase-8 that mediate its immune regulatory function. Some hypothesize that caspase-8 serves as a scaffolding platform for signal transduction that leads to gene expression [111, 112]. However, data from our lab suggest that caspase-8 enzymatic activity is required for maximal cytokine expression [75]. **Chapters 2** and **3** seek to address this question in the context of macrophage gene expression.

The second gap is the broader question of the mechanism by which caspase-8 promotes host defense. Given the observation that humans with caspase-8 deficiencies experience chronic infection with a variety of pathogens, and the requirement for caspase-8 in mouse survival during infection with *Yersinia pseudotuberculosis*, we sought to address the question of what biological property or properties of caspase-8 contribute to host protection. Previous work from our lab as well as others has demonstrated a broad cell-intrinsic role for caspase-8 in the regulation of immune cell homeostasis, inflammatory

cell death, and inflammatory gene expression. The spectrum of caspase-8 cellular functions provide several potential mechanisms by which caspase-8 promotes host survival during microbial infection. Data from **Chapters 5** and **6** seek to address this question during acute infection with *Toxoplasma gondii* and *Yersinia pseudotuberculosis*, respectively.

1.4 Figures

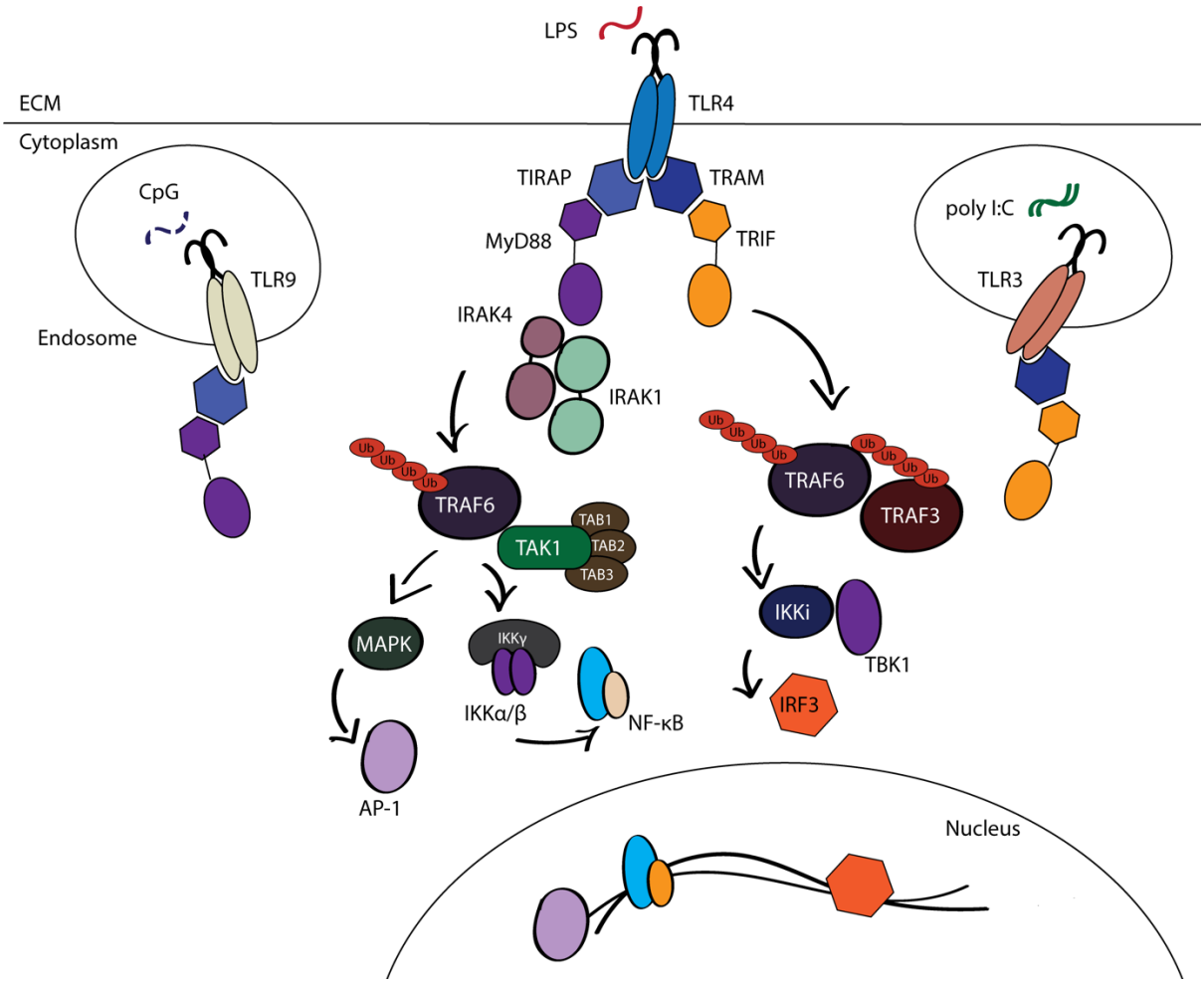

Fig 1.1 Schematic of signal transduction induced in response to TLR stimulation[162, 163].

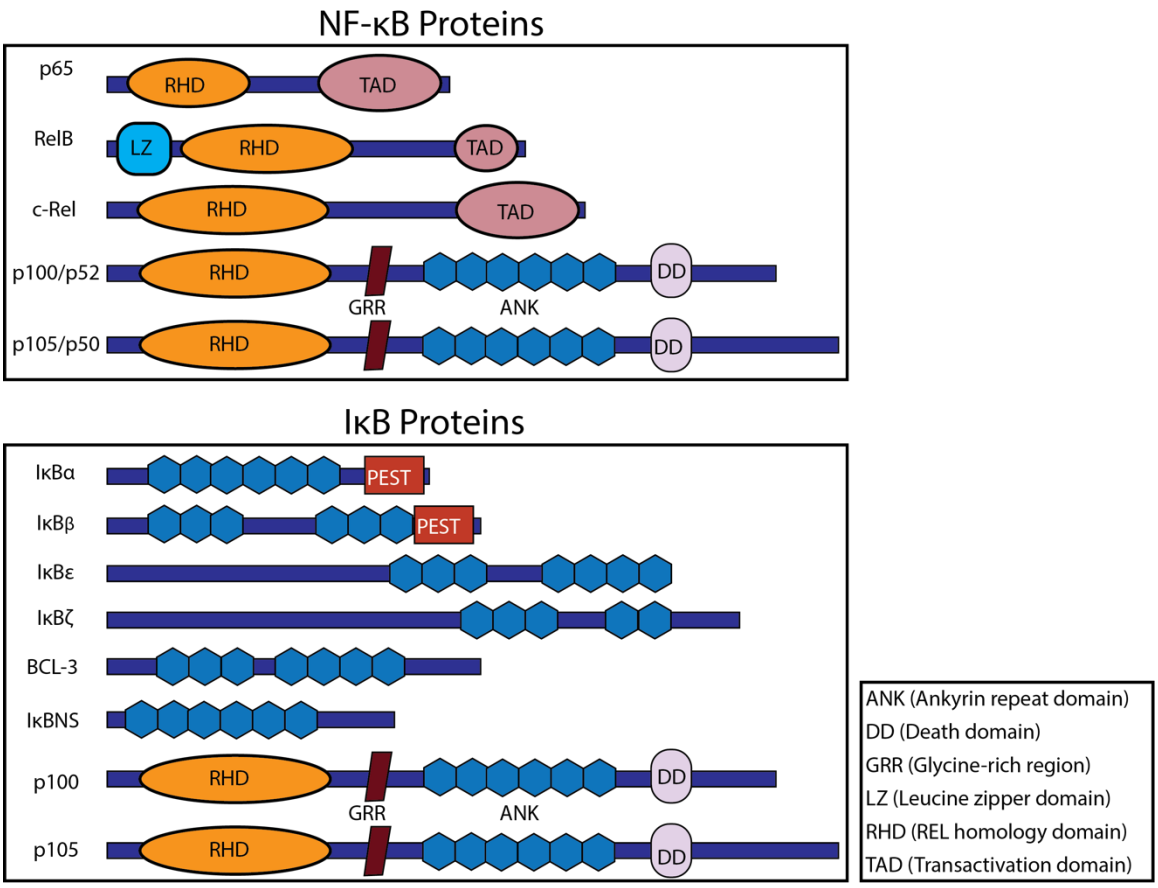

Fig 1.2 Schematic of NF-κB and IκB protein structure [56].

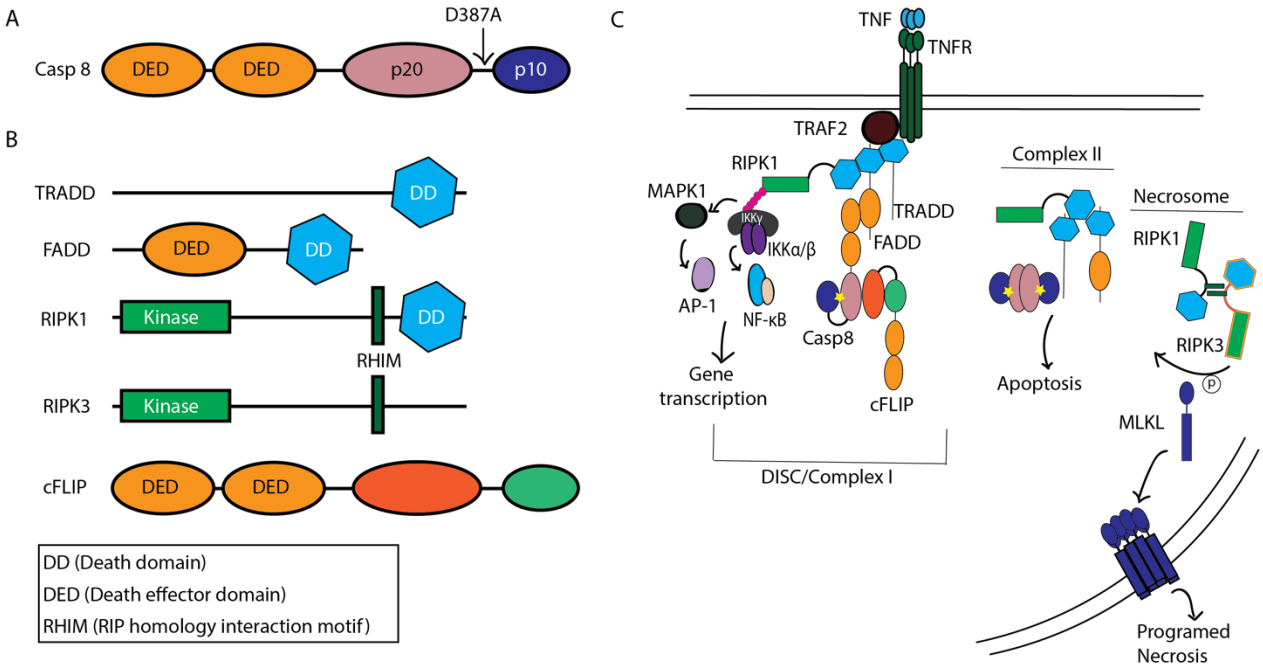

Fig 1.3 Schematic of proteins involved in death receptor signaling and the signal transduction cascade that mediates apoptosis and programmed necrosis [83, 87, 96].

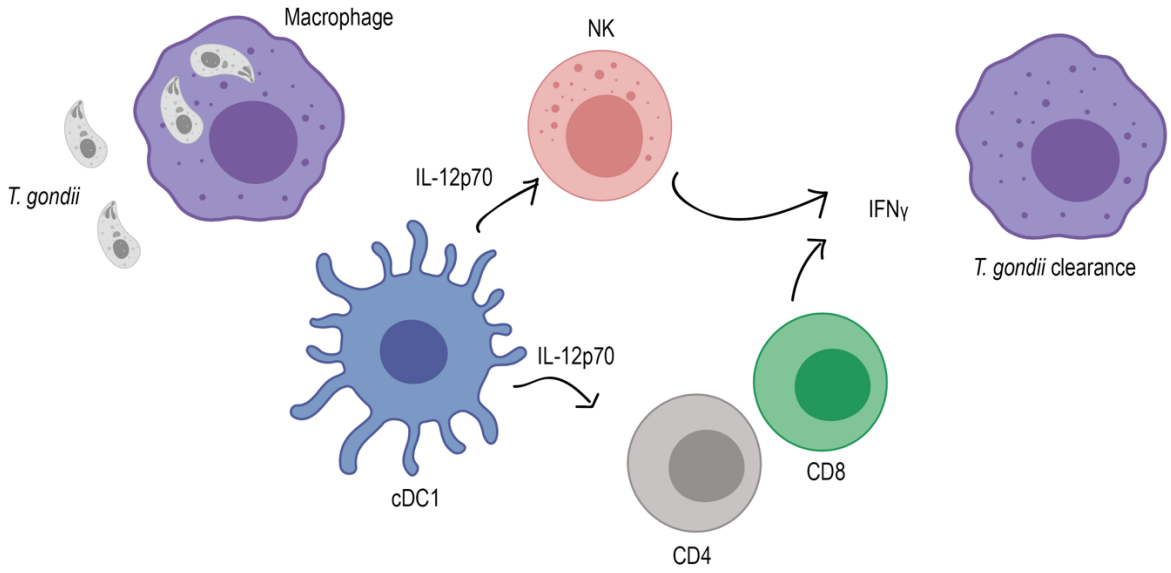

Fig 1.4. Model of IL-12-mediated clearance of *Toxoplasma gondii* infection.

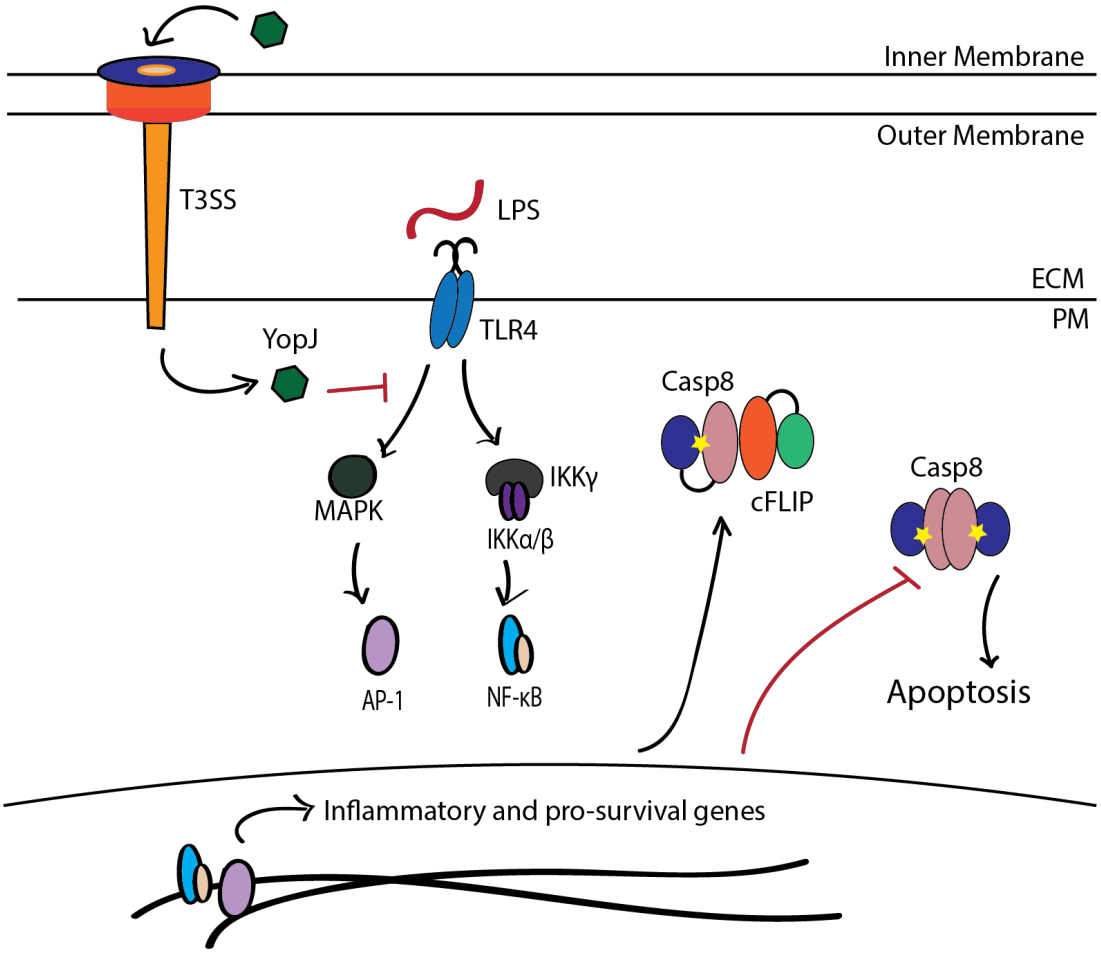

Fig 1.5 Schematic of *Yersinia pseudotuberculosis*-induced apoptosis in macrophages.

CHAPTER 2: Caspase-8 regulates TLR-induced macrophage gene expression through the NF-κB family member c-Rel.

2.1 Abstract

Our group as well as others have shown that caspase-8 has an important role in cell-intrinsic inflammatory gene expression. Macrophages lacking caspase-8 or the adaptor protein FADD have defective inflammatory cytokine expression, and inflammasome priming in response to bacterial infection and TLR stimulation. Macrophage cytokine secretion is a key regulator of host innate immunity. Therefore, defining the regulatory mechanisms that promote macrophage-mediated cytokine expression are essential to the development of clinical therapies that target these signaling pathways. We sought to specifically define the mechanism of caspase-8-dependent gene regulation in the context of TLR stimulation. Here we demonstrate that caspase-8 regulates a broad repertoire of inflammatory genes in response to multiple TLRs, and that caspase-8 exerts this function in part through regulation of IKK phosphorylation. This differential IKK phosphorylation affects translocation of the NF-κB family member c-Rel, but not p65, and overexpression of c-Rel was sufficient to restore expression of IL-12 and IL-1β in caspase-8-deficient cells. IKK phosphorylation in response to TLR4 and TLR9 is dependent on the presence of the adaptor protein FADD suggesting a mechanism by which both TLR activation and death receptor activation are coupled to caspase-8 signaling in macrophages. These findings provide new insight into a novel regulatory mechanism for the transcription factor c-Rel via caspase-8-mediated activation of IKK phosphorylation.

2.2 Introduction

Caspase-8-mediated apoptosis plays a critical role in immune homeostasis through the clearance of autoreactive cells [164-166], and tumor suppression [167]. Therefore, there has been considerable effort in elucidating the regulatory mechanisms governing this form of cell death. These studies have helped identify the critical adaptor molecules FADD [168, 169] and TRADD [170] that mediate caspase-8-recruitment to the death receptors Fas and TNFR1/2 respectively as well as the signals that govern the switch from pro-survival signaling at the plasma membrane to apoptotic signaling via Complex II in the cytoplasm [92, 93]. However, there is evidence that caspase-8 plays a role in host survival beyond its role in cell-extrinsic apoptosis.

Original reports of caspase-8 mutations in humans identified defects in T, B and NK cell activation [157], and subsequent work demonstrated that caspase-8 regulates NF-κB activation through interactions with NIK (NF-κB-inducing kinase) and RIKP1 [78]. These data led to the hypothesis that caspase-8 regulates lymphocyte activation through NF-κB signaling. This mechanism that was seemingly confirmed by subsequent studies in mice showing a role for caspase-8 in B cell survival in response to TLR stimulation, and decreased NF-κB signaling in the absence of caspase-8 in other cell types [158, 159]. However, two seminal studies published simultaneously in 2011 demonstrated a role for caspase-8 in the repression of another cell death pathway: programmed necrosis [104, 105]. In the absence of caspase-8 there is a de-repression of RIPK1/RIPK3-dependent programmed necrosis during embryonic development [92, 104, 105]. Dual ablation of caspase-8 and RIPK3 led to viable progeny, and abrogated the constitutive activation of programmed necrosis in response to death-inducing stimuli [105]. It was also shown that

caspase-8 negatively regulates programmed necrosis through the constitutive cleavage of the deubiquitinase CYLD [133]. CYLD cleaves K63 ubiquitin on RIPK1 which leads to its interaction with RIPK3 and subsequent activation of programmed necrosis [106].

These new data raised the possibility that previous studies demonstrating a role for caspase-8 in NF-κB signaling downstream of lymphocyte activation were confounded by the role of caspase-8 in the regulation of programmed necrosis. It was possible that the observed phenotype in lymphocytes was due to a defect in *survival* and not *activation*. In fact studies testing the impact of dual ablation of caspase-8-dependent apoptosis and RIPK3-mediated programmed necrosis in T cells showed no defect in proliferation—these mice also display normal T cell activation after infection with MHV [160]. These data conflict with earlier reports that caspase-8 was required for T cell activation in humans: T cells isolated from caspase-8-deficient patients had a decrease in IL-2 release after TCR stimulation [157]. However, these earlier studies did not test if these cells were *dying* in response to TCR activation which is a possible experimental outcome given our current understanding of caspase-8-dependent regulation of programmed necrosis. Another potential explanation for this discrepancy is that there are mouse- and human-specific differences in T cell activation after TCR stimulation, but these investigators did not directly test cell death in these cultures so this conflict remains unresolved.

Our initial interest in caspase-8 biology arose from its role in cell death in response to microbial infection. It has long been appreciated that apoptosis promotes clearance of virally infected cells, illustrated by the evolution of viral antagonism of caspase-8-mediated apoptosis [171, 172]. However, the role of caspase-8 in response to bacterial infection has yet to be completely defined. The gram-negative bacterial pathogen *Yersinia*

pseudotuberculosis (*Yp*), causes self-limiting gastroenteritis in humans, but in mice leads to bacterial dissemination that is similar to the systemic infection that is observed in humans infected with the related species *Yersinia pestis*—the causative agent of plague [148, 151]. *Y. pseudotuberculosis* is a potent activator of caspase-8-dependent apoptosis in macrophages [154, 173], and it was initially hypothesized that this induction of death mediated virulence in infected mice. However, strains of *Y. pseudotuberculosis* that induce less cell death *in vitro* have *increased* virulence *in vivo* [174], suggesting that caspase-8-mediated apoptosis is a host-derived mechanism of limiting virulence and dissemination of *Y. pseudotuberculosis*. These data suggest that caspase-8-medaited apoptosis is protective in the context of oral *Y. pseudotuberculosis* infection.

In an effort to determine the role of caspase-8-mediated apoptosis in immune cells during bacterial infection *in vivo* we generated bone marrow chimeras by transferring B6, *Ripk3*$^{-/-}$, and *Ripk3*$^{-/-}$*Casp8*$^{-/-}$ bone marrow progenitors into sublethally C57BL/6 mice. Consistent with the hypothesis that caspase-8-mediated apoptosis promotes host survival we found that mice deficient in both RIPK3 and caspase-8, but not RIPK3 alone, had an acute survival defect, and succumbed within 4-5 days of oral infection with *Y. pseudotuberculosis* [75]. This survival defect correlated to increased bacterial burdens, but we were surprised to discover that these mice had a marked impairment in cytokine production [75]. We went on to show that caspase-8-deficient cells have a cell-intrinsic defect in cytokine production *in vivo*, and caspase-8 was required for maximal cytokine secretion in macrophages stimulated with multiple TLR ligands [75]. Surprisingly, *Ripk3*$^{-/-}$*Casp8*$^{-/-}$ macrophages had consistent defects in the transcription of the pro-inflammatory genes *Il12b*, *Il1b*, *Il6* and *Tnf* among others [75].

Other groups have begun to identify a role for caspase-8 in inflammatory cytokine production as well. *Ripk3*$^{-/-}$*Casp8*$^{-/-}$ mice have reduced IL-1β production during oral infection with the gram-negative enteric pathogen *Citrobacter rodentium* [110]. Caspase-8 mediates pro-IL-1β expression during *in vitro* infection with *Salmonella typhimurium* [76], and mice infected with *Yersinia pestis* have defects in survival as well as inflammatory cytokine release [100]. The observed cytokine-regulatory role of caspase-8 is not restricted to bacterial pathogens as pro-IL-1β expression is decreased in the absence of caspase-8 during *in vitro* infection with the fungal pathogen *Candida albicans* [147]. However, the mechanism of caspase-8-mediated cytokine production in response to TLR activation remains unclear. Caspase-8 is known to promote NF-κB-mediated pro-survival gene expression in response to TNFR stimulation at the plasma membrane [84, 107]. However, the mechanism by which caspase-8 interacts with and signals from TLRs has yet to be defined. TLR4 and TLR3 can signal through the adaptor protein TRIF which is known to signal to caspase-8 in response to TLR4 activation [107], However, we also identified a role for caspase-8 in response to MyD88-dependent TLRs such as TLR9, and there is no reported interaction between caspase-8 and MyD88. Moreover, it is unclear if caspase-8 exerts it cytokine regulatory functions through the direct activation of NF-κB, indirect activation through a cytoplasmic intermediate, or another activation of transcription factor.

To address these questions we first identified the repertoire of genes regulated by caspase-8, and used promoter enrichment analysis to identify common transcription factor binding motifs. We found that many of these motifs were annotated for NF-κB family members, and that there was specifically impaired recruitment of c-Rel to the promoters of caspase-8-dependent genes upon TLR4 stimulation *in vitro*. Moreover, c-Rel

overexpression was sufficient to restore expression of IL-12 and IL-1β in caspase-8-deficient cells. We also demonstrated that caspase-8 exerts this function though differential IKK activation, and that the adaptor protein FADD was required for caspase-8-mediated cytokine production in response to both MyD88 and TRIF dependent TLRs. These studies provide insight into the divergent regulation of NF-κB proteins, and demonstrate an indirect role for caspsase-8-dependent regulation of NF-κB nuclear translocation.

2.3 Results

2.3.1 Caspase-8 regulates hundreds of inflammatory genes in response to TLR stimulation that are enriched for NF-κB binding motifs.

Caspase-8 deficient cells have defects in inflammatory gene transcription in response to both Myd88 and TRIF-dependent TLRs [75]. We sought to define the broad transcriptional program regulated by caspase-8 by measuring total RNA 2 and 6hrs post stimulation with the TLR4 and TLR9 agonists LPS and CpG respectively. We defined caspase-8 dependent genes as those that were differentially affected by the absence of caspase-8 (**Fig 2.1A**). Principle component analysis of our RNAseq data showed that samples segregated by the type of TLR ligand (PCA1) which accounted for 58% of the variance, and genotype was responsible for 8.8% of the variance (PCA2) (**Fig 2.1B**).We had observed a strong effect of caspase-8 on the transcription of *Il12b* and *Il1b* in response to LPS and CpG in previous *in vitro* experiments, but the repertoire of genes regulated by caspase-8 was much more extensive. Caspase-8 regulated 371 and 537 LPS inducible genes 2 and 6 hours post stimulation respectively (**Fig 2.1C**). 388 and 316 CpG-inducible genes were regulated 2 and 6 hours post stimulation respectively (**Fig 2.1C**). LPS is known to induce approximately 2000 genes in macrophages [63]; therefore, in our hands, caspase-8 regulates approximately 25% of all LPS-inducible genes after stimulation.

Heat map analysis of caspase-8-dependent genes showed that many of these genes were downregulated in the absence of caspase-8 at both 2 and 6hrs post LPS and CpG stimulation (**Fig 2.2A** and **Fig 2.2C**). We performed gene ontology analysis (GO) with the genes identified in each data set, and identified three distinct clusters of genes that were caspase-8 dependent in both the LPS and CpG conditions. These clusters are highlighted

on the heat maps, and further characterized in panels **2.2B** and **2.2D**. There was a defect in the induction of immune-regulated genes in response to both LPS and CpG in the absence of caspase-8. Interestingly, there was also a defect in cell cycle gene expression in both data sets as well. We performed promoter analysis to identify common transcription factor binding motifs in the promoters of caspase-8-dependent genes at 6 hours post LPS and CpG stimulation. We identified significant enrichment for NF-κB binding motifs which was concordant with the GO analysis identifying cytokine and immune response genes in the data set (**Fig 2.2E**). This data suggested that we would see a defect in overall NF-κB signaling in caspase-8-deficient macrophages stimulated with both LPS and CpG.

2.3.2 Caspase-8 promotes IKK phosphorylation in response to TLR stimulation.

Upon TNFR stimulation caspase-8 indirectly regulates NF-κB signaling by cleaving the K63 deubiquitinase CYLD to promote stable ubiquitination of RIPK1 [133]. Ubiquitinated RIPK1 serves as a scaffold for IKKα, IKKβ, and IKKγ and mediates pro-survival gene expression in response to TNF signaling[106]. However, it is unclear if caspase-8 signals to NF-κB in response to TLR activation. Two kinases proximal to TLR stimulation are TAK1—induced in response to MyD88-dependent TLRs—and TBK—induced in response to TRIF-dependent TLRs. Using immunoblotting we were unable to identify any differences in phosphorylation of TAK1 in response to both LPS and CpG (**Fig 2.3A**) and TBK1 in response to LPS (**Fig 2.3B**). However, in caspase-8-deficient cells we consistently saw a defect in phosphorylation of IKKα/IKKβ which is downstream of TAK1 activation (**Fig 2.3C**). We observed enrichment for AP-1 family member transcription factor binding motifs in our gene promoter analysis (data not shown). However, we did not observe a role

for caspase-8 in MAPK activation measured through immunoblotting for phosphorylated p38 (**Fig 2.3D**). We did not test other members of the MAPK signaling cascade comprehensively, and this is a potential area of further investigation. From these data we concluded that caspase-8 positively regulates IKK phosphorylation after TAK1 activation, placing caspase-8 upstream of IKK phosphorylation and downstream of TAK1 phosphorylation.

2.3.3 Caspase-8 promotes IκBε degradation in response to TLR4 stimulation.

NF-κB proteins are expressed in the cytoplasm as homo- and hetero-dimers [69]. IκB family members are bound to NF-κB proteins preventing their nuclear translocation until IκB proteins are phosphorylated and targeted for proteasomal degradation [175]. The observed requirement for caspase-8 in maximal IKKα/IKKβ phosphorylation suggested that caspase-8 would also indirectly regulate IκB protein degradation. We measured degradation of three IκB proteins (IκBα, IκBβ, and IκBε) in response to LPS and CpG. There was a slight, but consistent defect in IκBε degradation in response to LPS (**Fig 2.4A** and **Fig 2.4B**), and no defect in either IκBα or IκBβ (**Fig 2.4A** and **Fig 2.4C**). This was surprising given the profound defect we observed in IKKα/IKKβ phosphorylation in the absence of caspase-8. It is possible that IκBε is more sensitive to levels of phospho-IKK than other IκB proteins, or that the assays we used were not sensitive enough to measure small differences in degradation in the case of IκBα and IκBβ. The reported role for IκBε in the regulation of the NF-κB family members c-Rel and p65 [176] prompted us to investigate if there were measurable differences in nuclear translocation of these transcription factors in the absence of caspase-8.

2.3.4 Caspase-8 promotes c-Rel nuclear translocation in response to TLR4 and TLR9 stimulation.

Our previous observation that caspase-8 promoted IKK phosphorylation provoked the hypothesis that caspase-8 may exert its cytokine regulatory function through activation of the NF-κB family members c-Rel and p65. To test this hypothesis we used immunoblotting to measure the amount of c-Rel and p65 in nuclear enriched fractions of B6, *Ripk3*$^{-/-}$, and *Ripk3*$^{-/-}$*Casp8*$^{-/-}$ macrophages. We observed a defect in c-Rel translocation in response to both LPS and CpG—albeit slightly less so in response to CpG—and equivalent levels of p65 in nuclear fractions of B6 and *Ripk3*$^{-/-}$*Casp8*$^{-/-}$ macrophages (**Fig 2.5A** and **Fig 2.5B**). One possible interpretation of these data is that caspase-8 regulates overall c-Rel expression through its gene regulatory function, but we observed no difference in basal or inducible c-Rel levels in B6, *Ripk3*$^{-/-}$, and *Ripk3*$^{-/-}$*Casp8*$^{-/-}$ macrophages (**Fig 2.5C**). We then used confocal microscopy to directly quantify c-Rel nuclear translocation on a single-cell basis (**Fig 2.5E**). There was a consistent, and measurable defect in c-Rel translocation in *Ripk3*$^{-/-}$*Casp8*$^{-/-}$ macrophages stimulated with both LPS and CpG (**Fig 2.5D**, **Fig 2.5E**, and **Fig 2.5F**). We consistently observed that CpG stimulation revealed a smaller defect than LPS stimulation, which can likely be attributed to the relative intensity of both stimuli. LPS stimulation appears to induce a larger and more rapid response in wild type macrophages when compared to CpG stimulation; therefore, the magnitude of the response to LPS stimulation creates a larger dynamic range in which we can observe the effect of caspase-8 on the maximal response to TLR stimuli. These data suggested that caspase-8 regulates inflammatory gene expression through the

NF-κB family member c-Rel specifically. These data were surprising given that c-Rel is only reported to be required for *Il12b* expression in macrophages, and our transcriptional analysis implicated caspase-8 in the regulation of hundreds of LPS-and CpG-inducible genes. We next sought to determine if the defect in c-Rel translocation correlated with a measurable difference in recruitment to the promoters of caspase-8-depenent genes.

2.3.5 Caspase-8 promotes c-Rel recruitment to the promoters of caspase-8-dependent genes.

B6, *Ripk3*$^{-/-}$ and *Ripk3*$^{-/-}$*Casp8*$^{-/-}$ macrophages have equivalent levels of p65 bound to the promoters of several caspase-8-dependent genes (*Il12b*, *Il1b*, *Tnf*, and *Il6*) after LPS stimulation (**Fig 2.6A**). These data are concordant with our observation that caspase-8 has no impact on p65 nuclear translocation in response to TLR4 stimulation. We did observe a defect in c-Rel recruitment to the promoters of *Il12b*, *Il1b*, *Tnf*, and *Il6* after LPS stimulation (**Fig 2.6A**). Moreover, this defect occurred within 30 minutes LPS stimulation (**Fig 2.6B**). These data demonstrated that caspase-8 may mediate divergent regulation of p65 and c-Rel in response to TLR activation, as caspase-8 appears to be dispensable for p65 translocation, but not for c-Rel translocation. Given previous reports identifying a limited role for c-Rel in *Il12b* expression we next tested the requirement for c-Rel in transcription of other caspase-8-dependent genes.

2.3.6 c-Rel regulates several caspase-8-dependent genes in response to TLR stimulation.

Utilizing *Rel*$^{-/-}$ macrophages we sought to assess the role for c-Rel in the regulation of caspase-8-dependent genes. The expression of several inflammatory genes in addition

to *Il12b* were decreased in *Rel*$^{-/-}$ macrophages stimulated with both LPS and CpG (**Fig 2.7A**). This provided evidence that c-Rel was required for the expression of other inflammatory genes in addition to *Il12b*. We also observed a decrease in pro-IL-1β expression in the absence of c-Rel in response to both LPS and CpG which could be measured on a per cell basis (**Fig 2.7B**) as well using a bulk assay (**Fig 2.7C**). Surprisingly, we observed an increase in IL-6 secretion in *Rel*$^{-/-}$ macrophages stimulated with LPS despite the decrease we observed transcriptionally, and we observed no difference in TNF secretion between B6 and *Rel*$^{-/-}$ macrophages (**Fig 2.7D**). This suggested that although c-Rel regulates gene expression of several caspase-8-dependent genes there may be a threshold of transcript that is sufficient to mediate wild-type levels of cytokine secretion. There was a role for c-Rel in both the expression of *Il1b* and production of pro-IL-1β, which had not been previously identified. These data suggested that we could bypass the requirement for caspase-8 in IL-12p40 and pro-IL-1β production through the expression of c-Rel in caspase-8-deficient macrophages.

2.3.7 c-Rel expression restores IL-12p40 and pro-IL-1β expression in caspase-8-deficient macrophages.

We expressed c-Rel containing an IRES-GFP in macrophages lacking caspase-8. The inefficiency of this transfection created an internally controlled experiment by which we could measure the impact of c-Rel expression on a per-cell basis in cells expressing GFP compared to those that were GFP negative. Cells that are successfully transfected can be identified through GFP expression using flow cytometry (**Fig 2.8A**). After 6 hours the plasmid is expressed in approximately 30% of cells (**Fig 2.8A** and **Fig 2.8B**). We then used

intracellular cytokine staining with this mixed population of GFP^+ and GFP^- cells to determine if cell-intrinsic expression of c-Rel restored IL-12p40 and pro-IL-1β in individual cells. We found that expression of c-Rel restored IL-12p40 expression in *Ripk3*$^{-/-}$*Casp8*$^{-/-}$ macrophages in the absence of stimulation as well as in response to LPS and CpG (**Fig 2.9A**). The expression of IL-12p40 in the absence of TLR activation may be due to the lack of co-expression of the negative regulator IκBε, meaning all plasmid-derived c-Rel is able to translocate directly into the nucleus. Interestingly, only LPS stimulation coupled with c-Rel expression was sufficient to restore pro-IL-1β expression in the absence of caspase-8 (**Fig 2.9B**). These data suggest that another transcription factor synergizes with c-Rel to induce *Il1b* expression during CpG stimulation. It is also possible that a larger amount of c-Rel is required for induction of pro-IL-1β which is supported in part by the pronounced defect in pro-IL-1β in *Rel*$^{-/-}$ macrophages. The increase in IL-12p40 and pro-IL-1β observed in *Ripk3*$^{-/-}$*Casp8*$^{-/-}$ macrophages transfected with c-Rel was equivalent to expression observed in *Ripk3*$^{-/-}$ macrophages transfected with empty plasmid (**Fig 2.10A** and **Fig 2.10B**). This indicated that c-Rel expression in caspase-8-deficient cells was sufficient to restore IL-12p40 and pro-IL-1β expression to wild-type levels. These data collectively demonstrate that caspase-8 regulates *Il12b* and *Il1b* through the NF-κB family member c-Rel. This regulatory function seemed to be mediated indirectly through caspase-8-dependent activation of IKK. We next sought to define the adaptor proteins that coupled TLR activation to caspase-8.

2.3.8 Caspase-8 is coupled to TLR activation through the adaptor protein FADD.

The adaptor protein FADD is known to promote recruitment of caspase-8 to TNFR [84] which led us to hypothesize that it might play a similar role in response to TLR activation. Single ablation of FADD leads to the induction of programed necrosis in response to macrophage stimulation, but these cells can be rescued when proteins required for programmed necrosis are also ablated [160]. Therefore, we tested the role of the adaptor protein FADD in promoting IKK activation in response to TLR4 and TLR9 stimulation using *Fadd*$^{-/-}$*Mlkl*$^{-/-}$ macrophages which cannot undergo programmed necrosis. We observed a defect in IKKα/IKKβ phosphorylation in *Fadd*$^{-/-}$*Mlkl*$^{-/-}$ macrophages in response to both LPS and CpG stimulation (**Fig 2.11A** and **Fig 2.11B**). FADD-deficiency also leads to a decrease in IκBε degradation in response to both LPS and CpG (**Figure 2.11C**). *Fadd*$^{-/-}$*Mlkl*$^{-/-}$ macrophages had a decrease in the transcription of *Il12b, Il1b,* and *Il1a* (**Fig 2.11D**) as well as the secretion of IL-12p40, TNF and IL-6 (**Fig 2.11E**). These data suggest that caspase-8 may be coupled to the activation of both MyD88 and TRIF dependent TLRs through FADD, although, the effects we observed in the absence of caspase-8 are even more stark in the absence of FADD. It is possible that FADD interacts with other signaling molecules that mediate inflammatory gene expression in addition to caspase-8. Moreover, these data are also preliminary as the experiments depicted in panels **2.11C** and **2.11D** have only been performed once due to reagent limitations. However, the consistent impact of FADD on cytokine secretion and IKK phosphorylation suggests that this adaptor may be the mechanism by which caspase-8 is activated in response to TLR stimulation, although further studies are required.

2.4 Discussion

Previous work has demonstrated a critical role for caspase-8 in apoptosis, programmed necrosis, and cytokine expression [76, 102, 105, 125]. Here we define a mechanism by which caspase-8 regulates *Il1b* and *Il12b* via the NF-κB family member c-Rel (**Fig 2.12**). Caspase-8 promotes IKK phosphorylation which in turn induces IκBε degradation, c-Rel translocation, and c-Rel recruitment to the promoters of *Il12b* and *Il1b*. Despite our observation that caspase-8 regulates hundreds of LPS- and CpG-inducible genes, it appears that c-Rel is only required for expression of *Il12b* and *Il1b*. Therefore, there are likely other mechanisms of caspase-8-dependent inflammatory gene regulation that we have yet to identify. LPS and CpG promote expression of both overlapping, and distinct subsets, of caspase-8-depenent genes, suggesting that there is likely there is a common signaling mechanism for caspase-8 in response to both TLRs as well as TLR4 and TLR9 specific regulation that is also caspase-8 dependent.

Caspase-8-mediated c-Rel translocation appears to be specifically dependent on the sensitivity of IκBε to lower levels of IKK phosphorylation. Despite the strong decrease we observed in IKK phosphorylation, in the absence of caspase-8, IκBα and IκBβ degradation are indistinguishable from that observed in wild-type macrophages (**Fig 2.4**). There are studies demonstrating divergent temporal regulation of IκB proteins over the course of cellular activation [59], but it appears another mechanism of regulation may be differential sensitivity upstream kinases. The role of caspase-8 in the divergent regulation of p65 and c-Rel was also surprising. p65 and c-Rel are largely thought to be redundant during TLR activation in macrophages apart from the requirement for c-Rel in *Il12b* transcription [71]. However, our data suggest that c-Rel plays an important role in the expression of both

IL-12p40 and IL-1 family cytokines, offering a potential explanation for recent studies that have observed a role for caspase-8 in inflammasome priming via the induction of pro-IL-1β [76, 77, 111].

The mechanisms that govern disparate regulation of p65 and c-Rel in the cytoplasm have yet to be defined. Recent work has identified a novel cellular nucleic acid binding protein (CNBP) that is required for c-Rel translocation during TLR activation, but dispensable for p65 [24]. We did not observe a defect in CNBP enrichment in nuclear fractions of *Ripk3*$^{-/-}$*Casp8*$^{-/-}$ macrophages (data not shown), but our data suggest that caspase-8 may be another cytoplasmic factor that bifurcates p65 and c-Rel activation. We observed that c-Rel expression was sufficient to restore IL-12p40 production to wild-type levels in untreated as well as LPS and CpG stimulated cells (**Fig 2.9A** and **Fig 2.10A**); however, only LPS stimulation restored pro-IL-1β production (**Fig 2.9B**). This was surprising given the defect in pro-IL-1β production in *Rel*$^{-/-}$ macrophages stimulated with both LPS and CpG (**Fig 2.7B**). It is possible that there was insufficient c-Rel to restore pro-IL-1β production, or perhaps there is another regulatory factor that synergizes with c-Rel in this context.

Our preliminary data suggest a role for the adaptor protein FADD in activation of caspase-8 in response to TLR stimulation. This data is intriguing given that FADD is known to collaborate with caspase-8 during activation of death receptors [89, 112, 177]. FADD appears to promote IKK phosphorylation in response to TRIF- and MyD88-dependent TLRs which was surprising given recent work showing that MyD88 is dispensable for programed necrosis induced in response to TLR4 stimulation and caspase-8 inhibition [107]. However, it is possible that MyD88 interacts directly with FADD in the

context of TLR signaling under pro-survival conditions. The protein structure of FADD may shed light on the mechanism of collaboration between TRIF, MyD88, caspase-8 and FADD. FADD contains a death effector domain which can recruit caspase-8 via homotypic interactions. TRIF contains a region annotated for "sufficient to induce apoptosis" suggesting this might promote an interaction with FADD. Finally, MyD88 contains a death domain that could mediate a direct interaction with the death domain of FADD. Therefore, FADD may facilitate caspase-8 recruitment downstream of death receptors as well as TLRs. However, more mechanistic investigations are required to define the role of FADD in caspase-8-mediated cytokine expression.

In this chapter we have defined a mechanism for the regulation of *Il12b* and *Il1b* transcription by caspase-8. In **Chapter 3** we will interrogate the role of caspase-8 enzymatic activity in this system.

2.5 Figures

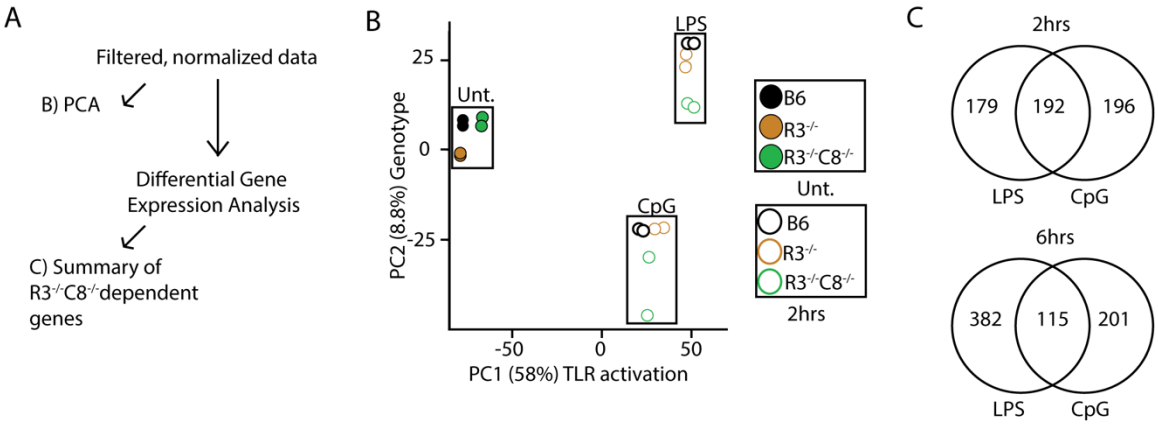

Fig 2.1. Caspase-8 regulates hundreds of genes in response to TLR stimulation.

(A) Diagram of RNAseq analysis experimental design.

(B) Principal component analysis of transcriptional profiling data from untreated or 2hrs post-LPS- or CpG-treatment of B6, *Ripk3*$^{-/-}$, and *Ripk3*$^{-/-}$*Casp8*$^{-/-}$ BMDMs.

(C) Total number of caspase-8-dependent genes at 2 and 6 hours post LPS or CpG stimulation. Venn diagrams demonstrating the overlap of caspase-8-dependent genes in both the LPS- and CpG-treated BMDMs.

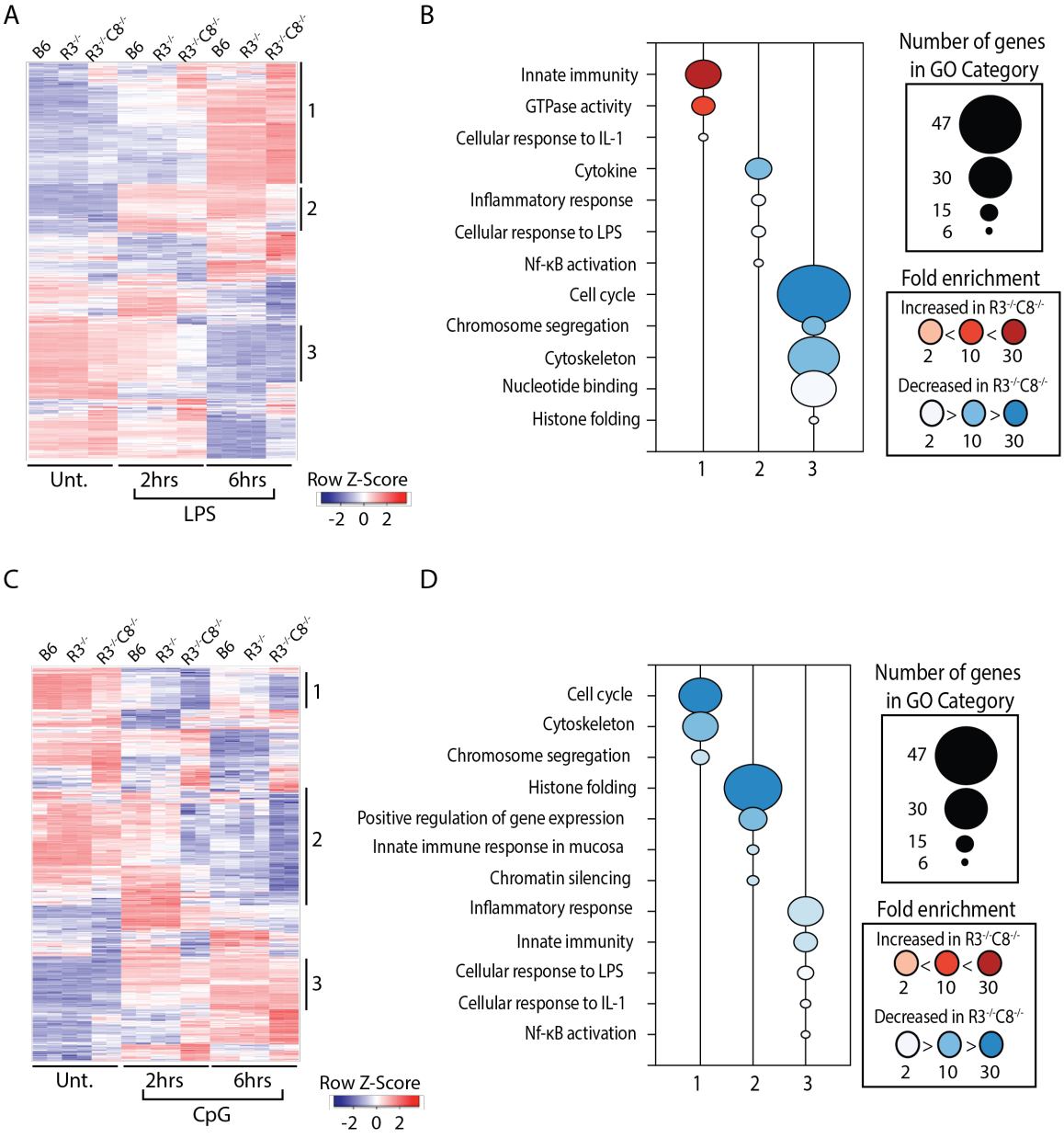

E

Motif name	Stim	% R3$^{-/-}$C8$^{-/-}$ genes with motif	Background sequences with motif	p-value	q-value
NF-κB (ThioMac LPS Expression)	LPS	7.68%	4.20%	1e^{-3}	0.0162
NF-κB (ThioMac LPS Expression)	CpG	42.8%	34.6%	1e^{-2}	0.2609
NF-κB (p65 ChIP Seq)	CpG	8.22%	4.16%	1e^{-2}	0.2897

Fig 2.2 Caspase-8 regulates inflammatory genes that are enriched for NF-κB binding motifs.

(A, C) Heat maps of the global transcriptional response of B6, *Ripk3*$^{-/-}$, and *Ripk3*$^{-/-}$*Casp8*$^{-/-}$ BMDMs 2 or 6 hours post stimulation with either LPS **(A)** or CpG **(C)**. Gene clusters containing caspase-8-dependent genes following LPS or CpG stimulation are numbered and indicated with a sidebar to the right of each heat map.

(B, D) Bubble plot representation of gene ontology enrichment analyses on caspase-8-dependent gene clusters shown in **(A)** and **(C)**. Bubble color indicates the degree to which genes associated with each term were upregulated (red) or downregulated (blue). Bubble size represents the number of genes within a cluster that were associated with each term.

(E) HOMER gene promoter analysis of caspase-8-dependent genes 6 hours post LPS or CpG stimulation.

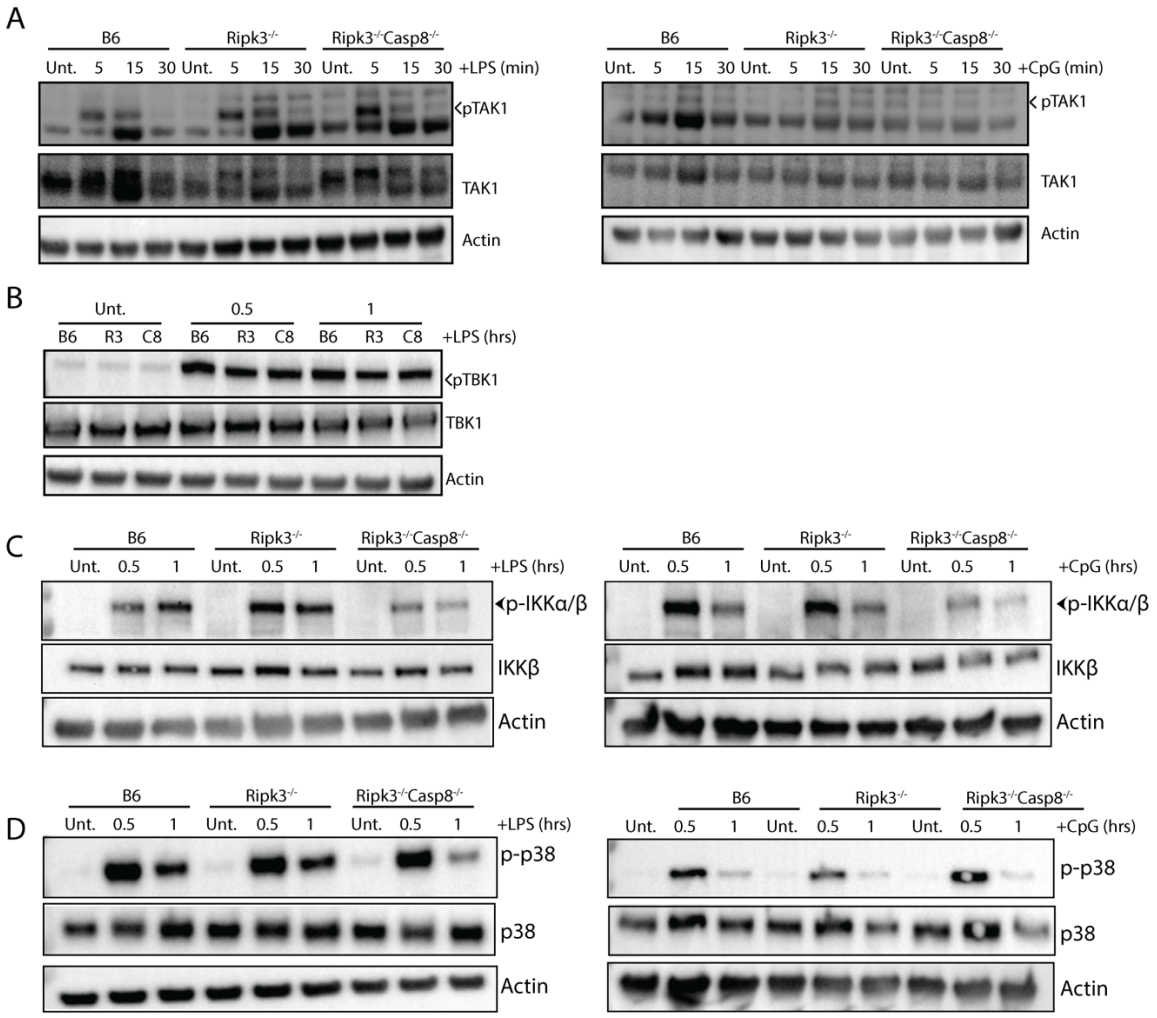

Fig 2.3 IKK phosphorylation is caspase-8-dependent in response to TLR stimulation.

(A) Immunoblots of phospho-TAK1 and total TAK1 in B6, *Ripk3*$^{-/-}$, and *Ripk3*$^{-/-}$*Casp8*$^{-/-}$ BMDMs following stimulation with LPS or CpG for indicated times.

(B) Immunoblots of phospho-TBK1 and total TBK1 in B6, *Ripk3*$^{-/-}$, and *Ripk3*$^{-/-}$*Casp8*$^{-/-}$ BMDMs following stimulation with LPS for indicated times.

(C) Immunoblots of phospho-IKKα/β and total IKKβ in B6, *Ripk3*$^{-/-}$, and *Ripk3*$^{-/-}$*Casp8*$^{-/-}$ BMDMs following stimulation with LPS or CpG for indicated times.

Fig 2.3 Continued: (D) Immunoblots of phospho-p38 and total p38 in B6, *Ripk3*$^{-/-}$, and *Ripk3*$^{-/-}$*Casp8*$^{-/-}$ BMDMs following stimulation with LPS or CpG for indicated times. **(A-B)** Representative of two independent experiments. **(C-D)** Representative of three independent experiments.

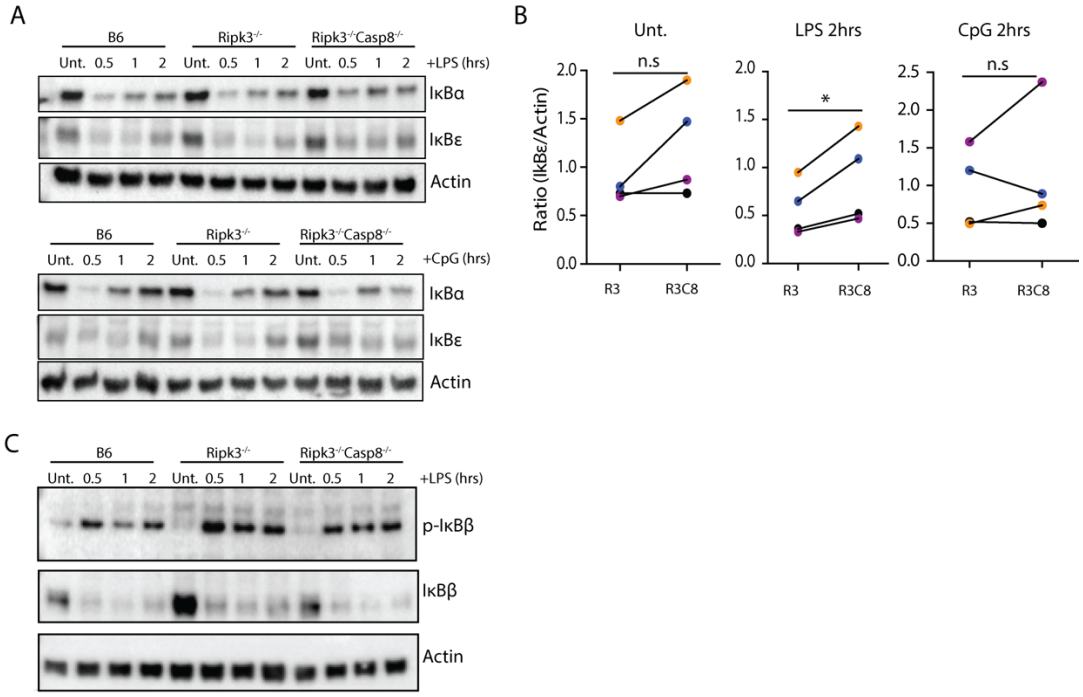

Fig 2.4 TLR4-induced IκBε degradation is impaired in the absence of caspase-8.

(A) Immunoblots of IkBε and IkBα in B6, *Ripk3*$^{-/-}$, and *Ripk3*$^{-/-}$*Casp8*$^{-/-}$ BMDMs stimulated with LPS or CpG.

(B) Quantification of immunoblots of IkBε in *Ripk3*$^{-/-}$ and *Ripk3*$^{-/-}$*Casp8*$^{-/-}$ BMDMs stimulated with LPS or CpG for 2hrs.

(C) Immunoblots of IkBβ in B6, *Ripk3*$^{-/-}$, and *Ripk3*$^{-/-}$*Casp8*$^{-/-}$ BMDMs stimulated with LPS.

Student's two-tailed paired t-test, * $p<0.05$. Data are representative of at least three independent experiments.

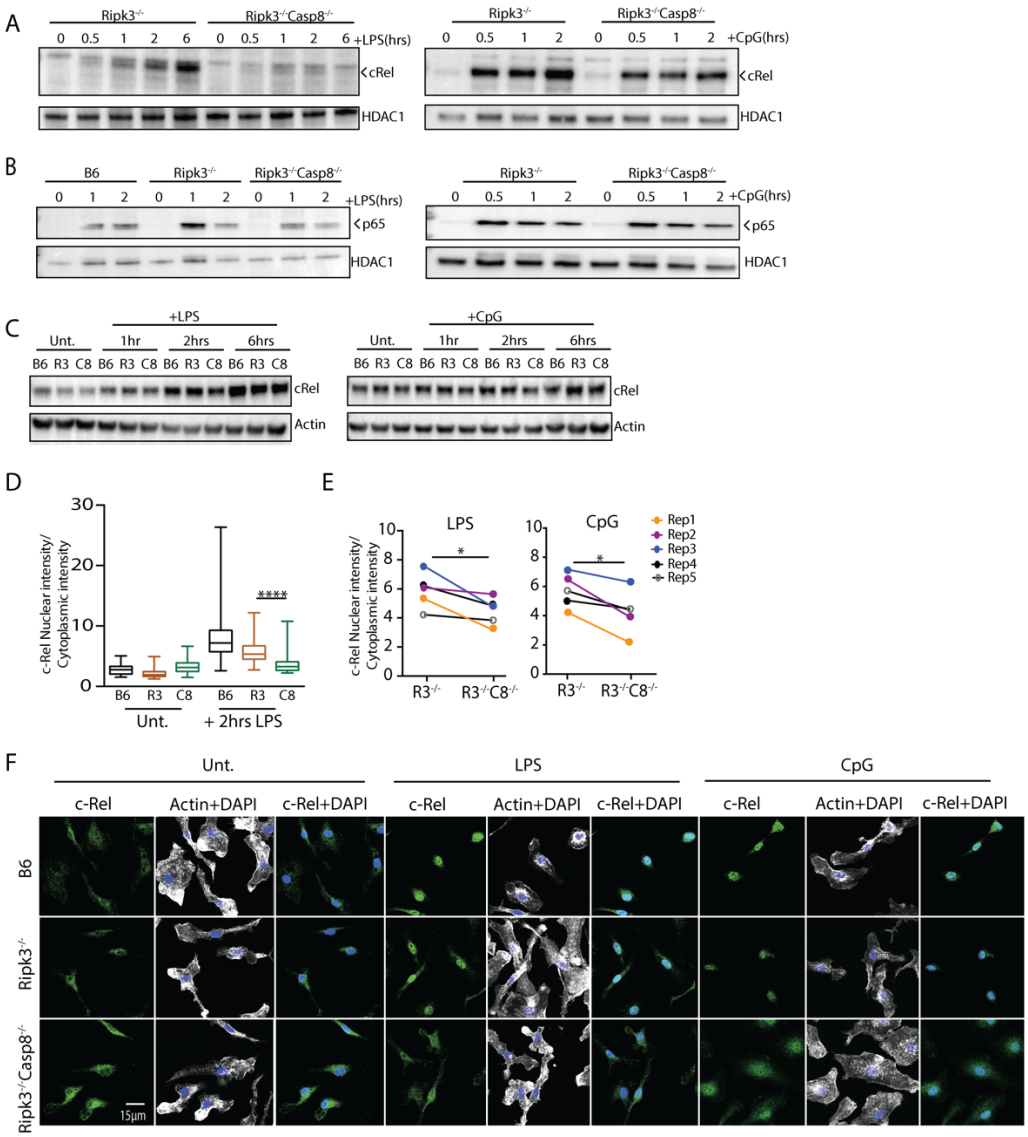

Fig 2.5 Caspase-8 promotes c-Rel translocation independently of p65.

(A) Immunoblots of c-Rel in nuclear fractions of *Ripk3*$^{-/-}$ and *Ripk3*$^{-/-}$*Casp8*$^{-/-}$ BMDMs following LPS or CpG stimulation for indicated times.

(B) Immunoblots of p65 in nuclear fractions of B6, *Ripk3*$^{-/-}$ and *Ripk3*$^{-/-}$*Casp8*$^{-/-}$ BMDMs following LPS or CpG stimulation for indicated times.

Fig 2.5 Continued: (C) Total c-Rel expression in B6, *Ripk3*$^{-/-}$, and *Ripk3*$^{-/-}$*Casp8*$^{-/-}$ BMDMs stimulated with LPS or CpG for the indicated times.

(D) Quantification of the ratio of mean fluorescence intensity of nuclear:cytoplasmic c-Rel in *Ripk3*$^{-/-}$ and *Ripk3*$^{-/-}$*Casp8*$^{-/-}$ BMDMs stimulated with LPS; box plots represent 60-150 individual cells per condition, Box plots indicate the median, upper and lower quartiles, and upper and lower extremes of the data.

(E) Quantification of the ratio of mean fluorescence intensity of nuclear:cytoplasmic c-Rel in *Ripk3*$^{-/-}$ and *Ripk3*$^{-/-}$*Casp8*$^{-/-}$ BMDMs stimulated with LPS or CpG; each datapoint indicates the mean of an individual experiment; Student's two-tailed paired t-test, * $p<0.05$.

(F) Representative confocal images of experiment quantified in **(D, E)**; B6, *Ripk3*$^{-/-}$ and *Ripk3*$^{-/-}$*Casp8*$^{-/-}$ BMDMs stimulated with LPS or CpG for 2hrs; c-Rel, actin and DAPI pseudo-colored in green, white and blue respectively.

Student's two-tailed unpaired t-test (n.s. not significant, **** $p<0.0001$). All data representative of at least three independent experiments.

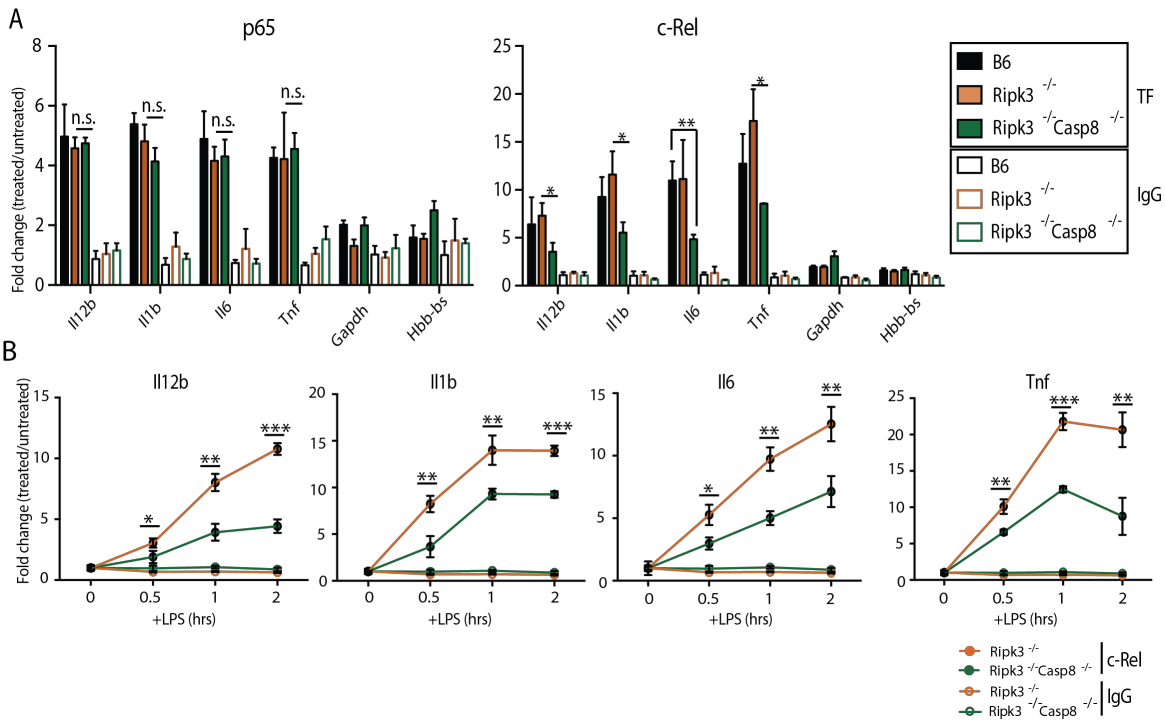

Fig 2.6 Caspase-8 promotes c-Rel recruitment to the promoters of caspase-8-dependent genes.

(A) ChIP-qPCR measuring fold-enrichment of p65 and c-Rel at the promoters of *Il12b, Il1b, Il6*, and *Tnf* 2hrs post LPS stimulation.

(B) Fold-enrichment of c-Rel at indicated cytokine gene promoters in *Ripk3*$^{-/-}$ and *Ripk3*$^{-/-}$*Casp8*$^{-/-}$ BMDMs following LPS treatment was determined by ChIP-qPCR at indicated times post-stimulation.

Student's two-tailed unpaired t-test (n.s. not significant, * $p<0.05$, ** $p<0.01$, *** $p<0.001$, **** $p<0.0001$). Error bars indicate ± SEM of triplicates. All data representative of at least three independent experiments.

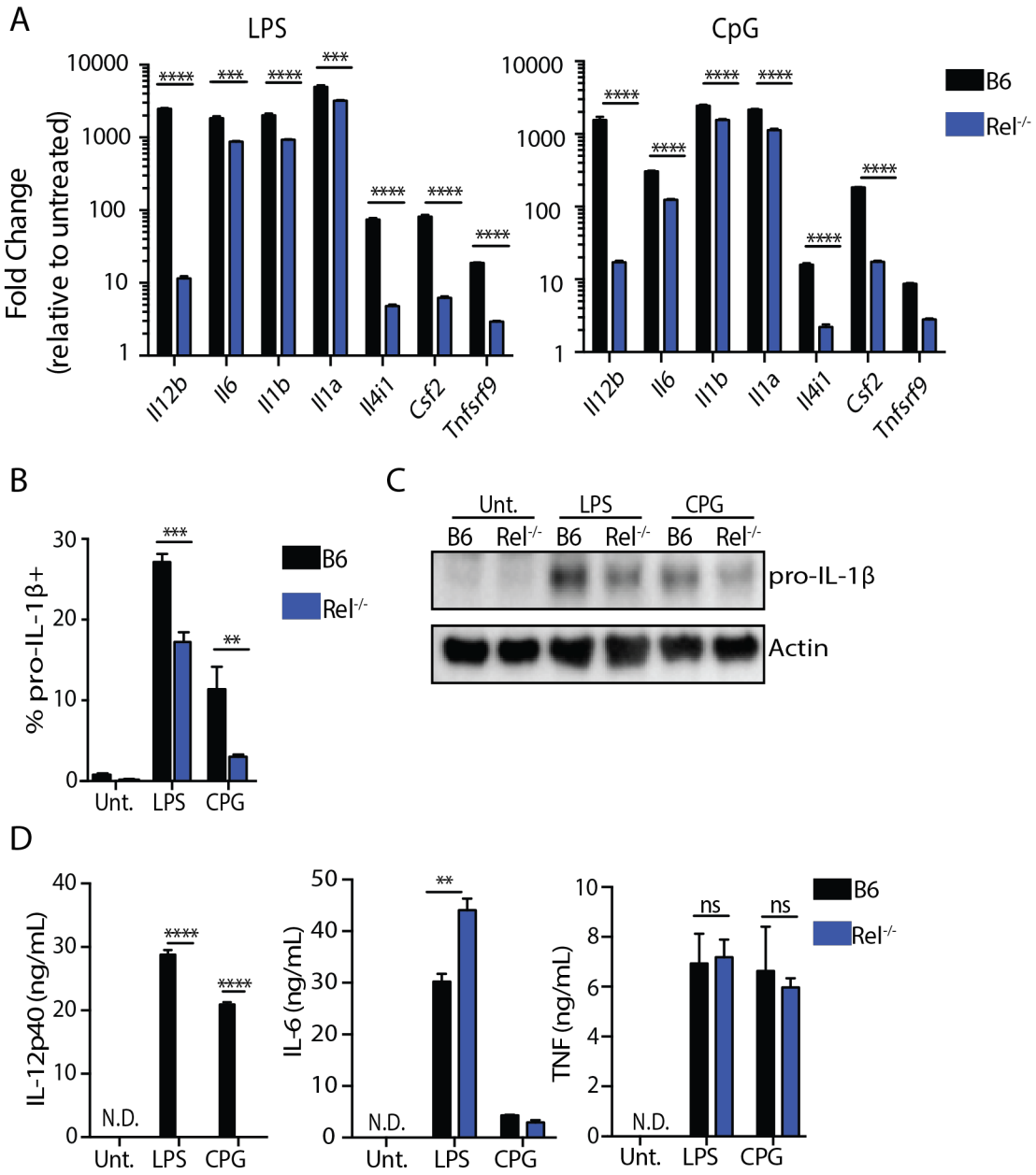

Fig 2.7 c-Rel regulates both IL-12p40 and pro-IL-1β expression in response to TLR activation.

(A) Fold-change in indicated inflammatory response genes in B6 and *Rel*$^{-/-}$ BMDMs 2hrs post-stimulation with LPS or CpG, as indicated.

(B) Flow-cytometry quantification and **(C)** immunoblot of intracellular pro-IL-1β expression in B6 and *Rel*$^{-/-}$ BMDMs stimulated with LPS or CpG for 6hrs.

Fig 2.7 Continued: (D) ELISA measurement of secreted IL-12p40, IL-6, and TNF in B6 and *Rel*$^{-/-}$ BMDMs following stimulation with LPS or CpG for 6hrs.

Student's two-tailed unpaired t-test (n.s. not significant, ** $p<0.01$, *** $p<0.001$, **** $p<0.0001$). Error bars indicate ± SEM of triplicates. All data representative of at least three independent experiments.

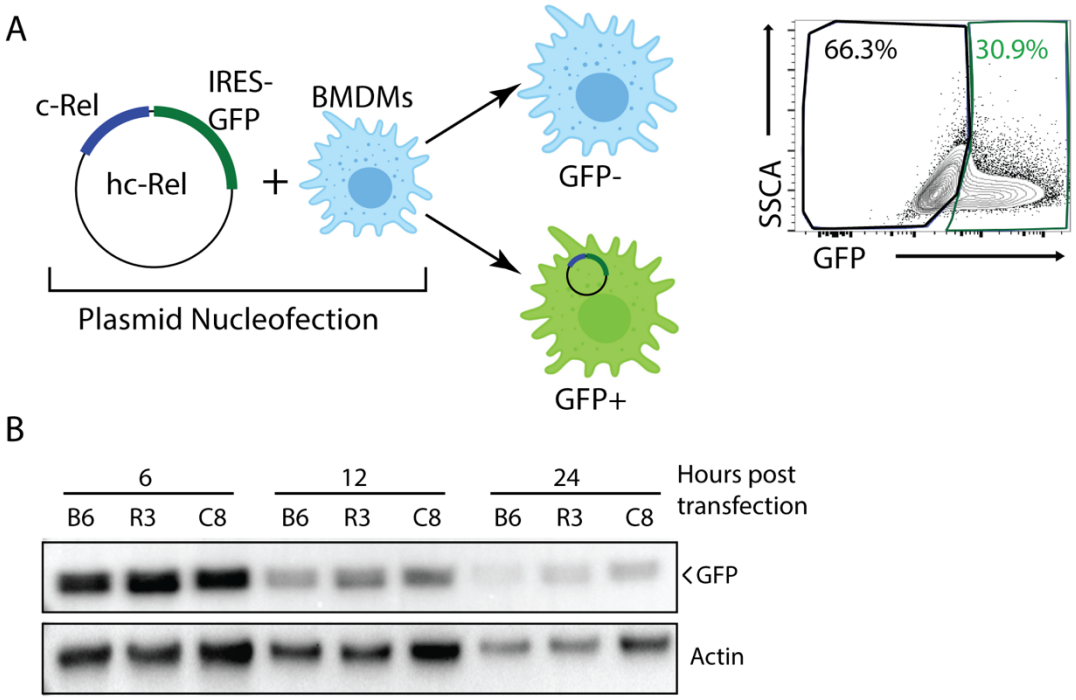

Fig 2.8 hc-Rel-IRES-GFP is expressed robustly in primary macrophages.

(A) Transfection schematic diagram indicating nucleofection of hc-Rel-IRES-GFP plasmid into primary BMDMs, and representative flow cytometry data indicating transfection efficiency measured 6hrs post-transfection.

(B) GFP expression was assayed in B6, *Ripk3*$^{-/-}$ and *Ripk3*$^{-/-}$*Casp8*$^{-/-}$ BMDMs 6, 12 and 24hrs post-transfection.

Data are representative of three independent experiments.

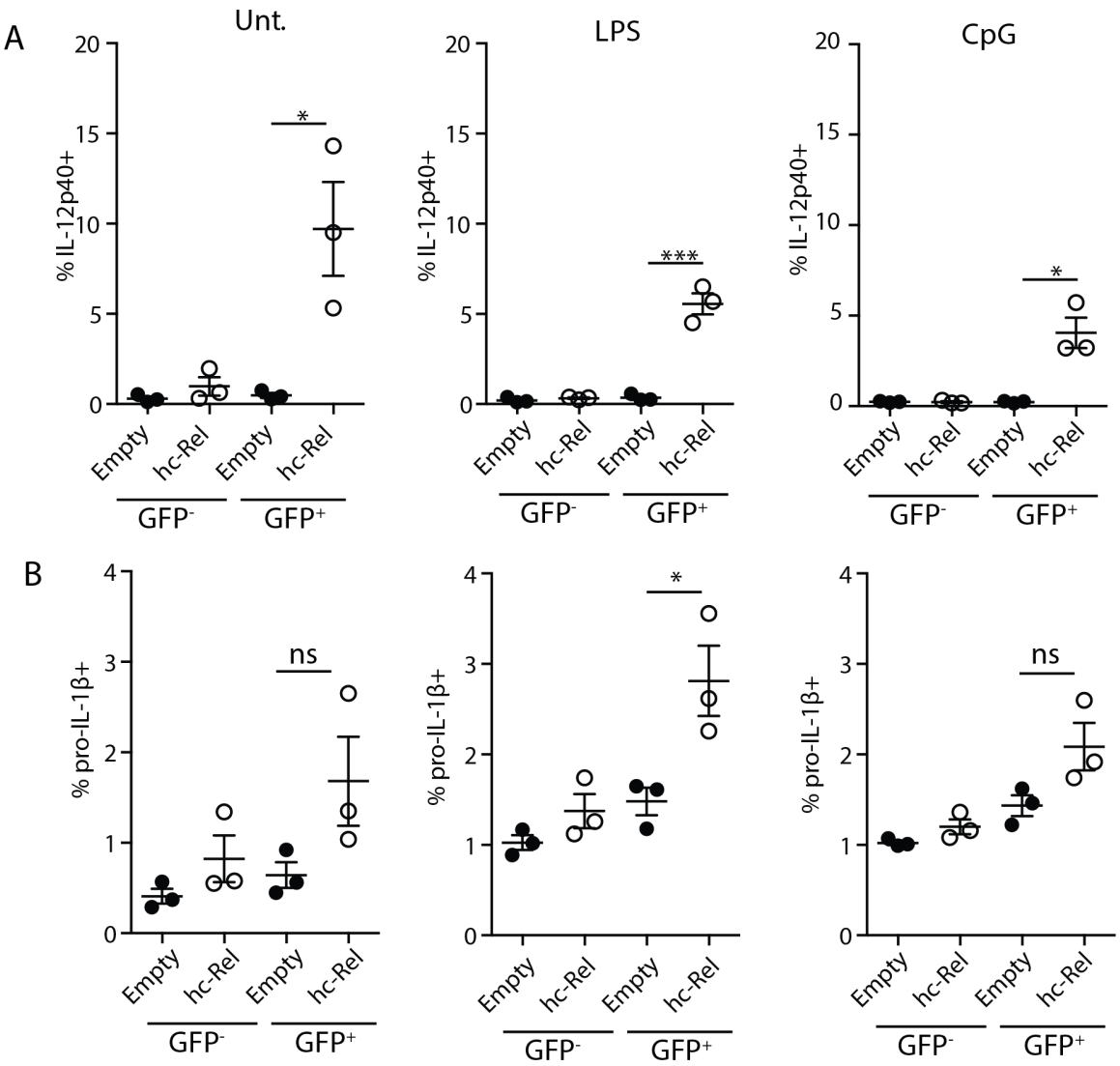

Fig 2.9 hc-Rel expression restores both IL-12p40 and pro-IL-1β production in the absence of caspase-8.

(A) Flow cytometry of intracellular IL-12p40 and **(B)** pro-IL-1β in *Ripk3*$^{-/-}$*Casp8*$^{-/-}$ BMDMs transfected with an IRES-GFP-expressing empty vector or hc-Rel-IRES-GFP-expressing plasmid and stimulated with LPS or CpG for 4hrs.

Fig 2.9 Continued: Student's two-tailed unpaired t-test (n.s. not significant, * $p<0.05$, *** $p<0.001$). Error bars indicate ± SEM of triplicates. All data representative of at least three independent experiments.

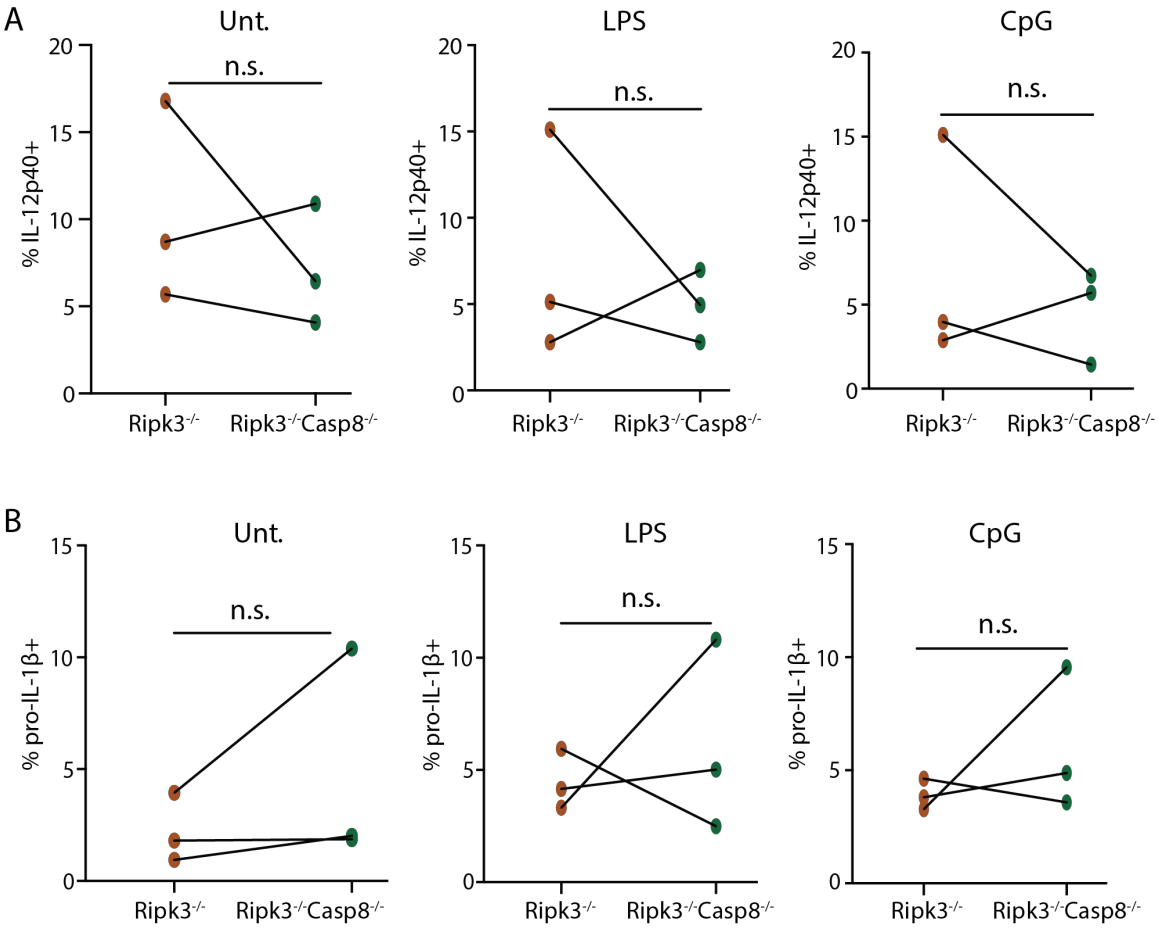

Fig 2.10 In the absence of caspase-8 hc-Rel expression restores both IL-12p40 and pro-IL-1β to levels observed in *Ripk3*$^{-/-}$ cells.

(A) Frequency of intracellular IL-12p40^{+} or **(B)** pro-IL-1β^{+} *Ripk3*$^{-/-}$ or *Ripk3*$^{-/-}$*Casp8*$^{-/-}$ BMDMs transfected with hc-Rel-IRES-GFP-expressing plasmid and stimulated with LPS or CpG for 4hrs.

Each data point represents the mean frequency of positive cells within an individual experiment. Lines link genotypes within the same experiment Student's paired two-tailed t-test (n.s. not significant).

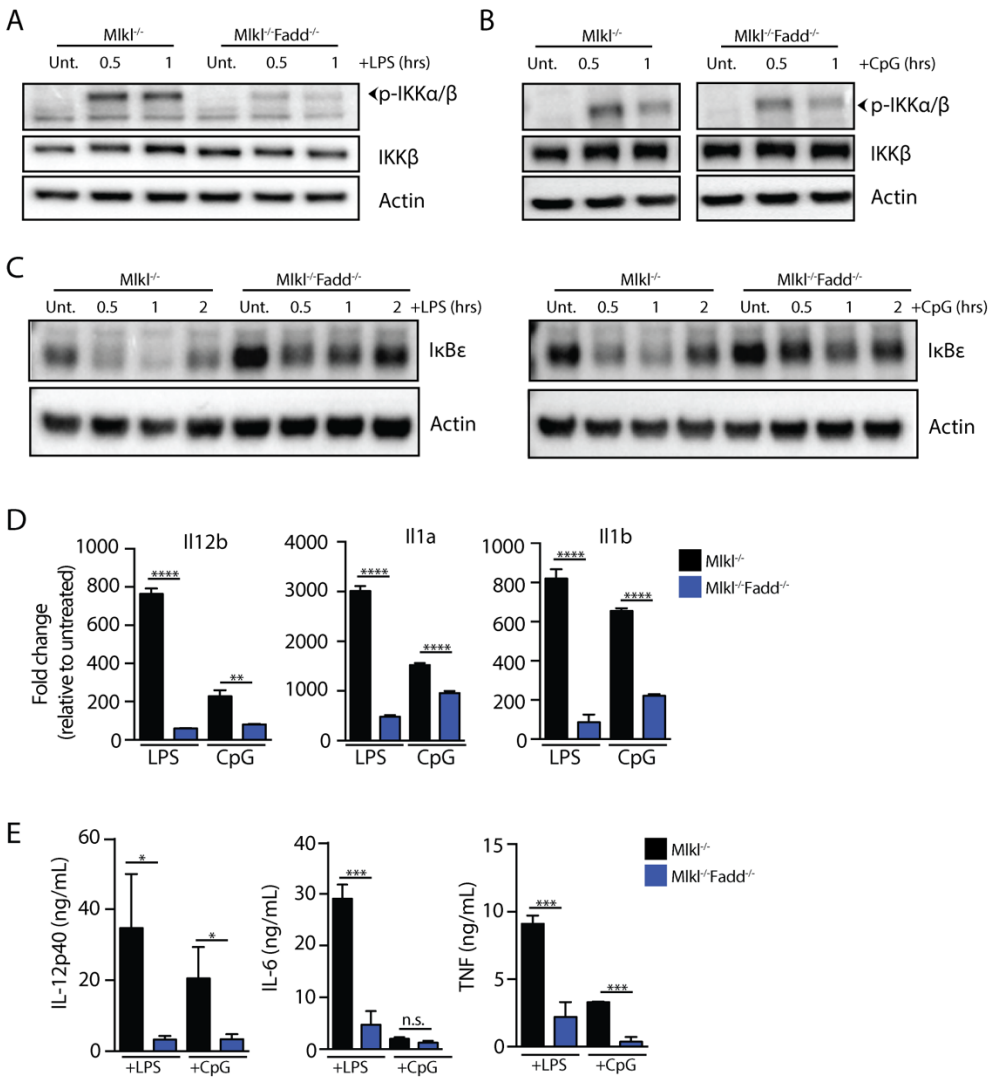

Fig 2.11 FADD promotes inflammatory gene expression and IKK phosphorylation in response to TLR activation.

(A, B) Immunoblot of phospho-IKKα/β and total IKKβ in *Mlkl*$^{-/-}$ and *Mlkl*$^{-/-}$*Fadd*$^{-/-}$ BMDMs stimulated with LPS **(A)** and CpG **(B)** for indicated times.

(C) Immunoblots of IkBε in *Mlkl*$^{-/-}$ and *Mlkl*$^{-/-}$*Fadd*$^{-/-}$ BMDMs stimulated with LPS or CpG for the indicated times.

Fig 2.11 Continued: (D) RT-qPCR of caspase-8-dependent genes in *Mlkl*$^{-/-}$ and *Mlkl*$^{-/-}$*Fadd*$^{-/-}$ BMDMs stimulated with LPS or CpG for 2hrs.

(E) ELISA of secreted IL-12p40, IL-6, and TNF in *Mlkl*$^{-/-}$ and *Mlkl*$^{-/-}$*Fadd*$^{-/-}$ BMDMs stimulated with LPS or CpG for 6hrs.

Experiments representative of one (**C, D**) or two (**A, B, E**) independent experiments. Error bars indicate ± SEM of triplicates. Student's two-tailed unpaired t-test (n.s. not significant, * $p<0.05$, ** $p<0.01$, *** $p<0.001$, **** $p<0.0001$).

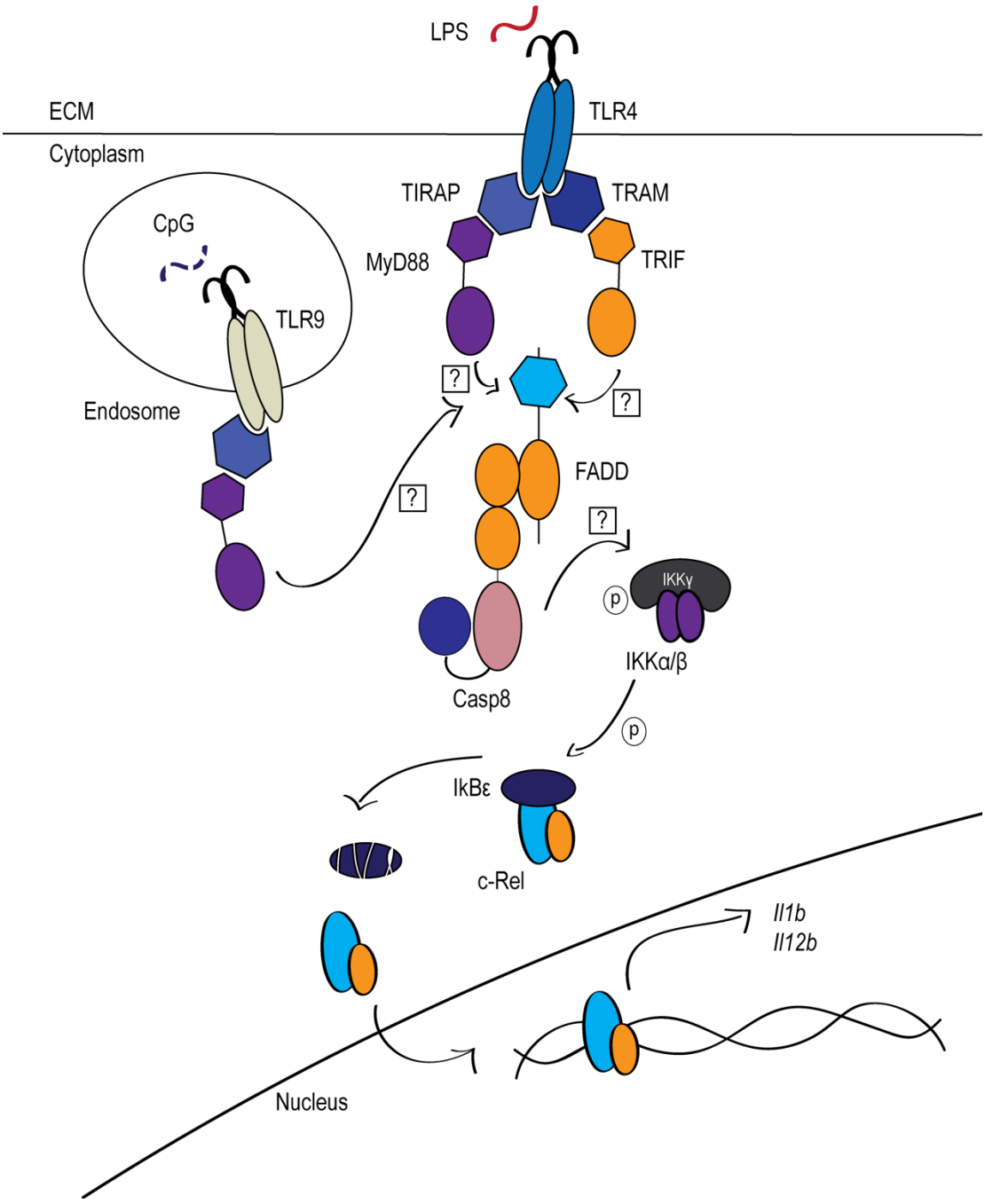

Fig 2.12 Graphical abstract and future directions: Caspase-8 promotes *Il12b* and *Il1b* expression through c-Rel.

CHAPTER 3: Caspase-8 enzymatic activity promotes inflammatory gene expression in macrophages.

3.1 Abstract

Caspase-8 enzymatic activity is required for its apoptotic function and for the repression of programmed necrosis; however, it is unclear if this activity is required for its role in cell-intrinsic inflammatory gene expression. Others have shown that ablation of caspsase-8 expression impairs inflammatory gene expression and inflammasome priming. Data from our lab suggest a role for caspase-8 enzymatic activity in macrophage TLR activation, but others have found that caspase-8 scaffolding is sufficient to mediate gene expression in response to TRAIL stimulation. Using both genetic and chemical approaches we identify a role for both caspase-8 enzymatic and non-enzymatic activity in response to TLR activation. We show that caspase-8 is enzymatically active in response to both TLR4 and TLR9 stimulation, and that inhibition of caspase-8 reduced the production of IL-12p40 and IL-1β. We also demonstrate that caspase-8 enzymatic activity promotes IKK phosphorylation and c-Rel nuclear translocation—one mechanism that we have identified for caspase-8-mediated inflammatory gene regulation. These experiments demonstrate a role for the enzymatic activity of caspase-8 in inflammatory gene expression in response to TLR activation, adding to our understanding of the diverse functions of caspase-8 in macrophages.

3.2 Introduction

Caspase-8 regulates two forms of cell death: apoptosis [102] and programmed necrosis [133]. In the context of apoptotic stimuli such as TNF or FasL caspase-8 is recruited to the death inducing signaling complexes (DISC) via its death effector domain [82, 85]. Apoptotic signals induce caspase-8 homodimerization, whereby each monomer undergoes auto-processing, and forms two catalytic sites that mediate cleavage of its apoptotic substrates [79, 80, 113]. Caspase-8 is also enzymatically active in heterodimers formed with a homologous protein cFLIP, as this enzymatic activity is required for the inhibition of programmed necrosis. Caspase-8 enzymatic activity under pro-survival and pro-apoptotic conditions is required for the cleavage of substrates that mediate programmed necrosis such as the K63 linear deubiquitinase CYLD [105]. It is hypothesized that caspase-8/cFLIP heterodimers are constitutively present under pro-survival conditions, and that caspase-8 monomers do not form stable catalytic sites without the presence of cFLIP [105]. Under pro-survival conditions caspase-8/cFLIP heterodimers mediate cleavage of CYLD, this cleavage promotes ubiquitination of RIPK1 (Receptor Interacting Serine/Threonine Kinase 1) which serves as a scaffold for the recruitment of IKKγ, and activation of NF-κB proteins to promote transcription of pro-survival genes [106]. Chemical or pathogen mediated blockade of NF-κB signaling leads to the down-regulation of cFLIP expression and induction of apoptosis [178-180].

Our group as well as other have demonstrated another role for caspase-8 in the cell-intrinsic expression of inflammatory cytokines [75, 77, 100]; however, the role of caspase-8 enzymatic activity in this context has yet to be resolved. We have demonstrated that both chemical inhibitors of caspase-8 catalytic activity and inhibition of cFLIP expression

impairs cytokine secretion in macrophages stimulated with TLR agonists [75]. These data support a model in which caspase-8 enzymatic activity mediates inflammatory gene expression. However, work from others has shown that caspase-8 scaffolding is sufficient to induce NF-κB activation in response to TRAIL (Tumor necrosis factor related apoptosis inducing ligand) stimulation in HeLa cells [112]. These models are not mutually exclusive as it is possible that there are cell-specific and stimuli-specific functions of caspase-8.

We utilized two approaches in an effort to elucidate the function of caspase-8 enzymatic activity in the context of gene expression. The first being chemical inhibition of caspase-8 catalytic activity in *Ripk3*$^{-/-}$ macrophages as well as macrophages derived from mice in which we ablated caspase-8-dependent apoptosis, but preserved its cytokine regulatory function. These mice express caspase-8 with a mutation in the linker region that mediates stabilization of the apoptotic conformation of caspase-8 [80, 113]. We refer to these mice, and cells derived from them, as *Casp8*$^{DA/DA}$. Our characterizations of these mice will be described in **Chapter 4**: briefly, macrophages from these mice are unable to undergo caspase-8 dependent apoptosis in response to *Yersinia pseudotuberculosis* (*Yp*) infection, but secrete wild-type levels of inflammatory cytokines in response to TLR stimulation [75]. We have crossed these mice with *Ripk3*$^{-/-}$ mice to eliminate the impact of programmed necrosis in this system: we refer to mice, and cells derived from them ,as *Ripk3*$^{-/-}$*Casp8*$^{DA/DA}$. In this chapter we seek to elucidate the role of the pro-survival conformation of caspase-8 on inflammatory gene expression as well as the enzymatic requirements for this function.

3.3. Results

3.3.1 TLR stimulation promotes caspase-8 catalytic activity.

We have previously shown that inhibition of caspase-8 catalytic activity reduced inflammatory cytokine secretion, but it is possible that this was mediated by off-target effects of these chemical compounds [75]. Therefore, we sought to directly test the activation of caspase-8 in response to TLR stimulation. Previous groups have shown that TLR4 stimulation promotes the cleavage of the linear deubiquitinase CYLD [107]. We found that caspase-8 catalytic activity was induced in response to both LPS and CpG in *Ripk3*$^{-/-}$ macrophages within 30 min of stimulation (**Fig 3.1A**). Interestingly, this activation was not to the same magnitude as that observed with the apoptotic stimulus staurosporine (**Fig 3.1A**). All caspase-8 activation was blocked by the pan-caspase inhibitor zVAD; therefore, we concluded that our previous findings demonstrating a role for caspase-8 in inflammatory cytokine secretion were likely not due to off target effects of zVAD (**Fig 3.1A**). We also found that CYLD was cleaved in response to LPS stimulation, and that this cleavage was partially blocked using both zVAD and the caspase-8-specific inhibitor IETD (**Fig 3.1B**). These data demonstrate that caspase-8 activity is induced in response to TLR activation, and that chemical inhibition—using zVAD or IETD—is sufficient to block a majority of caspase-8 activity.

3.3.2 Caspase-8 enzymatic activity promotes inflammatory gene expression and IKK phosphorylation.

We measured transcription of several caspase-8-dependent genes (described in **Chapter 2**) in *Ripk3*$^{-/-}$ macrophages stimulated with the TLR4 and TLR9 agonists LPS and

CpG respectively. zVAD inhibition reduced expression of *Il12b* in response to LPS but not CpG (**Fig 3.2A**). This result was surprising given the defect we observed in IL-12p40 secretion in LPS- and CpG-stimulated *Ripk3*$^{-/-}$ macrophages treated with zVAD (**Fig 3.2B**). Moreover, zVAD treatment was not sufficient to decrease LPS-induced *Il12b* transcription to the same magnitude as ablation of caspase-8, but it appears this was sufficient to reduce IL-12p40 secretion to similar levels observed in *Ripk3*$^{-/-}$*Casp8*$^{-/-}$ macrophages (**Fig 3.2A** and **Fig 3.2B**). These data suggest that there is a threshold of *Il12b* transcript required for secretion of IL-12p40, and the decrease we observed in the context of zVAD inhibition is sufficient to reduce cytokine secretion to levels observed in *Ripk3*$^{-/-}$*Casp8*$^{-/-}$ macrophages. There was a similar trend in the expression of *Il1b* in LPS-stimulated cells: zVAD treatment impaired transcription, and this reduction was sufficient to reduce pro-IL-1β expression to levels observed in *Ripk3*$^{-/-}$*Casp8*$^{-/-}$ macrophages (**Fig 3.2A** and **Fig 3.2B**). We measured a decrease in transcription of *Il1a* and *Il4i1* in LPS-stimulated *Ripk3*$^{-/-}$ macrophages treated with zVAD, but again this decrease was not to the same magnitude as caspase-8 ablation. There was no role for caspase-enzymatic activity in the transcription of *Il1a* or *Il4i1* in response to CpG which is consistent with what we observed for *Il12b* and *Il1b* (**Fig 3.2A**).

We interpret these data to mean that both caspase-8 enzymatic activity *and* scaffolding play a role in inflammatory gene expression, but the role of each appears to be gene and TLR-dependent. There seems to be more of a requirement for caspase-8 enzymatic activity in response to TLR4 stimulation, but it seems to be dispensable in some contexts in response to CpG. Based on these data we expected to observe a role for caspase-8 enzymatic activity in the phosphorylation of IKK in response to LPS, and not CpG, but

we were surprised to find zVAD treatment reduced IKK phosphorylation in both contexts (**Fig 3.2C**). It is possible that NF-κB-dependent genes display differing levels of sensitivity to IKK phosphorylation as we do not see a defect in transcription of *Il12b*, *Il1a*, and *Il4i1* in CpG-stimulated macrophages treated with zVAD (**Fig 3.2A**). One possible explanation is that the use of a pan-caspase inhibitor masked caspase-8-specific enzymatic requirements; therefore, we sought to test the impact of the caspase-8-specific inhibitor IETD on gene transcription.

3.3.3 Caspase-8 enzymatic activity promotes *Il12b* transcription and IL-12p40 secretion.

Consistent with our previous observations, *Ripk3*$^{-/-}$ macrophages treated with IETD have decreased IL-12p40 secretion in response to LPS (**Fig 3.3A**). We also discovered this was the case in response to CpG stimulation, again, suggesting a role for caspase-8 enzymatic activity in IL-12 secretion in response to both LPS and CpG (**Fig 3.3A**). Surprisingly, IETD reduced *Il12b* transcription in response to both LPS and CpG to the same magnitude as that observed in *Ripk3*$^{-/-}$*Casp8*$^{-/-}$ macrophages (**Fig 3.3B**). We interpret these data to mean that caspase-8 enzymatic activity is required for transcription of *Il12b*, and corresponding secretion of IL-12p40 in response to TLR activation. It is possible that because zVAD targets other caspases it is not sufficient to block all caspase-8 activity, but we could observe no measurable caspase-8 activity in our previous assay in *Ripk3*$^{-/-}$ macrophages treated with zVAD (**Fig 3.1A**). Based on our observations that caspase-8 catalytic activity mediated inflammatory gene expression and IKK phosphorylation we hypothesized that we would observe a decrease in c-Rel nuclear translocation in zVAD-treated cells (based on findings discussed in **Chapter 2**).

3.3.4 Caspase-8 enzymatic activity promotes c-Rel nuclear translocation.

We quantified nuclear translocation of c-Rel using single-cell analysis of *Ripk3*$^{-/-}$ macrophages treated with zVAD then stimulated with LPS or CpG. Consistent with the observed role for caspase-8 enzymatic activity on gene expression, zVAD treatment reduced c-Rel translocation (**Fig 3.4B**).. However, this reduction was not to the same magnitude as that observed in observed in *Ripk3*$^{-/-}$*Casp8*$^{-/-}$ macrophages (**Fig 3.4B**). *Ripk3*$^{-/-}$ macrophages treated with zVAD have much less nuclear c-Rel when compared to vehicle-treated cells stimulated with LPS or CpG. We interpret these data to mean that caspase-8 enzymatic activity promotes c-Rel translocation in response to both TLR4 and TLR9 agonists, but caspase-8 scaffolding also contributes to c-Rel translocation in this context. We next sought to determine if enzymatically inactive caspase-8 recapitulated our observations with *Ripk3*$^{-/-}$ macrophages treated with chemical inhibitors of caspase-8 activity.

3.3.5 Caspase-8 enzymatic activity promotes cytokine secretion.

We transduced wild-type caspase-8 (*Casp8*^{WT}), catalytically inactive caspase-8 (*Casp8*^{D3A}), and an empty vector into *Ripk3*$^{-/-}$*Casp8*$^{-/-}$ immortalized macrophages (**Fig 3.5A**). Each construct also expressed GFP allowing us to enrich for transduced cells after puromycin selection, resulting in an approximately 95% pure population (data not shown). We observed that cells expressing catalytically inactive caspase-8 had reduced secretion of TNF in response to both LPS and CpG; however, not to the magnitude observed in our empty vector controls expressing no caspase-8 (**Fig 3.5B**). These data are

consistent with our observations in primary *Ripk3*$^{-/-}$ macrophages treated with zVAD in which there are enzymatic and non-enzymatic contributions of caspase-8. One question raised by these data was whether some low-level of caspase-8 homodimers contribute to the observed requirement for caspase-8 enzymatic activity without causing measurable cell death.

3.3.6 Caspase-8 non-apoptotic activity mediates inflammatory cytokine expression and IKK phosphorylation.

It is hypothesized that caspase-8 homodimers do not form under pro-survival conditions, but it is formally possible that both caspase-8/cFLIP heterodimers and caspase-8 homodimers are present in *Ripk3*$^{-/-}$ macrophages under these conditions. To address this question we utilized macrophages in which caspase-8 apoptotic activity is inactive, but the protein is expressed and maintains catalytic activity (*Casp8*$^{DA/DA}$). *Casp8*$^{DA/DA}$ macrophages expressed *Il12b* to the same extent as B6 macrophages stimulated with LPS (**Fig 3.6A**). IKK phosphorylation in *Casp8*$^{DA/DA}$ macrophages was indistinguishable from B6 macrophages stimulated with LPS (**Fig 3.6B**). These data were consistent with our previous report that *Casp8*$^{DA/DA}$ macrophages produced cytokines to the same magnitude as B6 cells [75]. We have previously found no role for RIPK3 in gene expression, but we generated macrophages from *Ripk3*$^{-/-}$*Casp8*$^{DA/DA}$ to formally test the role for programed necrosis in this context. Surprisingly, we found that LPS-stimulated *Ripk3*$^{-/-}$*Casp8*$^{DA/DA}$ macrophages expressed *Il12b* to a higher magnitude than *Ripk3*$^{-/-}$*Casp8*$^{-/-}$ cells, but not to the same extent as *Ripk3*$^{-/-}$ cells (**Fig 3.6C**). This was concordant with the intermediate level of IKK phosphorylation observed in *Ripk3*$^{-/-}$*Casp8*$^{DA/DA}$ macrophages

stimulated with LPS (**Fig 3.6E**). However, *Ripk3*$^{-/-}$*Casp8*$^{DA/DA}$ macrophages secreted IL-12p40 equivalently to *Ripk3*$^{-/-}$ macrophages in response to LPS stimulation (**Fig 3.6D**). These data are similar to our previous observations that defects in cytokine gene transcription cannot be directly correlated to cytokine protein secretion. It is possible that despite the observed reduction in *Il12b* transcription, in *Ripk3*$^{-/-}$*Casp8*$^{DA/DA}$ macrophages stimulated with LPS, there was enough transcript to mediate wild-type levels of IL-12p40 secretion.

3.4 Discussion

Here we describe a role for caspase-8 enzymatic activity in inflammatory gene transcription in macrophages. Moreover, we were able to directly measure catalytic activity of caspase-8 in response to the Myd88-dependent TLR9. This was surprising given that there is limited data suggesting that caspase-8 can be activated downstream of MyD88. In support of a model in which MyD88 activates caspase-8, we observed defects in IKK phosphorylation, and c-Rel translocation in response to CpG stimulation (discussed in **Chapter 2)**, and here we report that this defect is in part due to the absence of caspase-8 catalytic activity. We also report for the first time that there is a defect in inflammatory cytokine secretion when caspase-8 catalytic activity is blocked in CpG-stimulated cells. The role for caspase-8 enzymatic activity is less clear with regards to CpG-induced gene transcription, as we cannot observe a decrease in transcription of *Il12b*, *Il1b*, *Il1a*, or *Il4i1* in zVAD-treated cells.

This is surprising given our observation that zVAD treatment blocks IKK phosphorylation as well as IL-12p40 and pro-IL-1β production to levels observed in *Ripk3*$^{-/-}$*Casp8*$^{-/-}$ macrophages in response to CpG stimulation. It is not likely that zVAD incompletely inhibits caspase-8 catalytic activity as we can detect no activity in response to LPS, CpG, or staurosporine in zVAD-treated cells (**Fig 3.1A**). However, the caspase-8-specific inhibitor IETD completely abrogates transcription of *Il12b* in response to both LPS and CpG. Therefore, it is possible that there is some latent caspase-8 activity in zVAD-treated cells that we cannot detect with our caspase-8-activity assay.

We also observed a partial block of c-Rel translocation in macrophages treated with zVAD, and we interpret these data to mean that both caspase-8 scaffolding and enzymatic

activity contribute to c-Rel translocation in response to LPS and CpG stimulation. These data are consistent with the observed dual contributions of caspase-8 enzymatic activity and scaffolding in gene transcription in response to LPS; however, it appears that this partial block is sufficient to inhibit cytokine secretion to levels observed in *Ripk3*$^{-/-}$*Casp8*$^{-/-}$ macrophages. It is clear from these data that cytokine secretion does not reflect gene transcription with enough fidelity for cytokine secretion to serve as a proxy for the levels of mRNA induced in response to TLR stimuli. These data also suggest that there is a threshold of transcript required in macrophages to mediate wild-type levels of cytokine secretion. If this is indeed the case, then caspase-8 enzymatic activity is critical for the purposes of cytokine secretion in macrophages, and its inhibition is sufficient to mimic complete ablation of caspase-8.

Our data demonstrated that immortalized *Ripk3*$^{-/-}$*Casp8*$^{-/-}$ macrophages transduced with catalytically inactive caspase-8 have intermediate levels of cytokine secretion, suggesting some contribution of caspase-8 scaffolding in this context. One caveat to these data are that immortalized macrophages secrete fewer cytokines than primary cells, and *Ripk3*$^{-/-}$*Casp8*$^{-/-}$ macrophages transduced with wild-type caspase-8 have no detectable IL-12p40 as measured by ELISA or flow-cytometry (data not shown). TNF is the only cytokine that is measurable in these cultures; therefore, it is possible that if we were able to generate primary cells expressing catalytically inactive caspase-8 we would observe a requirement for its activity in IL-12 secretion, as we see in chemically inhibited primary cells. However, this is entirely speculative given the technical limitations of this experiment.

We also reported a surprising role for RIPK3 in the context of a mutant form of caspase-8 that is unable to mediate apoptosis. *Ripk3*$^{-/-}$*Casp8*$^{DA/DA}$ macrophages had intermediate levels of IKK phosphorylation and gene expression when compared to *Ripk3*$^{-/-}$ and *Ripk3*$^{-/-}$*Casp8*$^{-/-}$ macrophages (**Fig 3.6C** and **Fig 3.6E**), whereas *Casp8*$^{DA/DA}$ macrophages phenocopied B6 macrophages stimulated with LPS (**Fig 3.6A** and **Fig 3.6B**). This suggests that RIPK3 promotes stabilization of the catalytic site of *Casp8*$^{DA/DA}$. This is surprising given that caspase-8 and RIPK3 are reported to exist in distinct complexes [105, 108]. However, RIPK3 is reported to be a substrate of caspase-8 [111] and other groups have implicated RIPK3 indirectly in apoptosis and [126] inflammasome activation [127]. Therefore, it is possible that RIPK1, RIPK3, cFLIP, FADD, TRADD, and caspase-8 interact more dynamically than is assumed in the Complex I, Complex II and necrosome transition model of different forms of cell death. It is likely that a combination of signals bias cells towards preferential interactions between these proteins, RIPK3/RIPK1 in the context of programed necrosis, RIPK1/caspase-8 in apoptosis, and RIPK1/cFLIP/caspase-8 under pro-survival conditions. Our data suggest that in response to TLR stimulation RIPK3 promotes the inflammatory gene regulatory function of *Casp8*$^{DA/DA}$, perhaps via stabilization of its catalytic site.

To our knowledge these studies represent the first report of caspase-8 activity in response to TLR9 activation. We also demonstrate a role for caspase-8 enzymatic activity in IKK phosphorylation, c-Rel translocation, and *Il12b* and *Il1b* transcription in response to both LPS and CpG (**Fig 3.7**). These data support a model in which caspase-8 enzymatic activity is a key component of inflammatory gene expression in response to multiple TLRs.

3.5 Figures

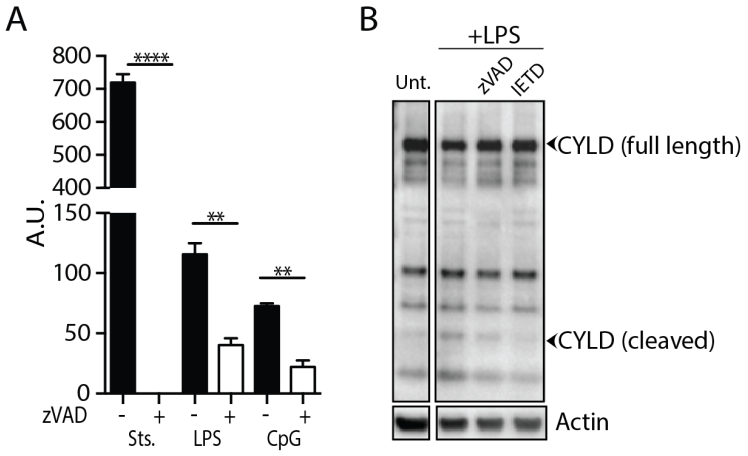

Fig 3.1 TLR stimulation promotes caspase-8 catalytic activity.

(A) IETDase activity (arbitrary fluorescence units) in *Ripk3*$^{-/-}$ BMDMs 3.5hrs post staurosporine treatment or 30min post LPS or CpG stimulation in the presence or absence of zVAD, as indicated.

(B) CYLD cleavage in *Ripk3*$^{-/-}$ BMDMs 4hrs post LPS stimulation was measured by immunoblotting cell lysates for CYLD in cells pre-treated with zVAD, IETD or vehicle control as indicated 1hr prior to stimulation.

Error bars indicate ± SEM of triplicates. Student's two-tailed unpaired t-test (** $p<0.01$, **** $p<0.0001$). **(A)** is from an individual experiment and **(B)** is representative of three independent experiments.

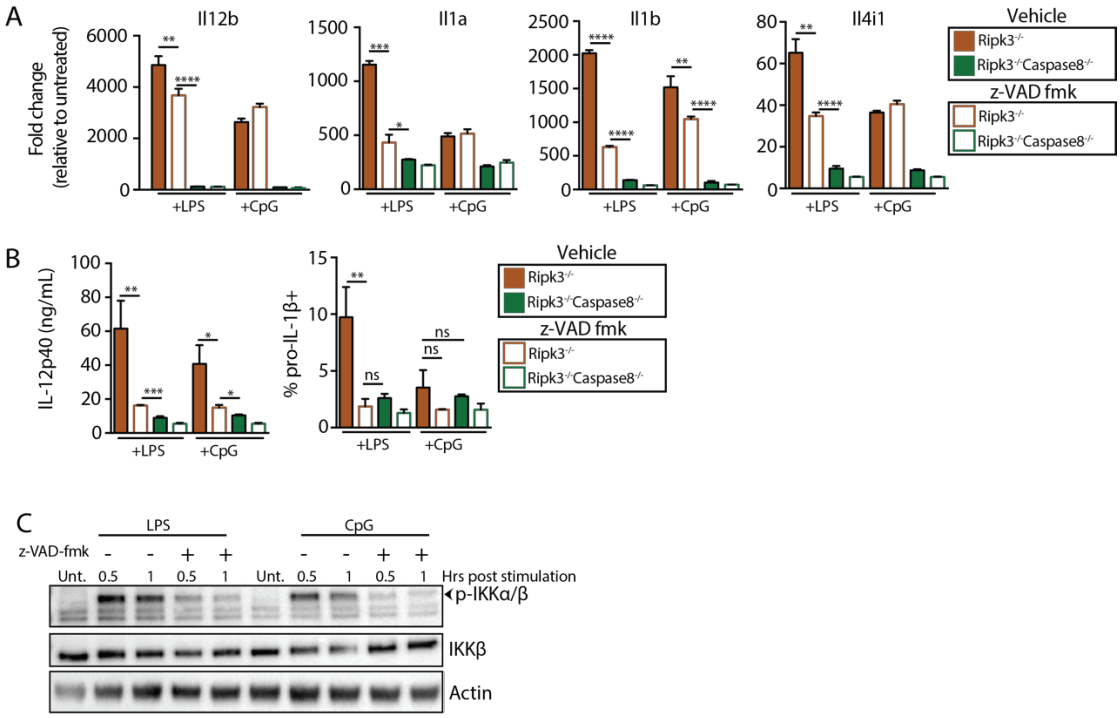

Fig 3.2 Caspase-8 enzymatic activity regulates activation of the IKK complex.

(A) Fold-change in mRNA expression of indicated genes in *Ripk3*$^{-/-}$ and *Ripk3*$^{-/-}$*Casp8*$^{-/-}$ BMDMs pre-treated with zVAD or vehicle control for 1hr followed by treatment with LPS or CpG for 2hrs.

(B) Levels of secreted IL-12p40, measured by ELISA, and frequency of intracellular pro-IL-1β expression, measured by flow cytometry, by *Ripk3*$^{-/-}$ and *Ripk3*$^{-/-}$*Casp8*$^{-/-}$ BMDMs pre-treated with zVAD or vehicle control for 1hr followed by LPS or CpG treatment for 5hrs.

(C) Immunoblots of phospho-IKKα/β and total IKKβ in *Ripk3*$^{-/-}$ BMDMs pre-treated with zVAD or vehicle control for 1hr and stimulated with LPS or CpG for the indicated times.

Error bars indicate ± SEM of triplicates. Student's two-tailed unpaired t-test (n.s. not significant, * $p<0.05$, ** $p<0.01$, *** $p<0.001$, **** $p<0.0001$). All data representative of three independent experiments.

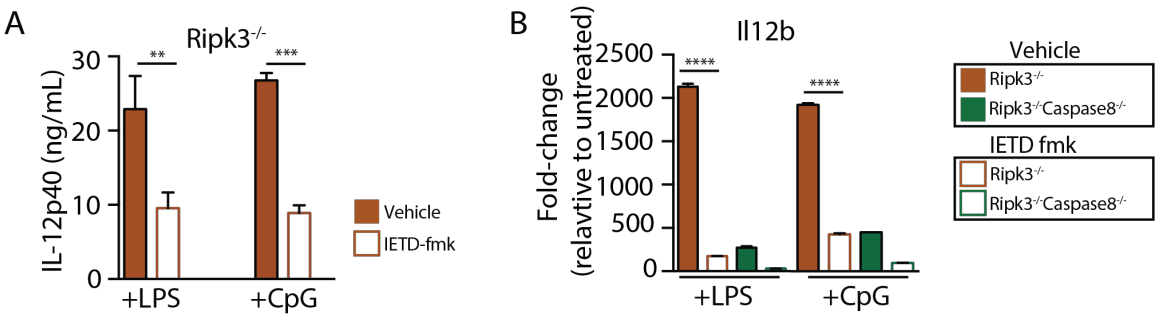

Fig 3.3 Caspase-8 enzymatic activity mediates *Il12b* expression in response to TLR activation.

(A) Secreted IL-12p40 assayed by ELISA in supernatants of *Ripk3*$^{-/-}$ BMDMs pre-treated with IETD or vehicle control (DMSO) for 1hr followed by 5hr stimulation with LPS or CpG.

(B) Fold change in *Il12b* expression in *Ripk3*$^{-/-}$ and *Ripk3*$^{-/-}$*Casp8*$^{-/-}$ BMDMs pre-treated with IETD or vehicle control for 1hr prior to 2hrsof LPS or CpG treatment.

Error bars indicate ± SEM of triplicates. Student's two-tailed unpaired t-test (** $p<0.01$, *** $p<0.001$, **** $p<0.0001$). Data are representative of two independent experiments.

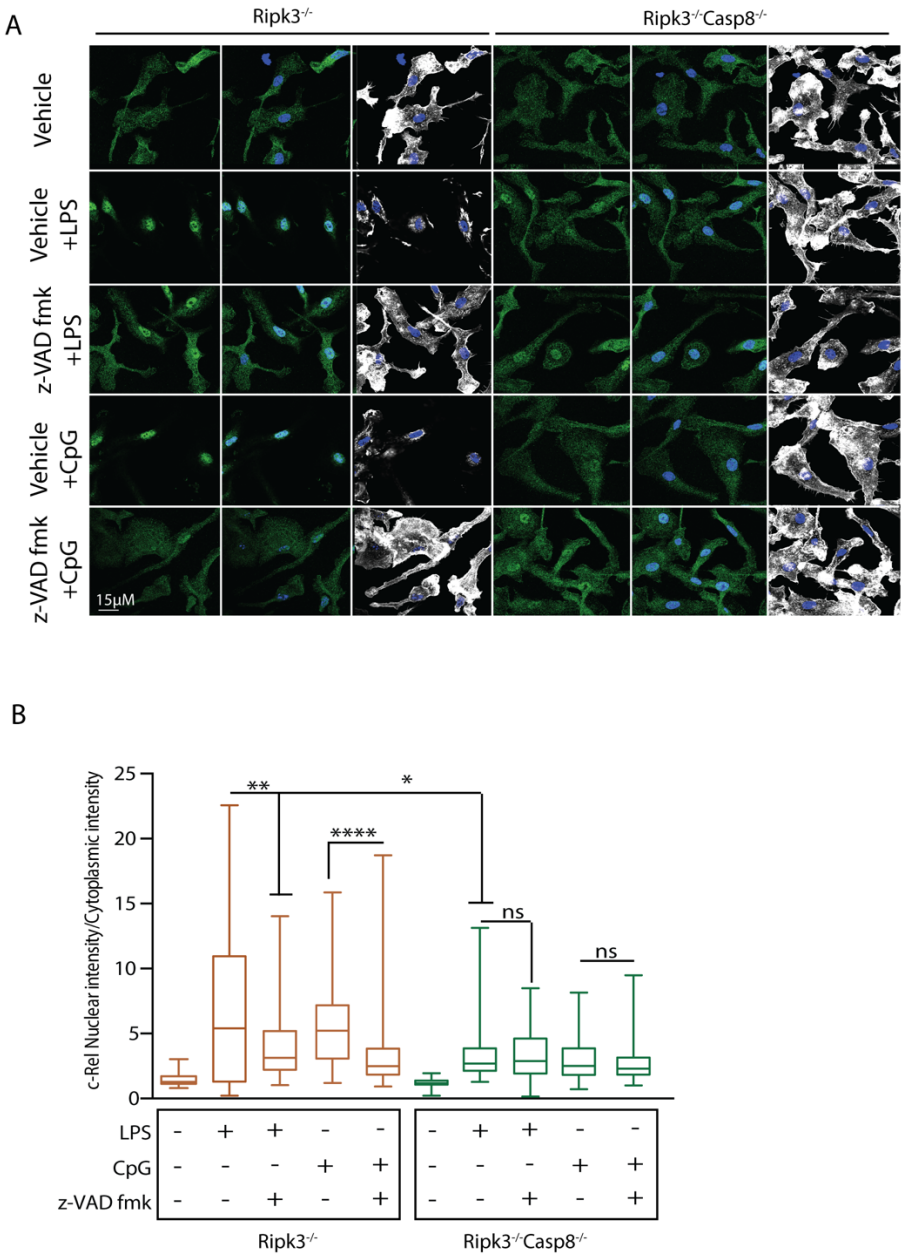

Fig 3.4 Caspase-8 enzymatic activity contributes to c-Rel nuclear translocation in response to TLR signaling.

(A) Representative confocal microscopy images of *Ripk3*$^{-/-}$ and *Ripk3*$^{-/-}$*Casp8*$^{-/-}$ BMDMs pre-treated with zVAD or vehicle control for 1hr followed by LPS or CpG stimulation as indicated for 2hrs; c-Rel, actin and DAPI pseudo-colored in green, white and blue respectively.

Fig 3.4 Continued: (B) Quantification of the mean fluorescence intensity of nuclear:cytoplasmic c-Rel in *Ripk3*$^{-/-}$ and *Ripk3*$^{-/-}$*Casp8*$^{-/-}$ BMDMs pre-treated with zVAD or vehicle control for 1hr prior to LPS or CpG treatment for 2hrs.

Box plots represent 60-150 individual cells per condition. Student's two-tailed unpaired t-test (n.s. not significant, * $p<0.05$, ** $p<0.01$, **** $p<0.0001$). Box plots illustrate the median, upper and lower quartiles, and upper and lower extremes of the data. All data representative of at least three independent experiments.

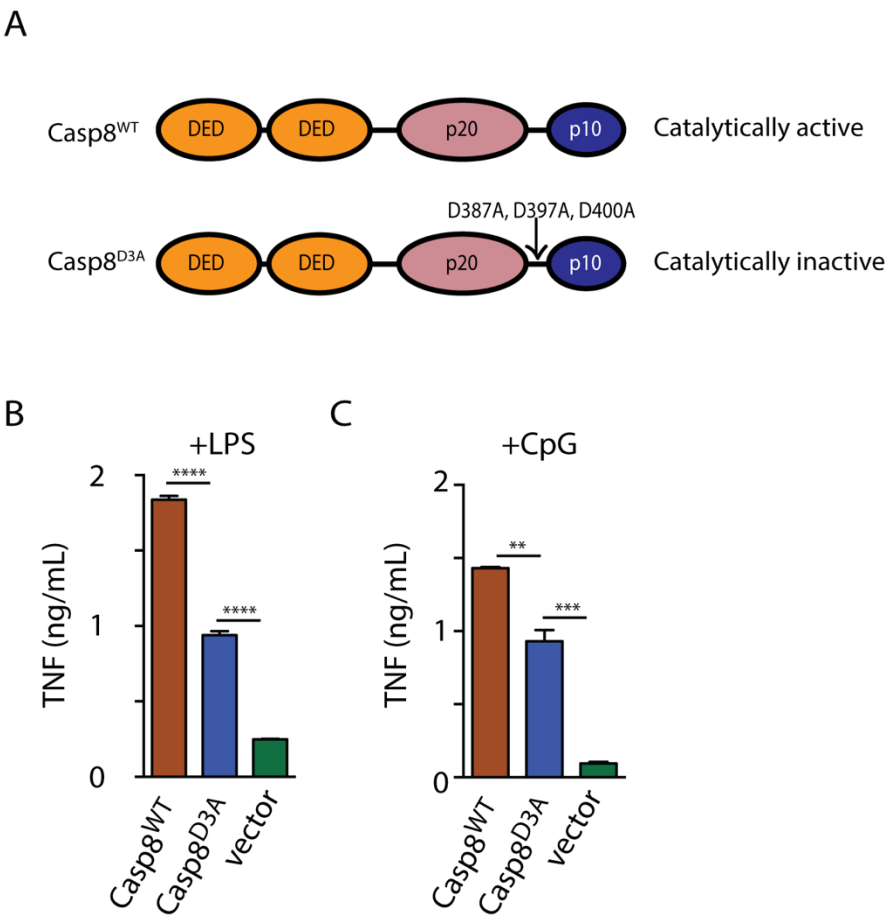

Fig 3.5 Caspase-8 enzymatic activity and scaffolding promote inflammatory cytokine secretion.

(A) Depiction of the caspase-8 constructs transduced into *Ripk3*$^{-/-}$*Casp8*$^{-/-}$ iBMDMs.

(B-C) ELISA measurement of secreted TNF in *Ripk3*$^{-/-}$*Casp8*$^{-/-}$ iBMDMs transduced with WT caspase 8 (Casp8^{WT}), catalytically inactive caspase 8 (Casp8^{D3A}), or an empty vector and stimulated with LPS or CpG as indicated for 12hrs.

Error bars indicate ± SEM of triplicates. Student's two-tailed unpaired t-test (** $p<0.01$, *** $p<0.001$, **** $p<0.0001$). Data are representative of two independent experiments.

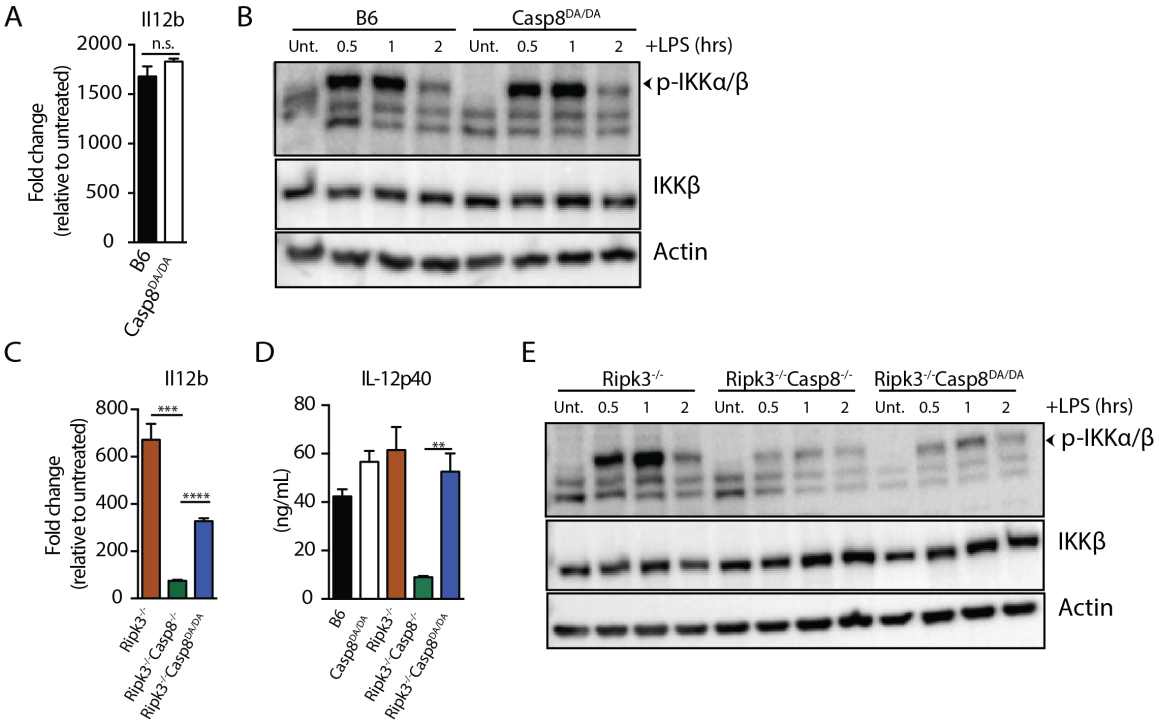

Fig 3.6 Non-cleavable caspase-8 promotes inflammatory gene expression and IKK phosphorylation in response to TLR stimulation.

(A) Fold-change in *Il12b* expression in B6 and *Casp8*$^{DA/DA}$ BMDMs stimulated with LPS for 2hrs.

(B) Immunoblots of phospho-IKKα/β and total IKKβ in B6 and *Casp8*$^{DA/DA}$ BMDMs stimulated with LPS for the indicated times.

(C) Fold-change in *Il12b* expression in *Ripk3*$^{-/-}$, *Ripk3*$^{-/-}$*Casp8*$^{-/-}$, and *Ripk3*$^{-/-}$*Casp8*$^{DA/DA}$ BMDMs stimulated with LPS for 2hrs.

(D) Secreted IL-12p40 assayed by ELISA in supernatants of B6, *Casp8*$^{DA/DA}$, *Ripk3*$^{-/-}$, *Ripk3*$^{-/-}$*Casp8*$^{-/-}$, and *Ripk3*$^{-/-}$*Casp8*$^{DA/DA}$ BMDMs stimulated with LPS for 6hrs.

(E) Immunoblots of phospho-IKKα/β and total IKKβ from *Ripk3*$^{-/-}$, *Ripk3*$^{-/-}$*Casp8*$^{-/-}$, and *Ripk3*$^{-/-}$*Casp8*$^{DA/DA}$ BMDMs after LPS stimulation for indicated times.

Fig 3.6 Continued: Error bars indicate ± SEM of triplicates. Student's two-tailed unpaired t-test (n.s. not significant, ** $p<0.01$, *** $p<0.001$, **** $p<0.0001$). Data are representative of three independent experiments.

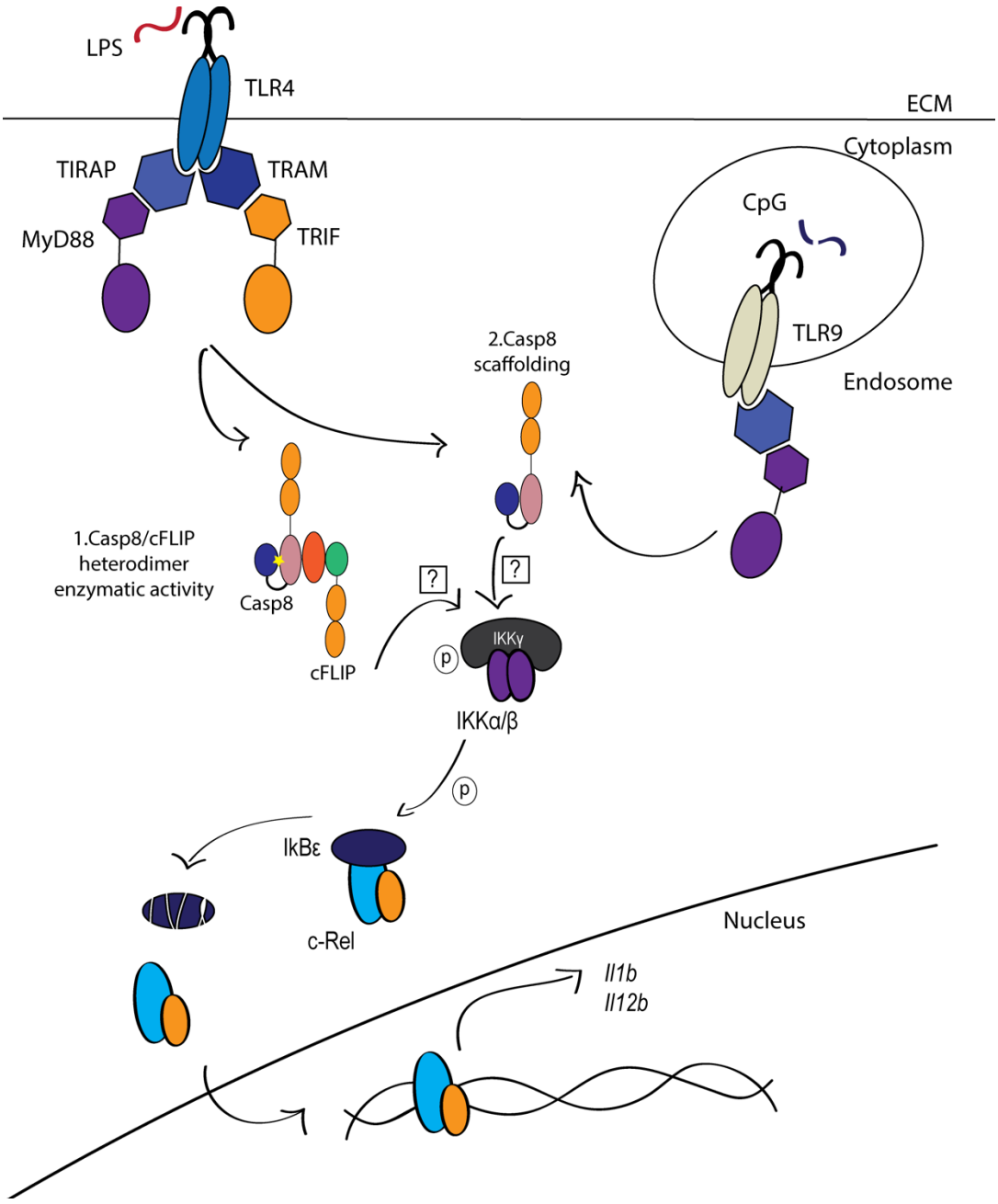

Fig 3.7 Graphical abstract and future directions: Caspase-8 enzymatic activity and scaffolding mediate inflammatory gene expression.

CHAPTER 4: Selective ablation of caspase-8 apoptotic activity protects thymocytes from Fas-mediated cell death and leads to the accumulation of myeloid cells.

4.1 Abstract

Two critical functions of caspase-8-mediated apoptosis are the clearance of autoreactive cells as well as pathogen-infected cells. Caspase-8-mediated apoptosis is induced upon activation of tumor necrosis factor receptor superfamily members; this family includes Fas/CD95 and TNFR1/2. Upon activation of these receptors by their cognate ligands FADD is recruited to the death domain of the cytoplasmic portion of these transmembrane proteins, and FADD in turn recruits caspase-8 via homotypic interactions between their death effector domains. Upon recruitment caspase-8 monomers undergo auto-processing through cleavage of the linker region between the p10 and p20 subunits of each monomer. This auto-processing stabilizes two catalytic sites in the caspase-8 homodimer which mediate the cleavage of the apoptotic substrate BID (BH3-interacting domain death agonist). Caspase-8 also negatively regulates another form of cell death: programmed necrosis. In the absence of caspase-8 programmed necrosis is de-repressed mediating embryonic lethality. Dual ablation of caspase-8 and the proteins that mediate programmed necrosis—MLKL and RIPK3—rescues these mice from embryonic lethality. *Ripk3*$^{-/-}$*Casp8*$^{-/-}$ mice display a lymphoproliferative disease that is characterized by splenomegaly, lymphadenopathy, and the accumulation of $CD3^{+}B220^{+}$ cells that begins 6-weeks postnatally. These characteristics are attributed to both a defect in programmed necrosis and apoptosis, which prevents homeostatic turnover of circulating lymphocytes in these mice. We sought to determine if specific ablation of caspase-8 apoptotic activity recapitulated the observations made in *Ripk3*$^{-/-}$*Casp8*$^{-/-}$ mice. We generated mice with a

non-cleavable linker sequence between the p10 and p20 subunit of the caspase-8 monomer referred to as *Casp8*$^{DA/DA}$ mice, and crossed these mice to RIPK3-deficient mice to generate *Ripk3*$^{-/-}$*Casp8*$^{DA/DA}$ mice. We were surprised to find that these mice display a unique lymphoproliferative disease, distinct from *Ripk3*$^{-/-}$*Casp8*$^{-/-}$ mice, that is characterized by the accumulation of innate immune cell populations. These data suggest that caspsase-8 apoptotic activity is dispensable for lymphocyte homeostasis, but required for maintenance of normal myeloid cell numbers.

4.2 Introduction

Caspase-8 plays a critical role in host survival through the clearance of autoreactive cells [181], tumorigenic cells [182], and infected cells [183]. It is thought that caspase-8 mediates these functions through caspase-8-dependent apoptosis activated in response to a variety of cell death stimuli. Broadly, death signals such as FasL (Tumor necrosis factor ligand superfamily member 6) or TNF (Tumor necrosis factor) bind to their cognate receptors which belong to the tumor necrosis receptor superfamily. Upon receptor activation the adaptor proteins FADD [168] (Fas-associated death domain protein) and TRADD [84] (Tumor necrosis factor receptor type 1-associated death domain protein) are recruited to the cytoplasmic domain of the transmembrane death receptor via their death domains (DD). TRADD and FADD indirectly or directly mediate recruitment of caspase-8 [184] forming the death inducing signaling complex (DISC). Under death inducing conditions caspase-8 monomers oligomerize [85], and undergo auto-processing which stabilizes their apoptotic activity [79]. Patients with non-functional caspase-8 display a lymphoproliferative disease [157] that is similar to disease displayed in patients with mutations in the death receptor Fas [165] as well as its cognate ligand FasL [185]. Studies elucidating the role caspase-8 in lymphocyte homeostasis *in vivo* were historically difficult as single ablation of caspase-8 results in embryonic lethality. However, in 2011 two groups demonstrated that dual ablation of caspase-8 and RIPK3 (Receptor-interacting serine/threonine-protein kinase 3), which mediates another cell death pathway known as program necrosis, resulted in viable progeny [104, 105]. These groups implicated caspase-8 in the negative regulation of programmed necrosis during development as well as during cellular activation [104, 105].

Mice in which both RIPK3 and caspase-8 are ablated display lymphoproliferative disease that resembles the phenotype of mice with Fas or FasL mutations: *lpr* and *gld* mice respectively [105, 186]. Lymphoaccumulation in *Ripk3*$^{-/-}$*Casp8*$^{-/-}$ mice begins 6 weeks postnatally, and is characterized by splenomegaly, lymphadenopathy, and accumulation of $CD3^{+}B220^{+}CD8^{-}CD4^{-}$ cells [105]. RIPK3-deficient mice do not display lymphoproliferative disease, which suggests that caspase-8-dependent apoptosis promotes clearance of circulating lymphocytes as mice age. These data were not entirely surprising given that Fas-mediated cell death is important for regulating autoreactive T cells [187] as well as total numbers of naïve T cells in the periphery [188].

In addition to its role in cell death caspase-8 has been implicated in the regulation of inflammatory gene expression. However, *in vivo* these studies were performed using *Ripk3*$^{-/-}$*Casp8*$^{-/-}$ mice which display a defect in caspase-8-dependent apoptosis as well as gene expression [75, 77, 110] during infection. In an effort to separate the gene-regulatory function of caspase-8 from its apoptotic function we generated mice in which the apoptotic confirmation of caspase-8 is rendered unstable. The apoptotic confirmation of caspase-8 is stabilized in part through auto-processing of the linker sequence between its p10 and p20 subunits [79, 80]. Therefore, we generated a mouse in which this sequence is mutated which we will refer to as *Casp8*$^{DA/DA}$ [75]. We have previously demonstrated that cells derived from these mice are able to produce inflammatory cytokines in response to the TLR4 agonist LPS, but do not undergo apoptosis when infected with the gram-negative bacterial pathogen *Yersinia pseudotuberculosis*—a potent activator of caspase-8-mediated apoptosis [75]. To further elucidate the role of caspase-8-mediated gene regulation in host defense *in vivo* we generated *Ripk3*$^{-/-}$*Casp8*$^{DA/DA}$ mice in which caspase-8-dependent

apoptosis and RIPK3-dependent programmed necrosis are ablated (**Fig 4.1**). In this chapter we discuss both our preliminary characterizations of these mice, and our discovery that caspase-8-dependent apoptosis may play a novel role in regulating myeloid cell populations in naïve mice.

4.3 Results

4.3.1 *Ripk3*$^{-/-}$*Casp8*$^{DA/DA}$ mice display a lymphoproliferative disease that is divergent from that of *Ripk3*$^{-/-}$*Casp8*$^{-/-}$ mice.

Previous studies have identified a role for caspase-8 in preventing splenomegaly and lymphadenopathy [104, 105], which has been attributed to caspase-8-mediated apoptosis in response to Fas stimulation. These mice are completely protected from Fas-mediated apoptosis leading to the accumulation of a $CD3^+B220^+CD4^-CD8^-$ cell population in the periphery [105]. In an effort to isolate the role of caspase-8-mediated inflammatory cytokine expression from its role in apoptosis we generated a mouse in which caspase-8-dependent apoptosis and RIPK3-mediated programed necrosis are ablated, but the cytokine regulatory function of caspase-8 is preserved (**Fig 4.1**). These mice will be referred to as *Ripk3*$^{-/-}$*Casp8*$^{DA/DA}$. We anticipated that these mice would display the same lymphoproliferative disease observed in *Ripk3*$^{-/-}$*Casp8*$^{-/-}$ mice, and *Ripk3*$^{-/-}$*Casp8*$^{DA/DA}$ mice do exhibit splenomegaly similar to *Ripk3*$^{-/-}$*Casp8*$^{-/-}$ mice (**Fig 4.2A** and **Fig 4.2B**). However, unlike mice in which caspase-8 is ablated there is no observable lymphadenopathy in *Ripk3*$^{-/-}$*Casp8*$^{DA/DA}$ mice (**Fig 4.2C**). Moreover, in *Ripk3*$^{-/-}$*Casp8*$^{DA/DA}$ mice we could not detect the $CD3^+B220^+CD4^-CD8^-$ T cell population that characterizes *Ripk3*$^{-/-}$*Casp8*$^{-/-}$ mice (**Fig 4.3A** and **Fig 4.3B**). These data were surprising given that the accumulation of this cell population is what mediates splenomegaly and lymphadenopathy in *Ripk3*$^{-/-}$*Casp8*$^{-/-}$ mice; therefore, we then took a histological approach to asses immune cell populations in the spleens of *Ripk3*$^{-/-}$*Casp8*$^{DA/DA}$ mice.

4.3.2 Ablation of capsase-8 apoptotic activity mediates splenomegaly that is characterized by both myeloid and lymphocyte infiltration.

Histological analysis of the spleens of *Ripk3*$^{-/-}$*Casp8*$^{DA/DA}$ mice revealed large disruptions in the overall splenic architecture (**Fig 4.4**) characterized by atypical lymphocyte expansion in the white pulp, lymphoid atrophy, and severe extramedullary erythropoiesis. This disruption in splenic architecture is not present in *Ripk3*$^{-/-}$*Casp8*$^{-/-}$ mice. Staining for immune populations (CD3^{+} T cell, CD45^{+} total immune cells, and F4/80^{+} monocytes/macrophage) also showed a divergent cellular infiltrate phenotype in the spleens of *Ripk3*$^{-/-}$*Casp8*$^{DA/DA}$ mice when compared to those of *Ripk3*$^{-/-}$*Casp8*$^{-/-}$ mice. *Ripk3*$^{-/-}$*Casp8*$^{DA/DA}$ mice had CD3^{+} cells that expanded into the while pulp compressing the remaining follicles, whereas follicular architecture was persevered in the *Ripk3*$^{-/-}$*Casp8*$^{-/-}$ mice and lymphocyte proliferation was restricted to the marginal zone (**Fig 4.4**). Surprisingly, *Ripk3*$^{-/-}$*Casp8*$^{DA/DA}$ mice had robust infiltration of macrophages and monocytes in both the white and red pulp of the spleen (**Fig 4.4**). These data implicated myeloid cells as well as CD3^{+} lymphocytes in the observed splenomegaly in *Ripk3*$^{-/-}$*Casp8*$^{DA/DA}$ mice. We then sought to characterize differences in circulating cell populations as well as those in secondary lymphoid structures that did not display differences in total organ weight or cellularity.

4.3.3 Ablation of the apoptotic activity of caspase-8 correlates with innate immune population expansion in secondary lymphoid organs.

Previous groups have described a population CD3^{+}B220^{+} cells that mediates the lymphadenopathy in *Ripk3*$^{-/-}$*Casp8*$^{-/-}$ mice [104, 105]. However, *Ripk3*$^{-/-}$*Casp8*$^{DA/DA}$ mice

do not have this population suggesting that there is a clear divergence between the phenotypes of *Ripk3*$^{-/-}$*Casp8*$^{DA/DA}$ and *Ripk3*$^{-/-}$*Casp8*$^{-/-}$ mice. Therefore, we characterized *Ripk3*$^{-/-}$*Casp8*$^{DA/DA}$ mice in comparison with *Ripk3*$^{-/-}$ controls, and observed that *Ripk3*$^{-/-}$*Casp8*$^{DA/DA}$ mice had no observable lymphadenopathy and even displayed a trend to overall lower cell counts in their mesenteric lymph nodes (mLNs) (**Fig 4.2C** and **Fig 4.5A**). In the mLNs we observed a decrease in overall $CD8^+$ T cells with a trend towards lower $CD4^+$ T cell numbers (**Fig 4.5B** and **Fig 4.6A**). In the blood there was also a trend towards an increase in $CD8^-CD4^-CD3^+$ cells which is concordant with our histological observations in the spleen (**Fig 4.5C**). There was a large increase in total numbers of monocytes/macrophages and neutrophils in the mLNs of *Ripk3*$^{-/-}$*Casp8*$^{DA/DA}$ mice when compared to *Ripk3*$^{-/-}$ mice (**Fig 4.5D**, **Fig 4.5E** and **Fig 4.6B**). These data suggested that caspase-8 apoptotic activity is required for maintenance of homeostatic levels of myeloid populations in secondary lymphoid organs. However, it is unclear why the expansion of myeloid cells was not observed in *Ripk3*$^{-/-}$*Casp8*$^{-/-}$ mice [105]. The other group describing these mice observed no differences in frequencies of neutrophils and monocytes in the lymph node that they analyzed [104]; however, they do not state which lymph node they isolated, and they did not calculate total cell numbers. Data that we will discuss in **Chapter 6** suggest that *Ripk3*$^{-/-}$*Casp8*$^{-/-}$ mice do not have increased numbers of myeloid cells in the context of bacterial infection. The observed decrease in $CD8^+$ T cells in the mLNs of *Ripk3*$^{-/-}$*Casp8*$^{DA/DA}$ mice prompted us to investigate if these mice had any defects in thymic development.

4.3.4 Caspase-8 apoptosis is dispensable for T cell development in the thymus.

The observed accumulation of $CD3^+CD4^-CD8^-$ cells in the spleen as well as the decrease in overall $CD8^+$ T cell numbers suggested a defect in the transition of DN to DP cells in the thymus. However, we were unable to observe any differences between *Ripk3*$^{-/-}$*Casp8*$^{DA/DA}$ and *Ripk3*$^{-/-}$ mice in progression from DN to DP nor in positive selection of $CD4^+$ and $CD8^+$ single positive cells expressing TCRβ (**Fig 4.7A**). Moreover we could not observe any difference in thymic weights or cellularity between *Ripk3*$^{-/-}$*Casp8*$^{DA/DA}$ and *Ripk3*$^{-/-}$ mice (**Fig 4.7B** and **Fig 4.7C**). We then measured the sensitivity of DP and single positive thymocytes to Fas stimulation with the expectation that they should be protected due to the ablation of caspase-8 apoptotic activity. However, we were surprised to find that only DP and $CD4^+$ thymocytes from *Ripk3*$^{-/-}$*Casp8*$^{DA/DA}$ mice were protected from Fas-dependent apoptosis (**Fig 4.7E** and **Fig 4.7F**). $CD8^+$ cells were not protected from Fas-dependent apoptosis, which could explain why we observed less overall $CD8^+$ cells in the mLNs of *Ripk3*$^{-/-}$*Casp8*$^{DA/DA}$ mice (**Fig 4.5B** and **Fig 4.7D**). These data were unexpected as complete ablation of caspase-8 protects thymocytes from Fas-dependent apoptosis, but the group that reported this phenotype only performed this analysis on bulk thymocytes [105] of which DP cells are the majority of the total population. We found that these cells have no defect in caspase-9-mediated apoptosis—cell death induced by the caspase-8/9 agonist staurosporine was more robust in *Ripk3*$^{-/-}$*Casp8*$^{DA/DA}$ single positive thymocytes (**Fig 4.7D**, **Fig 4.7E** and **Fig 4.7F**). Overall these data suggest that the non-apoptotic conformation of caspase-8 is sufficient to mediated Fas-dependent cell death in $CD8^+$ thymocytes, but not in $CD4^+$ or DP cells.

4.4 Discussion

Given the recent evidence that caspase-8 mediates cell death as well as inflammatory gene expression [75, 77, 110] we sought to specifically evaluate the contribution of caspase-8-dependent cytokine production to host defense *in vivo*. Caspase-8 apoptotic activity is stabilized through the auto-processing of a linker sequence between the p10 and p20 subunit of each caspase-8 monomer [79, 80]. We generated a mouse in which the residue that is required for this cleavage is mutated (D387A) [80] preventing auto-processing, and destabilizing the apoptotic conformation of caspase-8. We have previously demonstrated that macrophages derived from these mice are protected from caspase-8-dependent apoptosis, but produce inflammatory cytokines when stimulated with LPS [75]. These mice were further crossed onto *Ripk3*$^{-/-}$ mice to generate a line that was deficient for caspase-8-mediated apoptosis and RIPK3-dependent programmed necrosis, but sufficient for the cytokine regulatory function of caspase-8. These mice were generated in an effort to directly compare mice in which caspase-8 is completely ablated—which must be done on a RIPK3-deficient background—to mice expressing the conformation of caspase-8 that mediates inflammatory cytokine expression. We performed initial characterizations of the progeny of these crosses with the expectation that their phenotype would largely recapitulate that of *Ripk3*$^{-/-}$*Casp8*$^{-/-}$ mice. While there were superficial similarities between these mice, such as splenomegaly, there were pronounced differences in immune cell populations between each line.

Ripk3$^{-/-}$*Casp8*$^{DA/DA}$ display splenomegaly characterized by a disruption in splenic architecture (**Fig 4.4**). The reasons for this disruption are not clear as caspase-8-dependent apoptosis is known to play a role in overall embryonic development, but to our knowledge

no one has implicated this function in the development of germinal centers in the spleen. RIPK3 is dispensable for development of these structures as *Ripk3*$^{-/-}$ mice have no histological defects in their splenic architecture (**Fig 4.4**). Furthermore, a defect in apoptosis is not sufficient to explain the aberrant splenic architecture in *Ripk3*$^{-/-}$*Casp8*$^{DA/DA}$ mice as *Ripk3*$^{-/-}$*Casp8*$^{-/-}$ mice do not have this phenotype. It is possible that this disruption is not due to a defect in development per se, but rather due to myeloid and CD3^{+} lymphocyte infiltrate into the while pulp of the spleens isolated from *Ripk3*$^{-/-}$*Casp8*$^{DA/DA}$ mice; however, this explanation is entirely speculative.

The observed accumulation of myeloid cells in the mLNs of *Ripk3*$^{-/-}$*Casp8*$^{DA/DA}$ mice was surprising given that *Ripk3*$^{-/-}$*Casp8*$^{-/-}$ mice are not reported to display this type of cellular accumulation. One potential explanation is that because caspase-8 promotes the secretion of chemokines (**Chapter 2**) there is sufficient recruitment of myeloid cells from the bone marrow, but because apoptosis is impaired there is a defect in clearance under steady-state conditions. Neutrophils in particular have a very short circulating half-life (5-6hrs) [189]; therefore, caspase-8 apoptotic activity might play a critical role in control of neutrophil numbers. These data, while interesting, also require further mechanistic investigation to define the role of caspase-8-mediated apoptosis in monocyte and neutrophil turnover.

The most notable hallmark of the lymphoproliferative disease seen in *Ripk3*$^{-/-}$*Casp8*$^{-/-}$ mice is their accumulation of CD3^{+}B220^{+}CD4^{-}CD8^{-} lymphocytes—this phenotype largely mimics observations in *lpr* and *gld* mice which have defects in the genes encoding Fas and FasL respectively [105, 186]. Interestingly, we observed an accumulation of CD3^{+} cells in the spleens of *Ripk3*$^{-/-}$*Casp8*$^{DA/DA}$ mice as well as a trend towards

accumulation in the blood, but these cells do not express $B220^+$; suggesting they are an alternative population of double negative T cells. We hypothesized that this accumulation was due to a defect in thymic development leading to an increase in the circulation of double negative cells in the periphery, but our characterizations of thymic cellularity, thymic weight, and T cell development revealed no differences between *Ripk3*$^{-/-}$*Casp8*$^{DA/DA}$ and *Ripk3*$^{-/-}$ mice (**Fig 4.7**). More comprehensive analysis is required to determine what lymphocyte population these cells belong to, and whether these cells mediate the splenomegaly we observed in *Ripk3*$^{-/-}$*Casp8*$^{DA/DA}$ mice. More intriguingly, if this population of $CD3^+CD4^-CD8^-B220^-$ cells is limited by caspase-8-dependent apoptosis then these data implicate caspase-8 in the regulation of a novel cell population under steady-state conditions.

Overall, these data demonstrate a specific role for caspase-8-mediated apoptosis in maintenance of myeloid and $CD3^+$ lymphocyte populations in naïve mice; however, non-cleavable caspase-8 appears to be sufficient to prevent the accumulation of $CD3^+B220^+CD4^-CD8^-$ cells in the periphery. The expression of non-cleavable caspase-8 is also sufficient to mediate Fas-dependent apoptosis in $CD8^+$ thymocytes, but not in double positive or $CD4^+$ populations. In **Chapter 3** we demonstrated that *Ripk3*$^{-/-}$*Casp8*$^{DA/DA}$ and *Ripk3*$^{-/-}$ macrophages secrete cytokines to the same magnitude when stimulated with the TLR4 agonist LPS. We also observed that the cytokine regulatory function of caspase-8 is partially dependent on its enzymatic activity, which suggests that non-cleavable caspase-8 is enzymatically active in this context. It is possible that in $CD8^+$ cells the non-cleavable conformation of caspase-8 is sufficient to mediate Fas-induced apoptosis, which would reflect novel differences in caspase-8 enzymatic and structural requirements for the

induction of cell death in naïve T cell populations. In **Chapters 5** and **6** we explore the role non-cleavable caspase-8 plays in host defense *in vivo*.

4.5 Figures

Expected Phenotype	*Ripk3*$^{-/-}$	*Ripk3*$^{-/-}$ *Casp8*$^{DA/DA}$	*Ripk3*$^{-/-}$ *Casp8*$^{-/-}$
Apoptosis	+	−	−
Programmed Necrosis	−	−	−
Gene Expression	+	+	−

Fig 4.1 RIPK3-null *Casp8*$^{DA/DA}$ mice are expected to be deficient in cell death pathways.

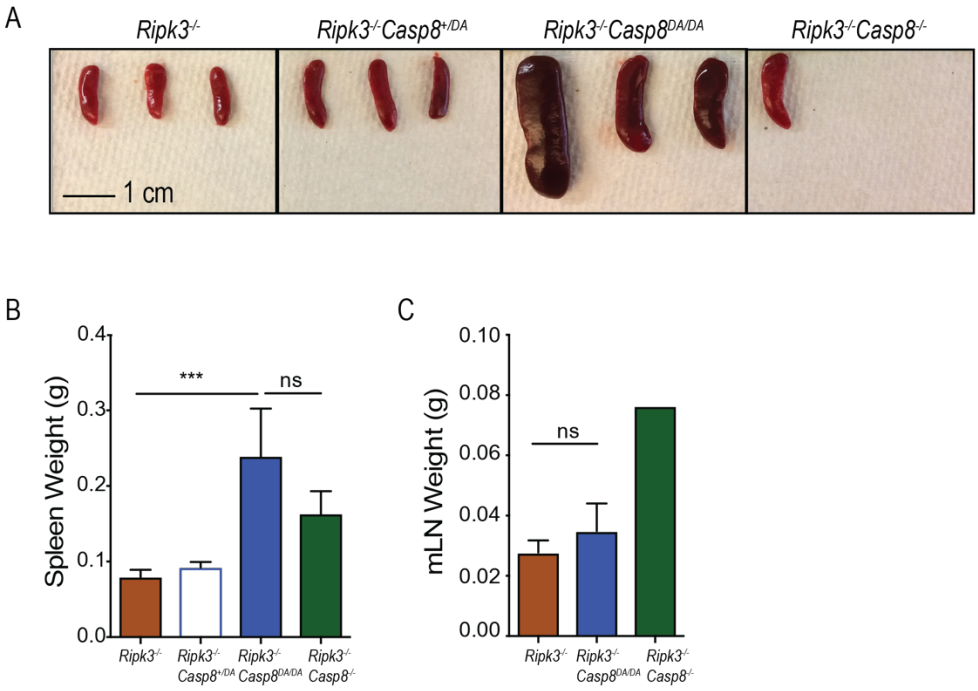

Fig 4.2 Ablation of capsase-8 apoptotic activity mediates splenomegaly.

(A) Images of spleens isolated from 16-week-old female littermates (*Ripk3*$^{-/-}$, *Ripk3*$^{-/-}$*Casp8*$^{DA/DA}$, *Ripk3*$^{-/-}$*Casp8*$^{DA/+}$ and *Ripk3*$^{-/-}$*Casp8*$^{-/-}$).

(B) Weights of spleens isolated from 16-week-old female mice (*Ripk3*$^{-/-}$, *Ripk3*$^{-/-}$*Casp8*$^{DA/DA}$, *Ripk3*$^{-/-}$*Casp8*$^{DA/+}$, and *Ripk3*$^{-/-}$*Casp8*$^{-/-}$; n=3-7 per mouse).

(C) Weights of mLNs isolated from 16-week-old female mice (*Ripk3*$^{-/-}$, *Ripk3*$^{-/-}$*Casp8*$^{DA/DA}$, and *Ripk3*$^{-/-}$*Casp8*$^{-/-}$; n=3-4 except *Ripk3*$^{-/-}$*Casp8*$^{-/-}$ n=1).

Student's two-tailed unpaired t-test (n.s. not significant, *** $p<0.001$). Error bars indicate ± SEM. Pooled data from two different experiments.

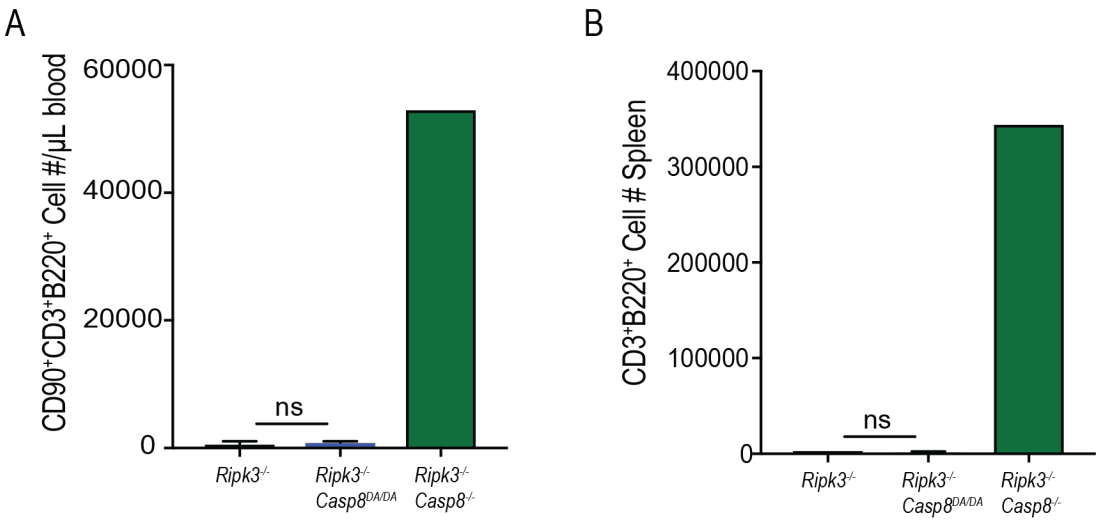

Fig 4.3 Non-cleavable capsase-8 protects mice from $CD3^+B220^+$ cell accumulation.

(A) Total numbers of live $Lin^-CD90^+CD3^+CD4^-CD8^-B220^+$ lymphocytes isolated from the blood of 16 week old female littermates (*Ripk3*$^{-/-}$, *Ripk3*$^{-/-}$*Casp8*$^{DA/DA}$, and *Ripk3*$^{-/-}$*Casp8*$^{-/-}$; n=3 except *Ripk3*$^{-/-}$*Casp8*$^{-/-}$ n=1).

(B) Total numbers of live $Lin^-CD3^+CD4^-CD8^-B220^+$ lymphocytes isolated from the spleens of 16-week-old female littermates (*Ripk3*$^{-/-}$, *Ripk3*$^{-/-}$*Casp8*$^{DA/DA}$, and *Ripk3*$^{-/-}$*Casp8*$^{-/-}$; n=3 except *Ripk3*$^{-/-}$*Casp8*$^{-/-}$ n=1).

Student's two-tailed unpaired t-test (n.s. not significant). Error bars indicate ± SEM. All data representative of two independent experiments. Lineage markers (CD19 and NK1.1)

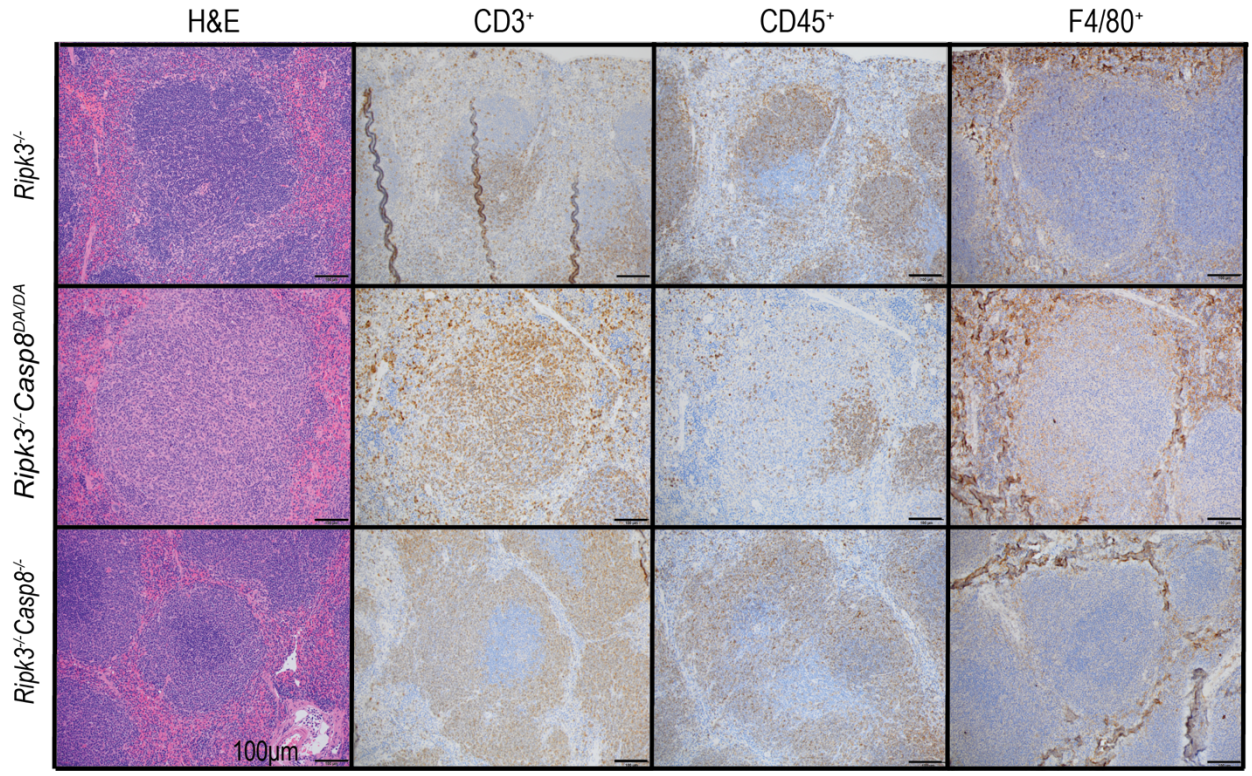

Fig 4.4 RIPK3-null *Casp8*$^{DA/DA}$ mice have disrupted splenic architecture and increased immune cell infiltrate.

Representative images from H&E, CD3, CD45 and F4/80 stained spleen paraffin sections prepared by the Children's Hospital of Philadelphia Pathology Core. Analysis of sections performed by Penn Veterinary Medicine Pathology Core (*Ripk3*$^{-/-}$ n=6, *Ripk3*$^{-/-}$*Casp8*$^{DA/DA}$ n=7, *Ripk3*$^{-/-}$*Casp8*$^{-/-}$ n=2).

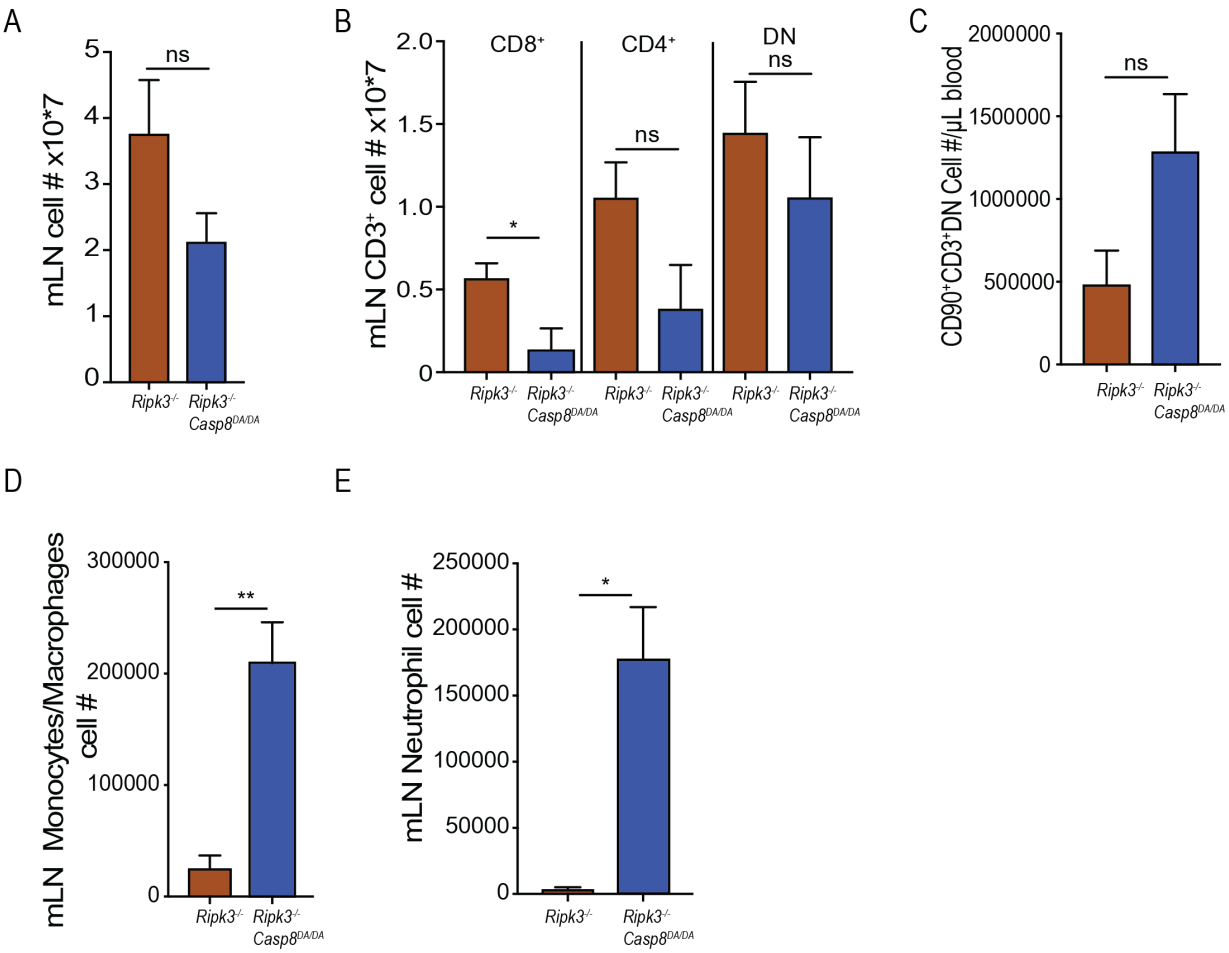

Fig 4.5 RIPK3-null *Casp8*$^{DA/DA}$ mice have expanded populations of myeloid cells in secondary lymphoid organs.

(A) Total cell numbers in mLNs isolated from *Ripk3*$^{-/-}$ and *Ripk3*$^{-/-}$*Casp8*$^{DA/DA}$ mice (n=3).

(B) Live^{+}CD3^{+} lymphocytes isolated from the mLNs of *Ripk3*$^{-/-}$ and *Ripk3*$^{-/-}$*Casp8*$^{DA/DA}$ mice (n=3).

(C) Live^{+}CD90^{+}CD3^{+}CD4^{-}CD8^{-} lymphocytes in the blood of *Ripk3*$^{-/-}$ and *Ripk3*$^{-/-}$*Casp8*$^{DA/DA}$ mice (n=3).

(D) Live^{+}CD3^{-}CD19^{-}CD45^{+}F4/80^{+} cells isolated from the mLNs of *Ripk3*$^{-/-}$ and *Ripk3*$^{-/-}$*Casp8*$^{DA/DA}$ mice (n=3).

Fig 4.5 continued: (D) Live^{+}CD3^{-}CD19^{-}CD45^{+}Ly6G^{+}Ly6C^{+} cells isolated from the mLNs of *Ripk3*$^{-/-}$ and *Ripk3*$^{-/-}$*Casp8*$^{DA/DA}$ mice (n=3).

Student's two-tailed unpaired t-test (n.s. not significant, * $p<0.05$, ** $p<0.01$). Error bars indicate ± SEM. All data representative of two independent experiments.

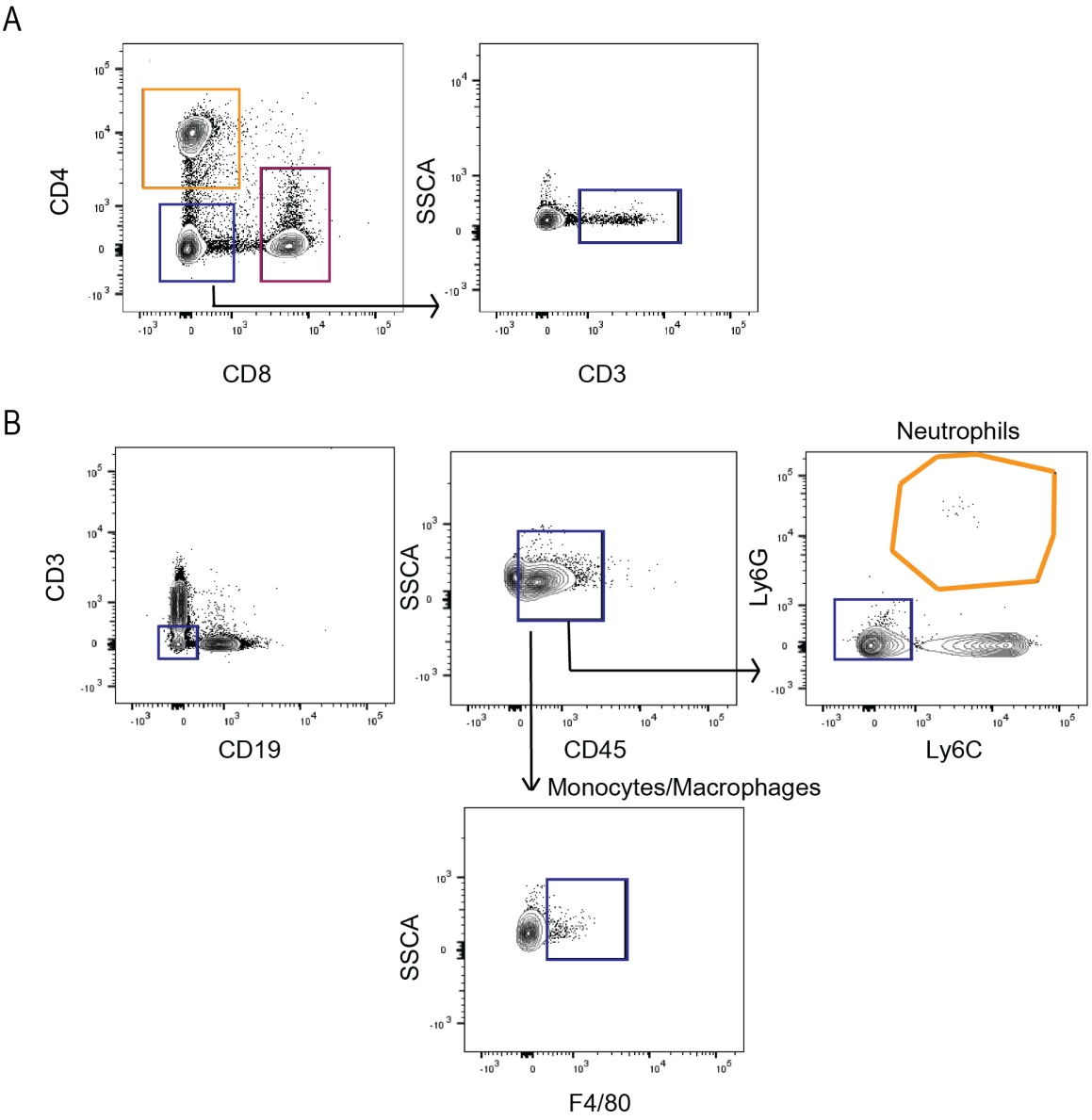

Fig 4.6 Representative gating strategy for the characterization of both innate and adaptive immune populations in RIPK3-null *Casp8*$^{DA/DA}$ mice.

(A). Flow contour plot showing gating strategy for classification of CD4^{+}, CD8^{+} and DN T cells isolated from the mLN of a *Ripk3*$^{-/-}$ mouse.

(B). Flow contour plot showing gating strategy for classification of innate immune cell populations isolated from the mLN of a *Ripk3*$^{-/-}$ mouse.

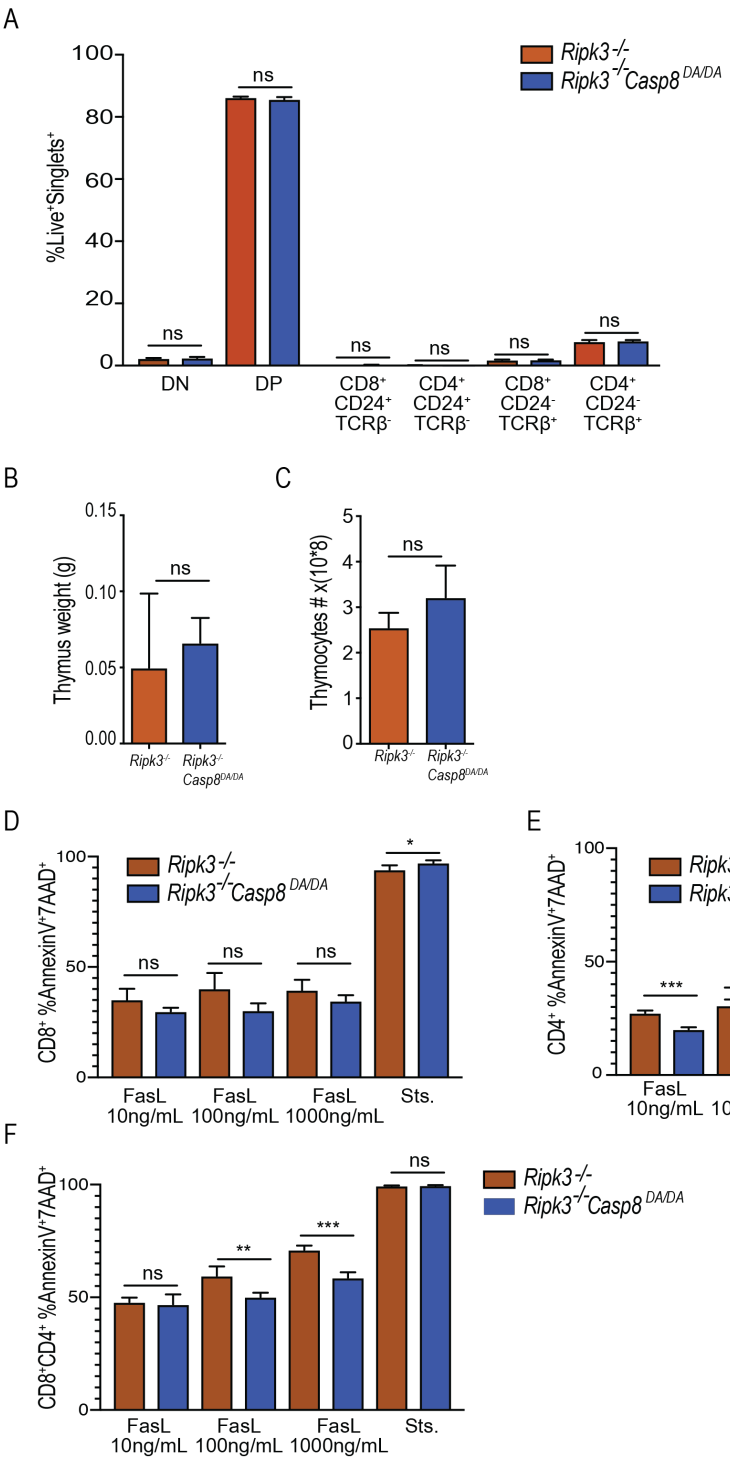
A
%Live+Singlets+
Ripk3-/-
Ripk3-/-Casp8DA/DA
ns
DN
DP
CD8+ CD24+ TCRβ-
CD4+ CD24+ TCRβ-
CD8+ CD24- TCRβ+
CD4+ CD24- TCRβ+
B
Thymus weight (g)
C
Thymocytes # x(10*8)
D
CD8+ %AnnexinV+7AAD+
E
CD4+ %AnnexinV+7AAD+
FasL 10ng/mL
FasL 100ng/mL
FasL 1000ng/mL
Sts.
F
CD8+CD4+ %AnnexinV+7AAD+

Fig 4.7 RIPK3-null *Casp8*$^{DA/DA}$ mice have normal T cell development and are partially protected from Fas-dependent apoptosis.

(A) Total numbers of DN, DP and single positive thymocytes isolated from *Ripk3*$^{-/-}$ and *Ripk3*$^{-/-}$*Casp8*$^{DA/DA}$ mice (n=3-4). Cells gated on live, singlets that were lineage negative. Lineage markers (CD11b, CD11c, CD19, CD49, and Gr-1).

(B). Total weights of thymi isolated from *Ripk3*$^{-/-}$ and *Ripk3*$^{-/-}$*Casp8*$^{DA/DA}$ mice (n=3-4).

(C). Total cell counts of thymi isolated from *Ripk3*$^{-/-}$ and *Ripk3*$^{-/-}$*Casp8*$^{DA/DA}$ mice (n=3-4).

(D-E). Frequency of Annexin V^{+}7AAD^{+} CD8^{+}, CD4^{+} and DP thymocytes isolated from *Ripk3*$^{-/-}$ and *Ripk3*$^{-/-}$*Casp8*$^{DA/DA}$ and stimulated with the indicated concentrations of FasL (with 25μg/mL cycloheximide) for 24hrs or 10μM staurosporine for 8hrs. (n=3-4 mice/group).

Student's two-tailed unpaired t-test (n.s. not significant, * $p<0.05$, ** $p<0.01$, *** $p<0.001$). Error bars indicate ± SEM. All data representative of two independent experiments.

CHAPTER 5: Caspase-8 promotes host survival during acute *Toxoplasma gondii* infection.

5.1 Abstract

Caspase-8 has been recently implicated in the regulation of inflammatory gene expression. Caspase-8-dependent cytokine secretion has been shown to mediate host defense in response to gram-negative bacterial pathogens *in vivo*; however, it is unclear if this function is required in other contexts. *Il12b* expression as well as the secretion of IL-12p40 are significantly impaired in macrophages lacking caspase-8. IL-12p40 serves as a subunit of both IL-23 and IL-12p70, two cytokines known to be important for host survival during infection with a variety of pathogens. IL-12p70 is specifically critical for the control of acute infection with the obligate, intracellular parasite *Toxoplasma gondii*. *T. gondii* belongs to the Apicomplexa phylum which contains other pathogens such as *Plasmodium* and *Cryptosporidium parvum*. *T. gondii* infects mammals through food or water contaminated with cysts excreted in cat feces leading to a significant amount of foodborne illness in the United States annually. C57BL/6 mice survive infection with the attenuated strain of *T. gondii* (Prunigard), and this survival is dependent on the secretion of IL-12p70 by dendritic cells. We show that caspase-8-deficient mice have an acute survival defect that largely recapitulates the observed phenotype in IL-12p40-deficient mice. Moreover, this defect is characterized by lower levels of IL-12p40 production by caspase-8-deficient dendritic cells, and impaired monocyte recruitment into the peritoneum of infected animals. Caspase-8-deficient animals can be rescued through exogenous injection of IL-12p70, leading to parasite clearance, and recruitment of inflammatory monocytes. To our knowledge these are the first studies implicating caspase-8-mediated cytokine secretion in host survival against a eukaryotic pathogen.

5.2 Introduction

Caspase-8 plays a cell-intrinsic role in inflammatory cytokine secretion *in vitro* and *in vivo* during infection with the gram-negative bacterial pathogen *Yersinia pseudotuberculosis* [75]. Others have demonstrated a role for caspase-8 in cytokine secretion during infection with another gram-negative enteric pathogen *Citrobacter rodentium* [110]. However, to our knowledge no one has tested the role for caspase-8 in survival during infection with a eukaryotic pathogen. *Toxoplasma gondii* is endemic to the United States, and causes a significant percentage of domestic foodborne illness cases annually [136]. Most carriers are asymptomatic, but pregnant women and immunocompromised individuals are at significant risk for life-threatening complications associated with toxoplasmosis [135]. C57BL/6 mice largely survive acute infection with the attenuated Prunigard strain of *T.gondii*, and this survival is dependent on the production of IL-12 [137], and *Il12b*$^{-/-}$ mice rapidly succumb to acute *T. gondii* infection [138].

The primary source of IL-12 during *T. gondii* infection is thought to be from uninfected inflammatory monocytes and conventional dendritic cells that detect *T. gondii* antigen [139]. Detection of *T. gondii* by dendritic cells is mediated in part by TLR11 and TLR12 upon recognition of profilin [190]. Secreted IL-12 then induces IFNγ production by NK cells in addition to cytotoxic CD8 and CD4 T cells; IFNγ promotes killing of infected cells through cell-extrinsic and cell-intrinsic mechanisms [140, 142, 191-193]. Interestingly, *T. gondii* actively suppresses apoptosis; therefore, the primary mechanism of clearance is T-cell-mediated killing or induction of intracellular reactive oxygen species in infected cells [142, 144, 145, 194]. Cytokine secretion is particularly important in this

context as it is required for the recruitment of T cells as well as paracrine signaling from bystander cells to infected cells.

We have shown that caspase-8-deficient macrophages have a defect in the expression of *Il12b* and secretion of IL-12p40 (**Chapter 2**). Moreover, *in vivo* there is a cell-intrinsic defect in IL-12p40 production in caspase-8-deficient monocytes and neutrophils during gram-negative bacterial infection [75]. These data provoked the hypothesis that caspase-8 may play a role in host defense during *T. gondii* infection via its cytokine regulatory function, specifically through the expression of IL-12. Although caspase-8 mediates both cell death and inflammatory cytokine expression, host defense during *T. gondii* infection is largely dependent on cytokine production by responding innate immune cells. Therefore, we hypothesized that caspase-8-mediated cell death would be dispensable for host survival during *T. gondii* infection.

We utilized two models to interrogate the role of caspase-8 in host defense against *T. gondii*: one in which caspase-8 was completely ablated, and one in which caspase-8-apoptotic activity was disrupted while preserving its cytokine regulatory function. We found a requirement for caspase-8 in host survival during *T. gondii* infection that was indistinguishable from the requirement for IL-12. Moreover, caspase-8-deficient animals had a defect in IL-12p40 production by dendritic cells, and survival of these mice could be completely rescued through the exogenous injection of IL-12p70. To our knowledge these data are the first to demonstrate a role for caspase-8 in host survival during infection with an intracellular, eukaryotic pathogen via the cytokine regulatory function of caspase-8.

5.3 Results

5.3.1 Caspase-8-deficient animals are acutely susceptible to *T. gondii* infection.

IL-12-deficient animals have a pronounced survival defect during intraperitoneal infection with a low dose (10,000 tachyzoites) of an attenuated strain of *T. gondii* (Prunigard, Pru). We observed a role for caspase-8 in the induction of *Il12b* in macrophages, but *Il12b* expression and IL-12p40 secretion are not completely abrogated in this context. Therefore, we were surprised to find that *Ripk3*$^{-/-}$*Casp8*$^{-/-}$ mice were just as susceptible to *T. gondii* infection as *Il12b*$^{-/-}$ mice (**Fig 5.1A**). *Ripk3*$^{-/-}$*Casp8*$^{-/-}$ mice had parasite burdens that were statistically indistinguishable from *Il12b*$^{-/-}$ mice suggesting that caspase-8 mediates host survival through control of parasite replication (**Fig 5.1C**). Cytospins of peritoneal exudate cells (PECs) also show that *Il12b*$^{-/-}$ and *Ripk3*$^{-/-}$*Casp8*$^{-/-}$ mice have similar numbers of parasites per cell (**Fig 5.1B** and **Fig 5.1D**). Dendritic cells (DCs) in the PECs of infected *Ripk3*$^{-/-}$*Casp8*$^{-/-}$ mice had impaired production of IL-12p40 (**Fig 5.2A)**. Representative flow plots show the gating strategy for identifying Lin^{-} CD64^{-}CD11c^{+}MHCII^{+} DCs as well as representative IL-12p40 staining in DCs from the PECs of B6, *Ripk3*$^{-/-}$, *Ripk3*$^{-/-}$*Casp8*$^{-/-}$, and *Il12b*$^{-/-}$ mice 5 days post infection (**Fig 5.2B** and **Fig 5.2C**). As dendritic cells are the primary mediators of IL-12p40 production during *T. gondii* infection these data suggest that impaired survival of caspase-8-deficient animals was due to failure to induce sufficient IL-12p40. Interestingly, IL-12p40 production by DCs in *Ripk3*$^{-/-}$*Casp8*$^{-/-}$ mice was not completely abrogated, but this amount of cytokine production appeared to be below the threshold required to mediate host survival.

5.3.2 IL-12 rescues caspase-8-deficient animals during acute *T. gondii* infection.

We hypothesized that exogenous IL-12 would restore host survival in caspase-8-deficient animals by compensating for the observed defect in IL-12 production by DCs. As expected IL-12 injections rescued *Il12b*$^{-/-}$ mice, and were also sufficient to completely rescue *Ripk3*$^{-/-}$*Casp8*$^{-/-}$ mice (**Fig 5.3A**). Moreover, IL-12 treatment reduced parasite burdens in *Ripk3*$^{-/-}$*Casp8*$^{-/-}$ mice to levels observed in B6 and *Ripk3*$^{-/-}$ mice (**Fig 5.3B** and **Fig 5.3C**). Another mechanism of parasite control is through infiltration of inflammatory monocytes that promote parasite killing [195]. We observed a defect in recruitment of inflammatory monocytes by total cell number as well as frequency into the peritoneum of caspase-8-deficient animals (**Fig 5.3D** and **Fig 5.3E**). Interestingly, this impaired recruitment was very similar to that observed in *Il12b*$^{-/-}$ mice, again suggesting that a threshold of IL-12 production is required to mount an innate response to *T. gondii* infection. We were also able to restore infiltration of inflammatory monocytes with the injection of exogenous IL-12. While these data are correlative they suggest that caspase-8-dependent IL-12 secretion mediates host defense during *T. gondii* infection.

5.3.3 IL-12 rescues c-Rel-deficient animals during acute *T. gondii* infection.

We have previously shown that in macrophages caspase-8 promotes *Il12b* expression in part through the transcription factor c-Rel (**Chapter 2**). Previous groups have shown that c-Rel-dependent IL-12 is important for the adaptive response in an oral model of *T. gondii* [196]. However, to our knowledge no one has investigated the contribution of c-Rel to intraperitoneal infection with *T. gondii* tachyzoites. We found that *Rel*$^{-/-}$ animals succumbed with similar kinetics to *Il12b*$^{-/-}$ animals, and that these mice were completely

rescued by exogenous IL-12 (**Fig 5.4**). We interpret these data to mean that c-Rel dependent IL-12 may also be protective in the intraperitoneal infection model of *T. gondii*, implicating caspase-8 in the c-Rel/IL-12 axis in this system.

5.3.4 Expression of non-cleavable caspase-8 reduced host mortality during acute *T. gondii* infection.

Although there is no reported role for caspase-8-dependent apoptosis in host defense during *T. gondii* infection—this pathway is repressed in *T.gondii*-infected cells—it was formally possible that caspase-8-dependent apoptosis contributes to survival. To specifically test the contribution of caspase-8-mediated inflammatory cytokine secretion during *T. gondii* infection we utilized a mouse model in which caspase-dependent apoptosis and RIPK3-mediated programmed necrosis are ablated while preserving caspase-8-cytokine secretion (*Ripk3*$^{-/-}$*Casp8*$^{DA/DA}$). *Ripk3*$^{-/-}$*Casp8*$^{DA/DA}$ mice had reduced mortality during *T. gondii* infection; however, not to the same magnitude as *Ripk3*$^{-/-}$ mice (**Fig 5.5A**). There was also considerable variance in the percentage of infected PECs isolated from *Ripk3*$^{-/-}$*Casp8*$^{DA/DA}$ mice 5 days post infection suggesting that some mice fail to control replication while others are able to (**Fig 5.5B**). These data implicated caspase-8-apoptotic activity in host defense; however, mice that are sufficient for RIPK3, but also express non-cleavable caspase-8 have no detectible parasites in their PECs 5 days post infection (**Fig 5.5C**). One possible explanation for this observation is that RIPK3 may be required to help stabilize the non-cleavable conformation of caspase-8 in dendritic cells during *in vivo* infection with *T. gondii*. This would be surprising given that we can find no role for RIPK3 in protection against *T. gondii*: *Ripk3*$^{-/-}$ mice have identical parasite burdens when

compared to B6 mice (**Fig 5.1C**). However, these data are preliminary as the experiments in panel B and C were only performed once. More experiments are required to determine if there is a synergistic effect between RIPK3 and non-cleavable caspase-8 during *T. gondii* infection.

5.3.5 Ablation of caspase-8 in hematopoietic cells results in increased parasite burdens and a defect in monocyte infiltration.

The observed decrease in IL-12 secretion from caspase-8-deficient DCs suggested that caspase-8-mediated cytokine production in the immune compartment was the primary mechanism that promoted host survival during acute *T. gondii* infection. To test this hypothesis we generated bone marrow chimeras in which B6 mice were sublethally irradiated, and reconstituted with bone marrow from B6, *Ripk3*$^{-/-}$, *Ripk3*$^{-/-}$*Casp8*$^{-/-}$, and *Il12b*$^{-/-}$ mice. These mice had parasite burdens that were concordant with our observations in mice lacking *Ripk3*$^{-/-}$*Casp8*$^{-/-}$ or *Il12b*$^{-/-}$ in both the hematopoietic and non-hematopoietic compartments, suggesting that control of parasite burdens is largely mediated by caspase-8 in immune cells (**Fig 5.6A**). B6 mice with caspase-8 deficiency in their hematopoietic compartment also have impaired monocyte recruitment into their peritoneum 5 days post infection, providing additional evidence that this infiltration is mediated by caspase-8 expression in immune cells (**Fig 5.6B**). These data demonstrate a role for caspase-8 expression in hematopoietic cells during acute *T. gondii* infection.

5.4 Discussion

To our knowledge these data implicate the cytokine regulatory function of caspase-8 in host defense during *T. gondii* infection for the first time (**Fig 5.7**). The defect in IL-12 production by caspase-8-deficient DCs suggests a broad role for caspase-8 in cytokine production in a variety of innate immune cell populations *in vivo*. The observed contribution of c-Rel to host survival provokes the hypothesis that the TLR/caspase-8/c-Rel axis may promote cytokine secretion by DCs as well as macrophages (**Fig 5.8**). We have not tested the *in vitro* requirement for caspase-8 in IL-12 production by DCs infected with *T. gondii* or stimulated with the *T. gondii* antigen STAg (soluble tachyzoite antigen), but it is possible that we would observe a defect in IL-12 production in this context as well.

These data also demonstrate the principle of thresholding in the immune response to inflammatory mediators. It appears that there is a threshold of IL-12 required for mice to mount an early innate response to *T. gondii.* Unlike *Il12b*$^{-/-}$ mice, caspase-8-deficient animals have some IL-12 production, but this amount of IL-12 is not sufficient to promote control of parasite replication or recruitment of inflammatory monocytes into the peritoneum of infected animals. These data are similar to our observations in which caspase-8 expression in immune cells is required for maximal production of cytokines during infection with *Yersinia pseudotuberculosis* [75]. However, the role of caspase-8 in IL-12 production during *T. gondii* infection remains correlative. Mice with cDC-specific depletion [197] would enable us to generate mixed bone marrow chimeras with bone marrow from mice lacking cDCs and bone marrow from mice lacking caspase-8. This will allow us to directly test the cell-intrinsic role of caspase-8, in cDCs *in vivo,* during *T. gondii* infection.

Given the requirement for caspase-8 in protection against an obligate, intracellular, eukaryotic pathogen it would be interesting to test its role in control of another member of the Apicomplexa phylum: *Cryptosporidium parvum.* Recent advances have made it possible to culture *C. parvum in vitro* and inoculate mice with a rodent-adapted strain of the parasite [198]. Very little is known about *C. parvum*-mediated antagonism of the host immune response or the mechanisms of host control; therefore, investigations into the possible role for caspase-8 in this model may provide insight into host-pathogen interactions during *C. parvum* infection *in vivo.*

In these studies we also demonstrated a role for caspase-8-dependent cytokine production separate from caspase-8-dependent apoptosis during *T. gondii* infection. However, on a RIPK3-null background expression of non-cleavable caspase-8 was not sufficient to mediate survival of all infected animals. We also observed significant variability in parasite burdens from PECs isolated from *Ripk3*$^{-/-}$*Casp8*$^{DA/DA}$ mice 5 days post infection. From experiments discussed in **Chapter 4** we know that *Ripk3*$^{-/-}$*Casp8*$^{DA/DA}$ mice have a defect in total numbers of CD8 T cells in their secondary lymphoid organs. CD8 T cells are critical for host defense against *T. gondii,* and can be recruited into the peritoneum very rapidly post infection [191]. Therefore, it is possible that the intermediate survival phenotype observed in *Ripk3*$^{-/-}$*Casp8*$^{DA/DA}$ mice could be attributed to a defect in cytotoxic CD8 T cell recruitment into the peritoneum after infection, and not due to impaired caspase-8-dependent apoptosis. We did not measure IFNγ production by NK cells or adaptive cell populations in any of the experiments we conducted, nor did we test the effector functions of these populations. These outstanding questions provide opportunities for future studies to determine if the observed defect in IL-12 production correlates with

impaired IFNγ production or impaired effector responses during *T. gondii* infection of caspase-8-deficient mice. Collectively, the data described here provide evidence for the broad protective role played by caspase-8 in response to infection, and the specific contribution of caspase-8-mediated cytokine expression to host defense during infection with a eukaryotic pathogen.

5.5 Figures

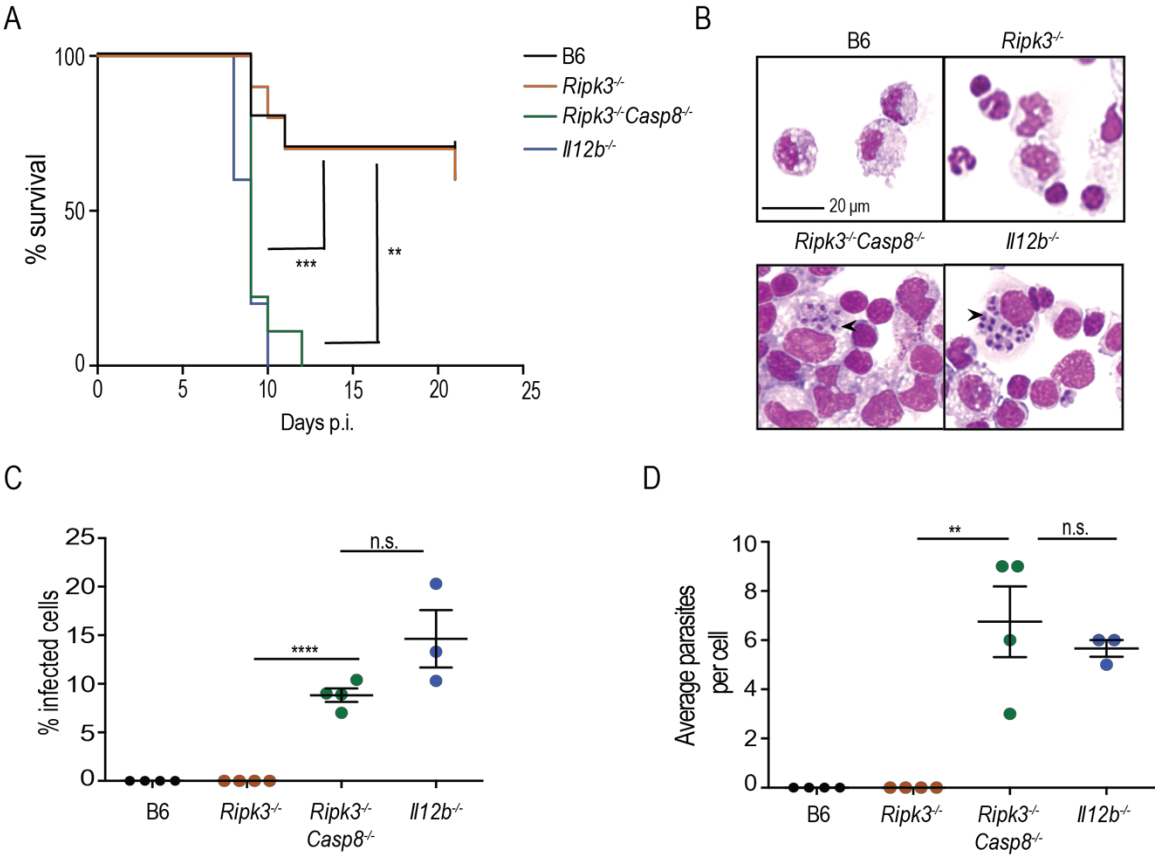

Fig 5.1 Caspase-8 promotes survival during acute *T. gondii* infection.

(A) Survival of B6, *Il12b*$^{-/-}$, *Ripk3*$^{-/-}$, and *Ripk3*$^{-/-}$*Casp8*$^{-/-}$ mice (n=5-10) infected intraperitoneally with *T.gondii*.

(B) Representative cytospins of infected cells in the PECs of *T.gondii*-infected B6, *Il12b*$^{-/-}$, *Ripk3*$^{-/-}$, and *Ripk3*$^{-/-}$*Casp8*$^{-/-}$ mice 5 days post-infection.

(C) Quantification of infected cell frequency and **(D)** parasites per cell in the PECs of *T. gondii*-infected B6, *Il12*$^{-/-}$, *Ripk3*$^{-/-}$, and *Ripk3*$^{-/-}$*Casp8*$^{-/-}$ mice 5 days post-infection; each data point represents a single mouse.

For all infections 10,000 Pru *T. gondii* parasites were injected i.p. (**A**) Mantel-cox test (** $p<0.01$, *** $p<0.001$). (**C**) and (**D**) Student's two-tailed unpaired t-test

Fig 5.1 Continued: (n.s. not significant, ** $p<0.01$, **** $p<0.0001$). Error bars indicate ± SEM. Data representative of three independent experiments.

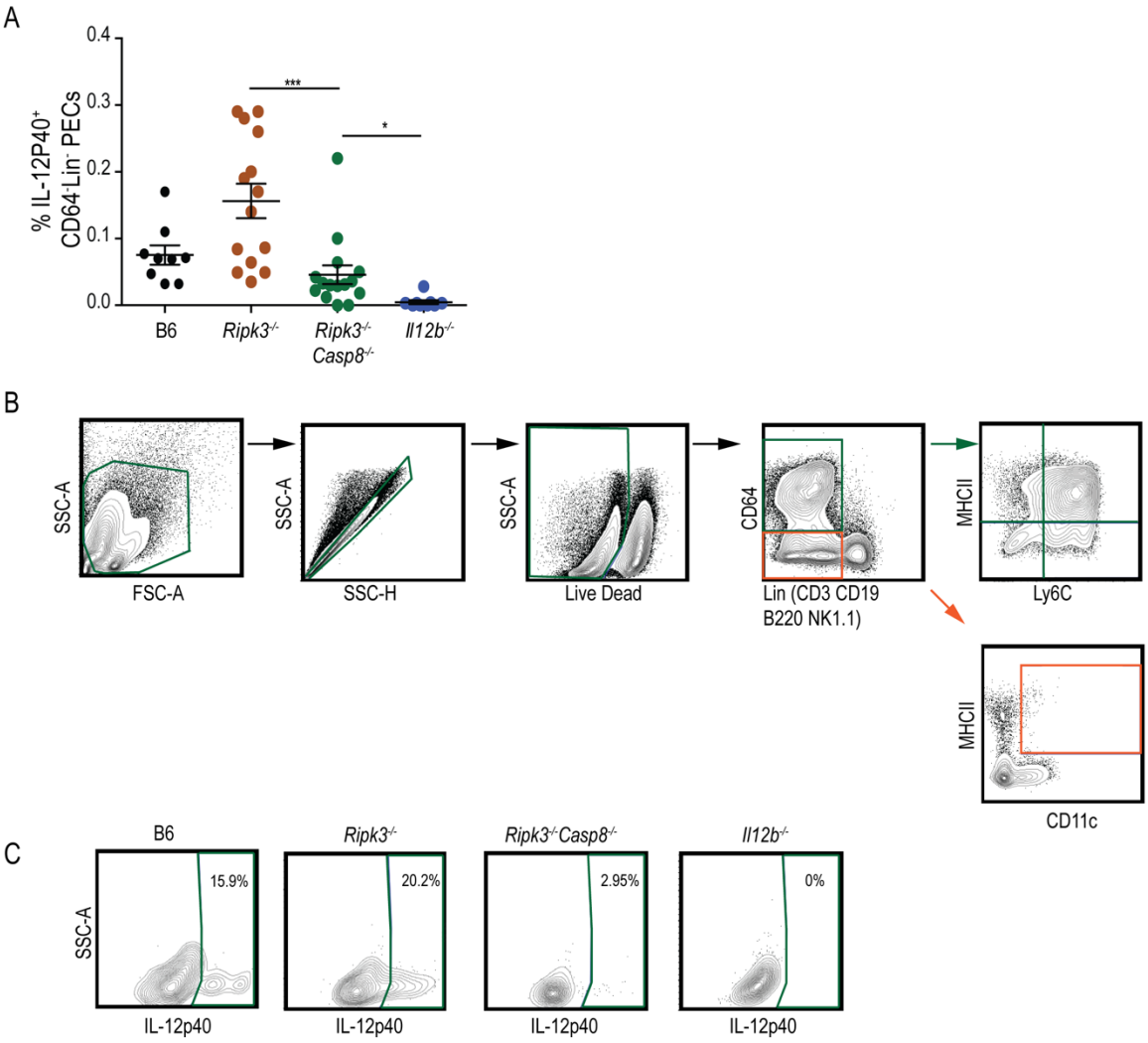

Fig 5.2. Caspase-8 promotes IL-12 production by DCs during acute *T. gondii* infection.

(A) Frequency of IL-12p40$^+$ CD64$^-$Lin$^-$ cells (Live$^+$Singlets$^+$CD19$^-$CD3$^-$B220$^-$ NK1.1$^-$CD64$^-$) in the PECs of *T. gondii*-infected B6, *Il12b*$^{-/-}$, *Ripk3*$^{-/-}$, and *Ripk3*$^{-/-}$*Casp8*$^{-/-}$ mice 5 days post infection.

(B) Representative flow contour plots of the gating strategy for CD11c$^+$MHCII$^+$ DCs (orange) and MHCII$^+$LY6C^{hi} inflammatory monocytes (green) in the PECs of a *T.gondii*-infected B6 mouse 5 days post infection.

(C) Representative flow contour plots of CD11c$^+$MHCII$^+$IL-12p40$^+$ cells from the PECs of *T.gondii*-infected B6, *Il12b*$^{-/-}$, *Ripk3*$^{-/-}$, and *Ripk3*$^{-/-}$*Casp8*$^{-/-}$ mice 5 days post infection.

Fig 5.2 Continued: For all infections 10,000 Pru *T. gondii* parasites were injected i.p. Student's two-tailed unpaired t-test (* $p<0.05$, *** $p<0.001$). Error bars indicate ± SEM. Panel **(A)** is composed to pooled data from three independent experiments.

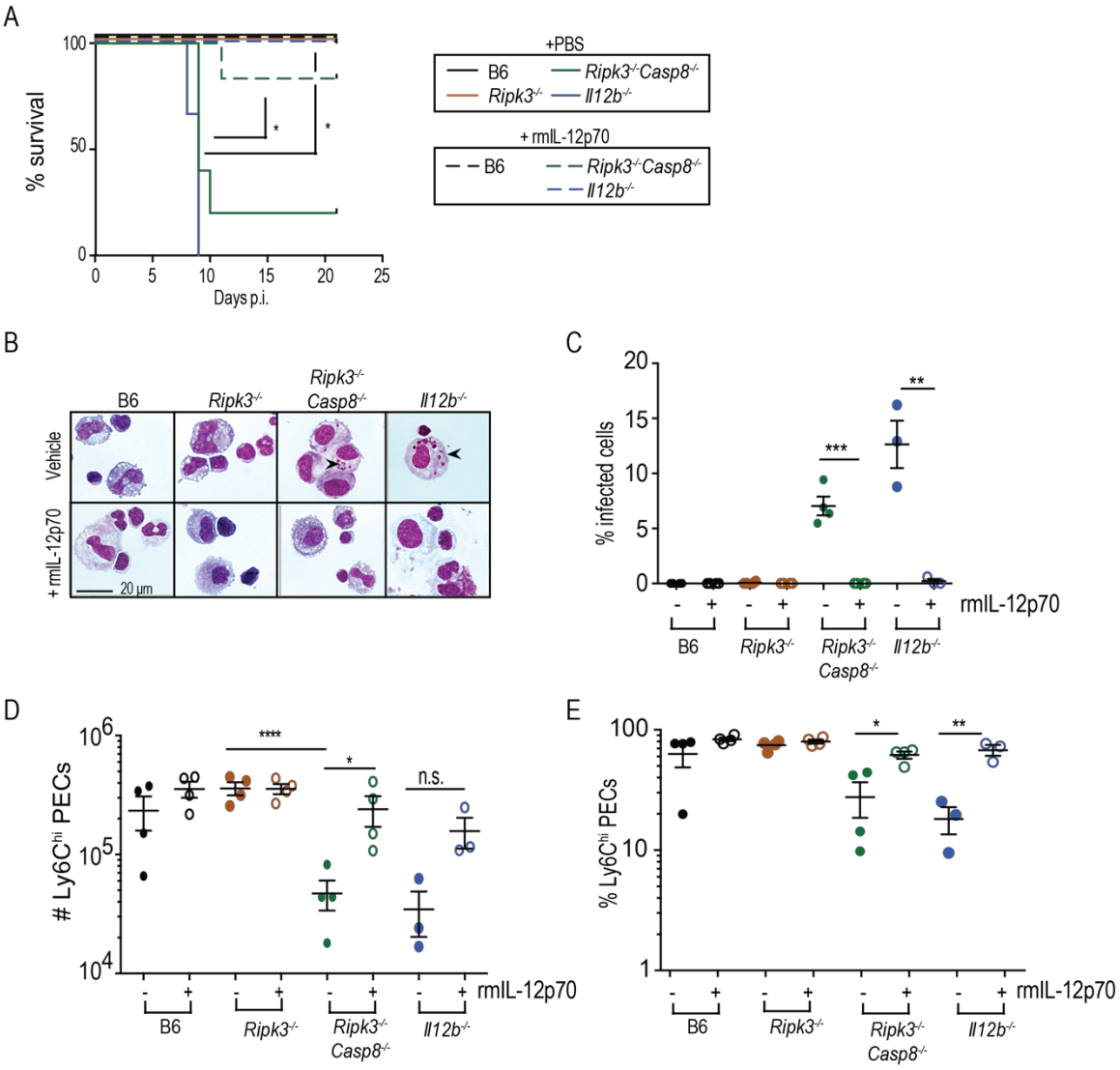

Fig 5.3. Exogenous IL-12 rescues caspase-8-deficient animals during acute *T. gondii* infection.

(A) Survival of mice infected with *T. gondii* and injected i.p. with PBS or rmIL-12p70 (200ng/mouse) for 7 days post infection (n=3-6).

(B) Representative cytospins from PECs isolated 5 days post infection from *T. gondii*-infected B6, *Il12b*$^{-/-}$, *Ripk3*$^{-/-}$, and *Ripk3*$^{-/-}$*Casp8*$^{-/-}$ mice injected i.p. with PBS or rmIL-12p70 for 5 days post infection.

Fig 5.3 Continued: (C) Quantification of the frequency of infected cells in the PECs of PBS or rmIL-12p70-injected *T.gondii*-infected B6, *Il12b*$^{-/-}$, *Ripk3*$^{-/-}$, and *Ripk3*$^{-/-}$*Casp8*$^{-/-}$ mice 5 days post infection, each data point represents a mouse.

(D) Number and **(E)** frequency of inflammatory monocytes (Live^{+}Singlets^{+}CD19^{-}CD3^{-} B220^{-}NK1.1^{-} CD64^{+}MHCII^{+}LY6C^{hi} cells) in the PECs of PBS or rmIL-12p70-injected *T. gondii*-infected B6, *Il12b*$^{-/-}$, *Ripk3*$^{-/-}$, and *Ripk3*$^{-/-}$*Casp8*$^{-/-}$ mice 5 days post infection. Each data point represents one mouse.

For all infections 10,000 Pru *T. gondii* parasites were injected i.p. (**A**) Mantel-cox test (* $p<0.05$). (**B**), (**D**), and (**E**) Student's two-tailed unpaired t-test (n.s. not significant, * $p<0.05$, ** $p<0.01$, *** $p<0.001$, **** $p<0.0001$). Error bars indicate ± SEM. Panels representative of two independent experiments.

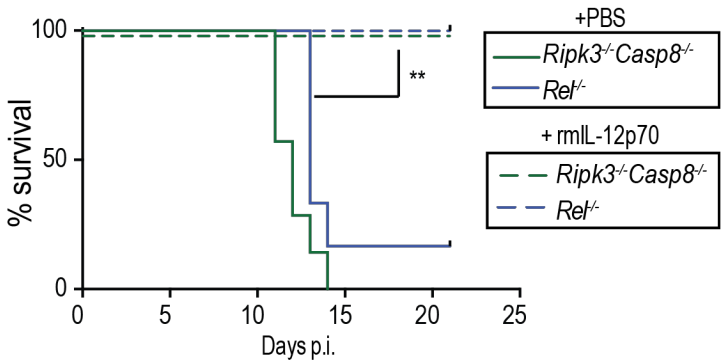

Fig 5.4. Exogenous IL-12 rescues c-Rel-deficient animals during acute *T. gondii* infection. Survival of *Ripk3*$^{-/-}$*Casp8*$^{-/-}$ and *Rel*$^{-/-}$ mice following *T. gondii* infection and injected i.p. with PBS or rmIL-12p70 (200ng/mouse) for 7 days post infection (n=7 per group). Mantel-cox test (** $p<0.01$). For all infections 10,000 Pru *T. gondii* parasites were injected i.p. Representative of two independent experiments.

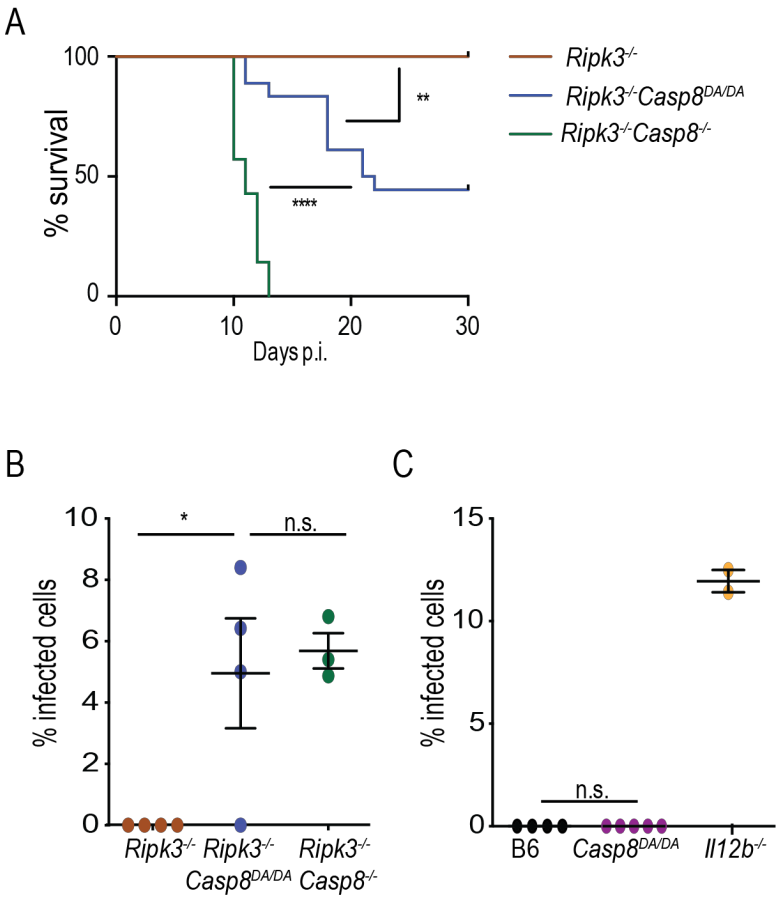

Fig 5.5. Non-cleavable caspase-8 promotes host survival during acute *T. gondii* infection.

(A) Survival of *Ripk3*$^{-/-}$, *Ripk3*$^{-/-}$*Casp8*$^{-/-}$, and *Ripk3*$^{-/-}$*Casp8*$^{DA/DA}$ mice infected with *T. gondii* (n=7-18).

(B) Frequency of infected cells in the PECs of *T.gondii*-infected *Ripk3*$^{-/-}$, *Ripk3*$^{-/-}$*Casp8*$^{-/-}$, and *Ripk3*$^{-/-}$*Casp8*$^{DA/DA}$ mice 5 days post infection, each data point represents a mouse.

(C) Frequency of infected cells in the PECs of *T.gondii*-infected B6, *Casp8*$^{DA/DA}$ mice, and *Il12b*$^{-/-}$ mice 5 days post infection, each data point represents a mouse.

For all infections 10,000 Pru *T. gondii* parasites were injected i.p. (**A**) Mantel-cox test (** $p<0.01$, *** $p<0.001$). (**B**) and (**C**) Student's two-tailed unpaired t-test (n.s. not significant, * $p<0.05$). Error bars indicate ± SEM. Panel (**A**) represents 3 pooled independent experiments. Panels (**B**) and (**C**) were performed once.

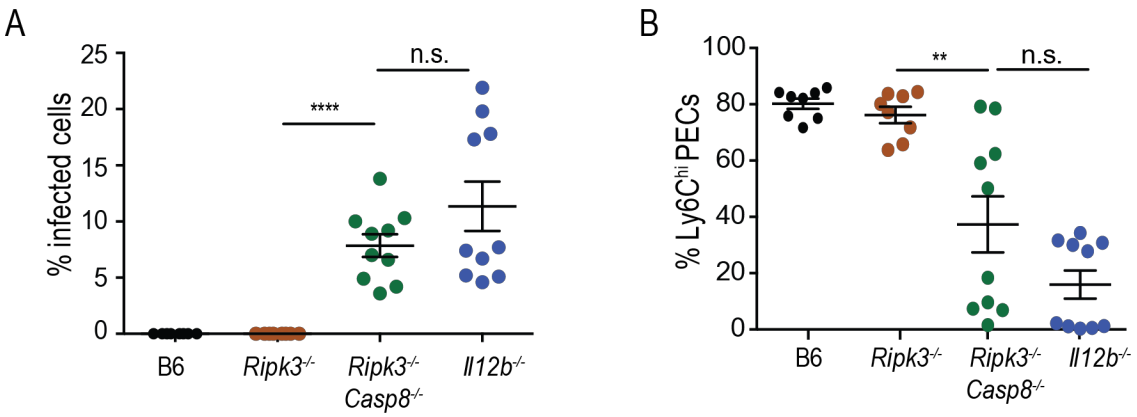

Fig 5.6. Caspase-8 deficiency in hematopoietic cells leads to increased parasite burdens and impaired monocyte infiltration during *T. gondii* infection.

(A) Frequency of infected cells in the PECs of *T. gondii*-infected B6.SJL mice irradiated and reconstituted with B6, *Il12b*$^{-/-}$, *Ripk3*$^{-/-}$, and *Ripk3*$^{-/-}$*Casp8*$^{-/-}$ bone marrow 5 days post infection, each data point represents an individual mouse.

(B) Frequency of inflammatory monocytes (Live^{+}Singlets^{+}CD19^{-}CD3^{-}B220^{-}NK1.1^{-}CD64^{+}MHCII^{+}LY6C^{hi} cells) in the PECs of B6.SJL mice reconstituted with B6, *Il12b*$^{-/-}$, *Ripk3*$^{-/-}$, and *Ripk3*$^{-/-}$*Casp8*$^{-/-}$ bone marrow and infected with *T. gondii* 5 days post infection. Each data point represents a mouse.

For all infections 10,000 Pru *T. gondii* parasites were injected i.p. Student's two-tailed unpaired t-test (n.s. not significant, ** $p<0.01$, *** $p<0.001$). Error bars indicate ± SEM. Panels show two pooled experiments from a total of three independent experiments.

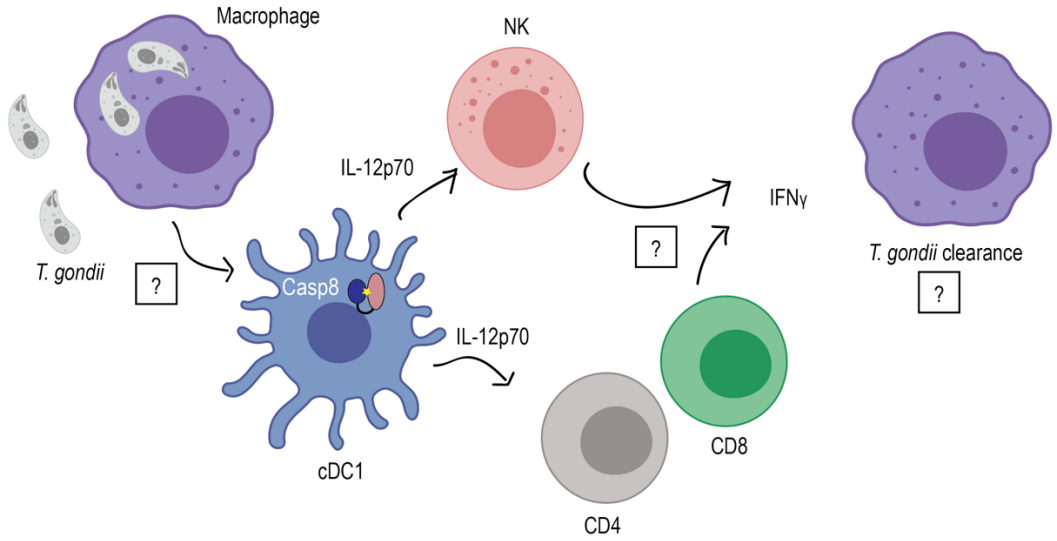

Fig 5.7. Graphical abstract: Caspase-8 promotes secretion of IL-12 in response to *T. gondii* infection.

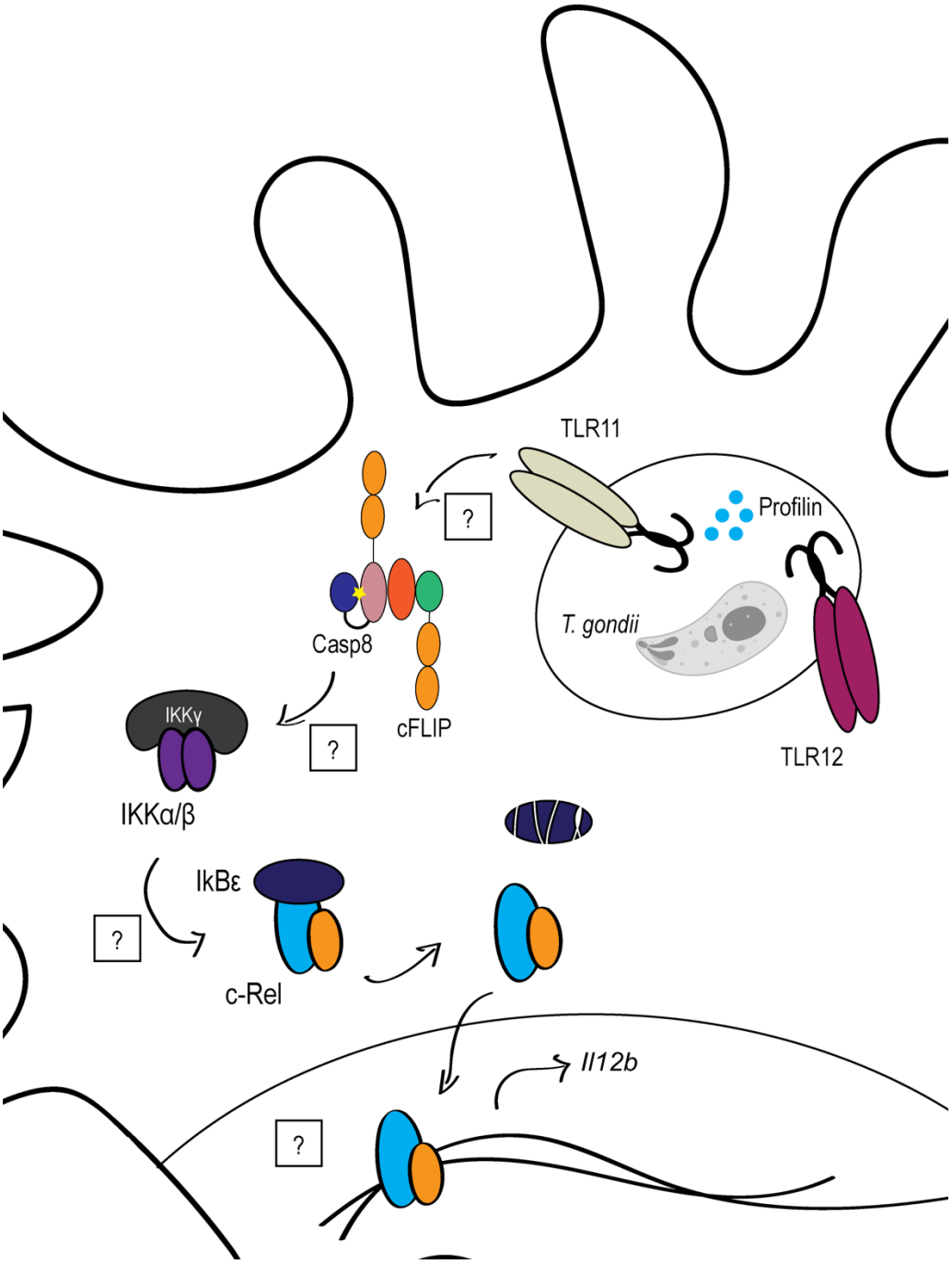

Fig 5.8. Future directions: Potential *in vitro* mechanism of caspase-8-dependent *Il12b* expression in DCs during *T. gondii* infection.

CHAPTER 6: Non-cleavable caspase-8 mediates host survival during infection with the gram-negative bacterial pathogen *Yersinia pseudotuberculosis.*

6.1 Abstract

Caspase-8 positively regulates cell-extrinsic apoptosis and constitutively represses RIPK3-mediated programmed necrosis, functions critical to immune homeostasis and host defense. In addition to its well-characterized role in cell death, caspase-8 regulates inflammatory cytokine secretion *in vitro* and *in vivo*. Data from our lab as well as others have implicated caspase-8 in the immune response during infection with the gram-negative enteric pathogens *Citrobacter rodentium* and *Yersinia pseudotuberculosis* (*Yp*). During oral infection *Yp* mice deficient in caspase-8 in hematopoietic cells have an acute survival defect and a cell-intrinsic defect in cytokine production. However, the relative contribution of caspase-8-mediated cell death and inflammatory gene expression during *Yp* infection has yet to be elucidated. To begin to resolve this question we generated mice in which caspase-8 apoptotic activity was ablated while preserving its cytokine regulatory function. We further crossed these mice onto a RIPK3-deficient background to directly compare mice without caspase-8 expression to those expressing non-cleavable caspase-8 (non-apoptotic caspase-8). Mice lacking caspase-8 in both their hematopoietic and nonhematopoietic cell populations were acutely susceptible to oral infection with *Yp*. Moreover, expression of non-cleavable caspase-8 was sufficient to rescue mice during infection, and these mice had reduced bacterial burdens. However, we were surprised to find that, contrary to what has been observed in mice specifically lacking caspase-8 in their hematopoietic cells, mice lacking caspase-8 in all cell populations had no defect in cytokine production. These data suggest that the mortality observed in caspase-8-deficient mice was

not due to the inability to mount an inflammatory cytokine response or apoptotic response, but an alternative function of caspase-8 that is mediated by its non-cleavable conformation.

6.2 Introduction

Caspase-8 is a cysteine protease that mediates cell-extrinsic apoptosis in response to activation of death receptors such as Fas and TNFR [102], a function that is critical for clearance of autoreactive cell populations [181, 199], tumorigenic cells [182], and virally infected cells [128, 183]. Caspase-8 also negatively regulates another form of cell death known as programmed necrosis [104, 105] through the cleavage of the K63 deubiquitinase CYLD to prevent the activation of RIPK1/RIPK3-dependent necrosis [133]. In addition to its role in cell death, caspase-8 has a recently described function in inflammatory cytokine expression [75, 100, 110]. Caspase-8 is required for the expression of inflammatory mediators in response to fungal [147] and bacterial [77] pathogens *in vitro* as well as to bacterial pathogens *in vivo* [75, 110]. We have also identified a role for caspase-8-mediated cytokine expression in host defense against the eukaryotic, obligate, intracellular pathogen *Toxoplasma gondii* (**Chapter 5**). However, the relative contributions of caspase-8-mediated cell death and caspase-8-mediated cytokine secretion to survival during bacterial infection has yet to be defined. In this chapter we address the contributions of both of these pathways to survival during infection with the gram-negative bacterial pathogen *Yersinia pseudotuberculosis*.

Yersinia pseudotuberculosis is closely related to two other pathogenic *Yersinia spp*.: *Yersinia enterocolitica* and *Yersinia pestis*. *Yersinia enterocolitica* and *Yersinia pseudotuberculosis* cause self-limiting gastroenteritis in humans [148, 149], whereas *Yersinia pestis*, the causative agent of plague, has a case-fatality rate of 30-90% when left untreated, and is still endemic to the United States [153]. In rodents *Y. pseudotuberculosis* mimics the systemic bacterial dissemination and disease symptomology observed in

humans infected with *Yersinia pestis* [152, 200]. *Yersinia spp.* are potent activators of apoptosis in immune cells via the effector protein YopJ (Yersinia outer protein J) which antagonizes gene transcription [154, 155, 178]. We have previously shown that strains of *Yersinia spp.* with reduced YopJ injection are more virulent [174], and apoptosis limits *Y. pseudotuberculosis* virulence *in vivo* [132]. There is also evidence that *in vivo* cytokine production, particularly IL-12 and TNF, promote host survival to *Yersinia* infection [98, 201]. Therefore, it is possible that there are distinct contributions of caspase-8-mediated cell death and caspase-8-mediated cytokine secretion to host survival during infection with *Y. pseudotuberculosis.*

We have previously shown that mice lacking caspase-8 in hematopoietic cells are acutely susceptible to oral infection with *Y. pseudotuberculosis* [114]. Moreover, these mice have increased bacterial burdens, and a defect in cytokine production in caspase-8-deficient monocytes and neutrophils [114]. To test the specific contribution of caspase-8-mediated cytokine production to host survival during *Y. pseudotuberculosis* we generated a mouse in which the linker sequence between the p10 and p20 subunit of caspase-8 is mutated to prevent auto-processing and stabilization of the apoptotic conformation of the protein [79, 80]. We have previously shown that macrophages generated from these mice are resistant to *Yersinia*-induced apoptosis, but are able to produce cytokines in response to TLR stimuli [75]. These mice were also crossed onto RIPK3-null mice to generate a mouse in which both apoptosis and programed necrosis are ablated while preserving the cytokine regulatory function of caspase-8. This approach allowed us to specifically interrogate the role of caspase-8-mediated cytokine secretion to host defense during oral

infection with *Yersinia pseudotuberculosis*. In this studies we describe an *in vivo* role for caspase-8 that is independent of both its cell death and cytokine regulatory functions.

6.3 Results

6.3.1. Non-cleavable caspase-8 promotes host survival during oral infection with *Yersinia pseudotuberculosis*.

We have previously shown that mice lacking caspase-8 in their hematopoietic cells succumb to oral infection with *Yersinia pseudotuberculosis* (*Yp*) within 6 days of infection [114]. Surprisingly, mice in which caspase-8 was ablated in all cell populations were even more susceptible to *Yp* infection. Mice began to die 3 days post infection, and all mice succumbed within 4 days (**Fig 6.1A**). We observed a role for RIPK3 in survival beginning 9 days post infection, which had not previously been observed in mice with hematopoietic-specific ablation of RIPK3 (**Fig 6.1A**) [114]. These data potentially implicate RIPK3 in the adaptive response to *Yp* infection which has not been previously reported. One of the seven effector proteins expressed by *Yp* is YopJ, which is known to promote systemic dissemination of *Yersinia* [200]; however, YopJ-mediated apoptosis is also important for host survival during *Yersinia* infection in some contexts [202]. To address the contribution of caspase-8-dependent apoptosis *in vivo* in mice lacking caspase-8 in both their hematopoietic and non-hematopoietic cell populations we orally infected *Ripk3*$^{-/-}$*Casp8*$^{-/-}$ mice with ΔYopJ. We hypothesized that if caspase-8-dependent apoptosis played a role in host survival, mice deficient in caspase-8 would have increased survival during ΔYopJ infection, which has been observed in mice with hematopoietic-specific caspase-8 ablation [114]. However, *Ripk3*$^{-/-}$*Casp8*$^{-/-}$ mice infected with ΔYopJ succumbed with kinetics indistinguishable from mice infected with the parental strain of *Yp* (**Fig 6.1A**). These data suggested that caspase-8-dependent apoptosis does not mediate host survival during infection with *Yersinia*.

We then utilized mice expressing a non-cleavable form of caspase-8 that prevents caspase-8-mediated apoptosis while preserving caspase-8-mediated cytokine secretion. We found that the apoptotic conformation of caspase-8 was dispensable for survival as the kinetics of mortality in *Casp8*$^{DA/DA}$ and *Ripk3*$^{-/-}$*Casp8*$^{DA/DA}$ mice were indistinguishable from B6 and *Ripk3*$^{-/-}$ mice respectively (**Fig 6.1B**). From these data we concluded that expression of non-cleavable caspase-8 was sufficient to rescue mice from mortality during oral *Yp* infection, implicating caspase-8-mediated cytokine production in host defense independently of the role of caspase-8 in apoptosis.

6.3.2. Non-cleavable caspase-8 expression correlates with reduced bacterial burdens during oral infection with *Yersinia pseudotuberculosis*.

Mice expressing non-cleavable caspase-8 had reduced bacterial burdens in their Peyer's Patches, spleens, and livers 2 days post infection (**Fig 6.2A**, **Fig 6.2C** and **Fig 6.2D**). However, we could observe no difference in mLN bacterial burdens between any groups of infected mice (**Fig 6.2B**). Previous work has shown that there are distinct replicating pools of *Yp* in the oral model of infection [152]. The spread of bacteria is not a linear route through Peyer's Patches to the draining lymph node (mLN), but rather replication in the Peyer's patches occurs in parallel to replication in the small intestine. Bacteria originating from the small intestine disseminate to the spleen and liver directly to mediate colonization and replication. Therefore, the observed differences in the Peyer's Patches are likely due to differences in the first wave of colonization, and the observed differences in the spleen and liver likely reflect dissemination from the small intestine

directly. Interestingly, expression of non-cleavable caspase-8 is sufficient to reduce bacterial burdens during both forms of colonization.

6.3.3. Systemic IL-12p40 is produced independently of caspase-8 expression.

We previously reported that mice with caspase-8 deficiency in their hematopoietic cells had reduced levels of inflammatory cytokines in their serum 6 days post infection [114]. Therefore, we were surprised to find that mice, in which caspase-8 is ablated in all cell populations have wild-type levels of serum IL-12p40 2 days post infection (**Fig 6.3**). We interpret these data to mean that caspase-8 expression is not required to mediate cytokine production in this context Furthermore, we observed no additive effect of the expression of non-cleavable caspase-8 on a wild-type or RIPK3-null background (**Fig 6.3**). We then tested the inflammatory response on a per-cell basis to determine if immune-cell specific cytokine production was impaired in this context.

6.3.4 Cell-intrinsic IL-12p40 expression occurs independently of caspase-8 expression.

Two innate cell populations that mount the early inflammatory response to *Yp* are monocytes and neutrophils [75, 98, 114, 132]. In an effort to measure immune-cell specific intracellular cytokine responses we selected the mLN, an organ in which bacterial burdens were statistically indistinguishable amongst the mice used in these studies. We used this approach to control for differences in immune cell recruitment that can be mediated by bacterial replication rather than the specific immune state of the host. Using this approach we found that mLNs isolated from *Ripk3*$^{-/-}$*Casp8*$^{-/-}$ mice had a higher frequency of IL-12p40 positive monocytes and equivalent cell numbers of IL-12p40 positive monocytes

when compared to *Ripk3*$^{-/-}$ controls (**Fig 6.4**, **Fig 6.5A** and **Fig 6.5B**). We also observed a similar trend in IL-12p40 positive neutrophils (**Fig 6.4**, **Fig 6.6A** and **Fig 6.6B**). These data were surprising given our findings that caspase-8-deficient hematopoietic cells have a cell-intrinsic defect in cytokine production [75]. We interpret these data to mean that caspase-8 is not required for IL-12 production in this context.

We also observed greater overall numbers of IL-12p40 positive monocytes in *Ripk3*$^{-/-}$*Casp8*$^{DA/DA}$ mice, and a higher frequency of IL-12p40 positive monocytes in *Casp8*$^{DA/DA}$ mice. One possible explanation for these data were differences in overall monocyte numbers. Therefore, we measured total inflammatory monocytes in naïve and infected mice, and found that similar to the phenotype we described in **Chapter 4**, *Ripk3*$^{-/-}$*Casp8*$^{DA/DA}$ mice had higher overall numbers of inflammatory monocytes during infection (**Fig 6.7A** and **Fig 6.7B**). These results may provide an explanation for the higher overall numbers of IL-12p40 positive cells observed in *Ripk3*$^{-/-}$*Casp8*$^{DA/DA}$ mice. We did not observe a difference in total numbers of monocytes in naïve or infected *Casp8*$^{DA/DA}$ mice when compared to B6 controls, suggesting that the higher frequency of IL-12p40 positive cells reflects an increased inflammatory response in these mice (**Fig 6.7C** and **Fig 6.7D**).

There was no additive effect of non-cleavable caspase-8 expression for on a RIPK3-null background for cytokine production as measured by neutrophil-derived IL-12p40 production (**Fig 6.6**). This was surprising given the higher overall neutrophil numbers we observed at baseline in *Ripk3*$^{-/-}$*Casp8*$^{DA/DA}$ mice (**Fig 6.8A**). We did observe an increase in total neutrophil numbers in infected *Ripk3*$^{-/-}$*Casp8*$^{DA/DA}$ mice when compared to *Ripk3*$^{-/-}$ controls, but this did not correspond to an increase in total IL-12p40 positive

neutrophils in these mice (**Fig 6.6** and **Fig 6.8B**). Interestingly, opposite of our observation in monocytes, non-cleavable caspase-8 on a wild-type background mediated an increase in overall numbers of IL-12 positive neutrophils, but did not impact frequency (**Fig 6.6 C** and **Fig 6.6D**). We observed a trend toward increased neutrophil infiltrate in the mLNs of *Casp8*$^{DA/DA}$ mice at steady-state and during infection, but this was not statistically significant when compared to B6 controls (**Fig 6.8C** and **Fig 6.8D**). Collectively, these data demonstrate that monocytes and neutrophils produce IL-12p40 independently of caspase-8 expression; however, in some cases non-cleavable caspase-8 expression can enhance intracellular cytokine production. In all assays that we used we did not observe lower levels of global or intracellular cytokine production from *Ripk3*$^{-/-}$*Casp8*$^{-/-}$ mice when compared to *Ripk3*$^{-/-}$ controls, indicating that mice lacking global caspase-8 expression have a distinct phenotype from those lacking caspase-8 expression in just the hematopoietic compartment.

6.4 Discussion

We have previously shown that caspase-8 deficiency in hematopoietic cells leads to acute mortality in response to oral infection with the gram-negative bacterial pathogen *Yersinia pseudotuberculosis* (*Yp*) [114]. Here we demonstrate that complete ablation of caspase-8 in both hematopoietic and non-hematopoietic cells leads to an even more acute survival defect in which mice succumb within 4 days of infection. We also observed no role for caspase-8-dependent apoptosis in this context as these mice were equally susceptible to an isogenic strain of *Yp* lacking the effector YopJ (ΔYopJ). Mice with hematopoietic-specific ablation of caspase-8 largely survive infection with ΔYopJ, but mice with global ablation of caspase-8 succumb with kinetics indistinguishable from those infected with *Yp* expressing YopJ. These data led us to conclude that caspase-8-dependent apoptosis was dispensable for survival during infection, implicating the cytokine regulatory function of caspase-8.

Two inflammatory cytokine that are critical for host defense during *Yp* infection are TNF and IL-12 [98, 201]. We have previously shown that macrophages derived from mice expressing a non-cleavable form of caspase-8 produce endogenous levels of cytokines, but to not undergo YopJ-mediated apoptosis during *in vitro Yp* infection [75]. We used these mice as a model to test the contribution of caspase-8-mediated cytokine production specifically, and found that these animals survived oral infection with *Yp,* and had reduced bacterial burdens when compared to caspase-8-deficient mice. These data were consistent with a model in which caspase-8-dependent cytokine production was required for control of *Yp* infection *in vivo*.

We originally hypothesized that global caspase-8-deficiency would largely recapitulate our observations with hematopoietic-specific ablation of caspase-8. However, we were surprised to find that mice lacking caspase-8 had no defect in serum cytokines or intracellular cytokine production in innate immune cells. Expression of non-cleavable caspase-8 was sufficient to reduce bacterial burdens and mediate survival; however, this effect appears to be independent of caspase-8-mediated cytokine secretion. Caspase-8-deficient mice, and mice expressing non-cleavable caspase-8, largely had no detectible differences in serum cytokines or intracellular cytokine production by monocytes or neutrophils. We interpret these data to mean that caspase-8 expression is not required for the early cytokine response to *Yp.* Intriguingly, these data suggested that there is an alternative role for caspase-8 in regulating bacterial dissemination or replication independently of cell death or cytokine secretion.

One possible explanation for the discrepancy between mice with total caspase-8 ablation and mice with hematopoietic-specific ablation is developmental differences between these mice. There are no reported developmental defects in the intestines of *Ripk3*$^{-/-}$*Casp8*$^{-/-}$ mice. However, this may be due to the focus on the immune compartment of these mice as they display acute lymphoproliferative disease [104, 105]. We have previously implicated caspase-8 in pro-inflammatory gene expression in macrophages downstream of TLR signaling, but it is possible that it interacts with some of these signaling intermediates in other cell types such as intestinal epithelial cells. Homeostatic turnover of intestinal epithelial cells is primarily mediated by TNF signaling, which is upstream of caspase-8 activation [203]. Additionally, mice deficient in TAK1 or the transcription factor p65 in their intestinal epithelium have increased ROS production and

intestinal apoptosis respectively [203, 204]. c-Rel has also been implicated in epidermal homeostasis through the regulation of cell cycle genes [205], but it is also possible that this regulation also occurs in intestinal epithelial cells. In **Chapter 2** we note that caspase-8 deficiency leads to impaired expression of cell cycle genes in macrophages in response to TLR stimulation. Therefore, it would be interesting to see if caspase-8 and c-Rel also play a role in intestinal epithelial cell homeostasis. If caspase-8 mediates development of the small intestine or barrier integrity during steady-state then the survival defect we observed in mice globally deficient in caspase-8 may be due to failure to control bacterial dissemination from the small intestine. Expression of non-cleavable caspase-8 may be sufficient to maintain barrier integrity, in turn promoting survival of the host. Future studies that interrogate the role of caspase-8 in intestinal epithelial cell homeostasis and barrier integrity may help elucidate the mechanism of caspase-8-dependent protection during oral infection with *Yp*. Collectively, these studies show, for the first time, that caspase-8 non-apoptotic activity is sufficient to mediate survival during *Yp* infection, and that this protection occurs independently of the cytokine regulatory function of caspase-8 (**Fig 6.9**).

6.5 Figures

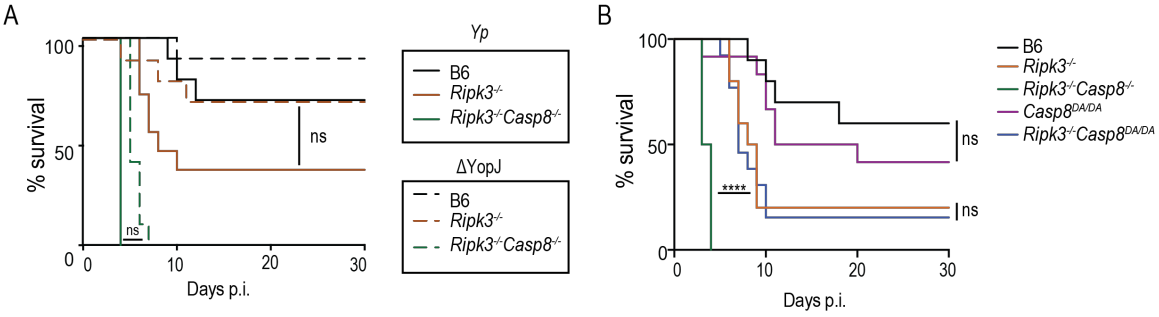

Fig 6.1. Non-cleavable caspase-8 promotes host survival during oral infection with *Yersinia pseudotuberculosis*.

(A) Survival of B6, *Ripk3*$^{-/-}$, and *Ripk3*$^{-/-}$*Casp8*$^{-/-}$ mice (n=10-11) infected o.g. (3-4x10^8 CFU/mouse) with *Yersinia pseudotuberculosis* (IP2777) and *Δ*YopJ *Yersinia pseudotuberculosis* (IP2777).

(**B**) Survival of B6, *Ripk3*$^{-/-}$, *Ripk3*$^{-/-}$*Casp8*$^{-/-}$, *Ripk3*$^{-/-}$*Casp8*$^{DA/DA}$, and *Casp8*$^{DA/DA}$ mice (n=10) infected o.g. (4x10^8 CFU/mouse) with *Yersinia pseudotuberculosis* (IP2777)

Mantel-cox test (n.s. not significant , **** p<0.0001). Panel (**A**) and (**B**) performed once.

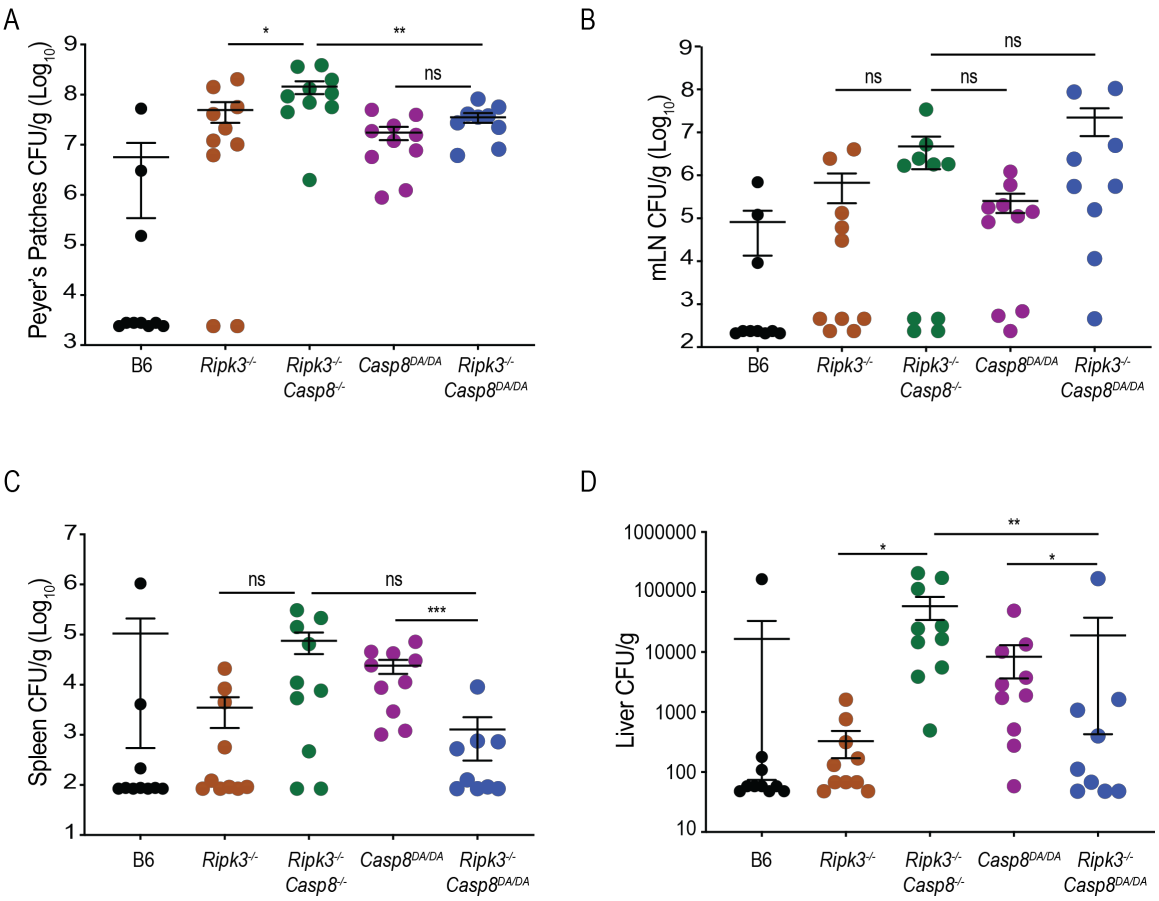

Fig 6.2. Non-cleavable caspase-8 expression correlates with reduced bacterial burdens during oral infection with *Yersinia pseudotuberculosis*.

Bacterial burdens in the Peyer's Patches (**A**), mLNs (**B**), spleens (**C**) and livers (**D**) of B6, *Ripk3*$^{-/-}$, *Ripk3*$^{-/-}$*Casp8*$^{-/-}$, *Ripk3*$^{-/-}$*Casp8*$^{DA/DA}$, and *Casp8*$^{DA/DA}$ mice infected o.g. (2-3x10^8 CFU/mouse) with *Yersinia pseudotuberculosis* (IP2777) 2 days post-infection. Each circle represents a mouse.

Student's two-tailed unpaired t-test (n.s. not significant, *p<0.05, **p<0.01, *** p<0.001). Error bars indicate ± SEM. Data pooled from two independent experiments.

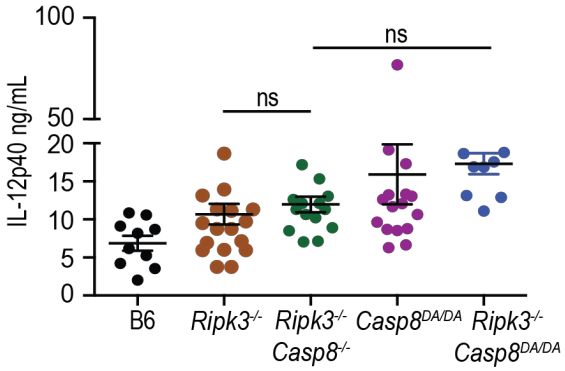

Fig 6.3. Systemic IL-12p40 is produced independently of caspase-8 expression.

ELISA measurement of serum IL-12p40 from B6, *Ripk3*$^{-/-}$, *Ripk3*$^{-/-}$*Casp8*$^{-/-}$, *Ripk3*$^{-/-}$*Casp8*$^{DA/DA}$, and *Casp8*$^{DA/DA}$ mice infected o.g. (2-3x10^8 CFU/mouse) with *Yersinia pseudotuberculosis* (IP2777) 2 days post-infection. Each circle represents a mouse.

Student's two-tailed unpaired t-test (n.s. not significant). Error bars indicate ± SEM. Data pooled from two independent experiments.

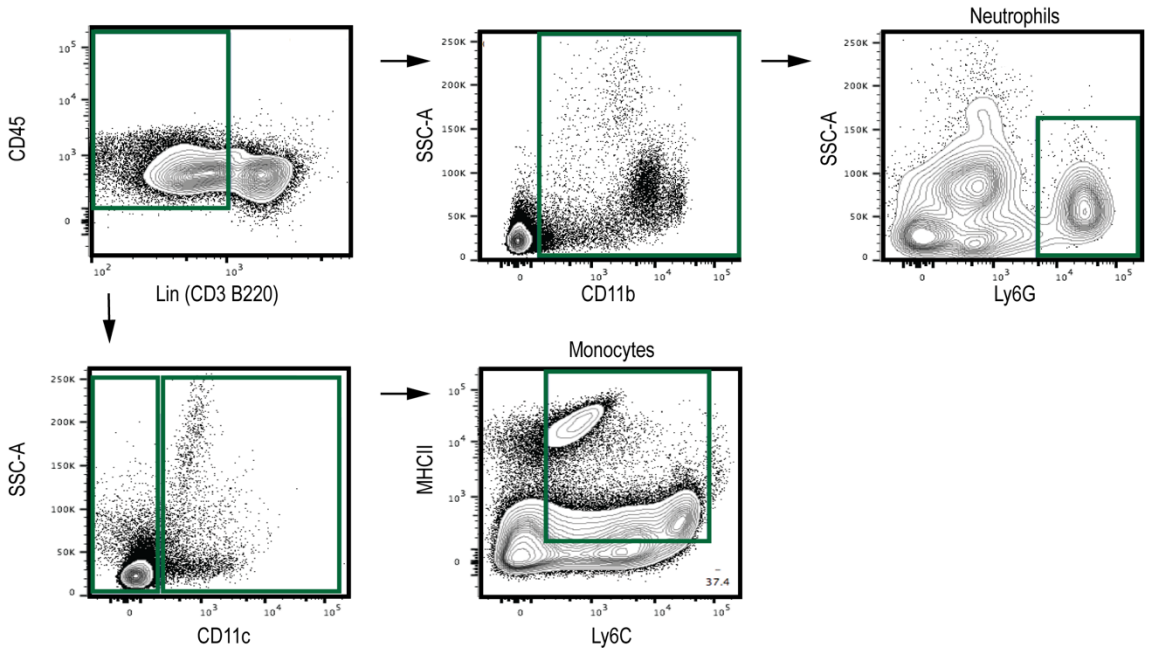

Fig 6.4. Flow-cytometry gating strategy for innate immune populations during oral infection with *Yersinia pseudotuberculosis*.

Representative flow contour plots of the gating strategy for neutrophils ($CD45^{+}Lin^{-}CD11b^{+}Ly6G^{+}$) and inflammatory monocytes ($CD45^{+}Lin^{-}CD11c^{-}Ly6C^{hi}MHCII^{+}$) in the mLN of a B6 mouse infected o.g. (3x10^8 CFU/mouse) with *Yersinia pseudotuberculosis* (IP2777) 2 days post-infection. All samples pre-gated on live single cells. Lin markers (CD3, B220).

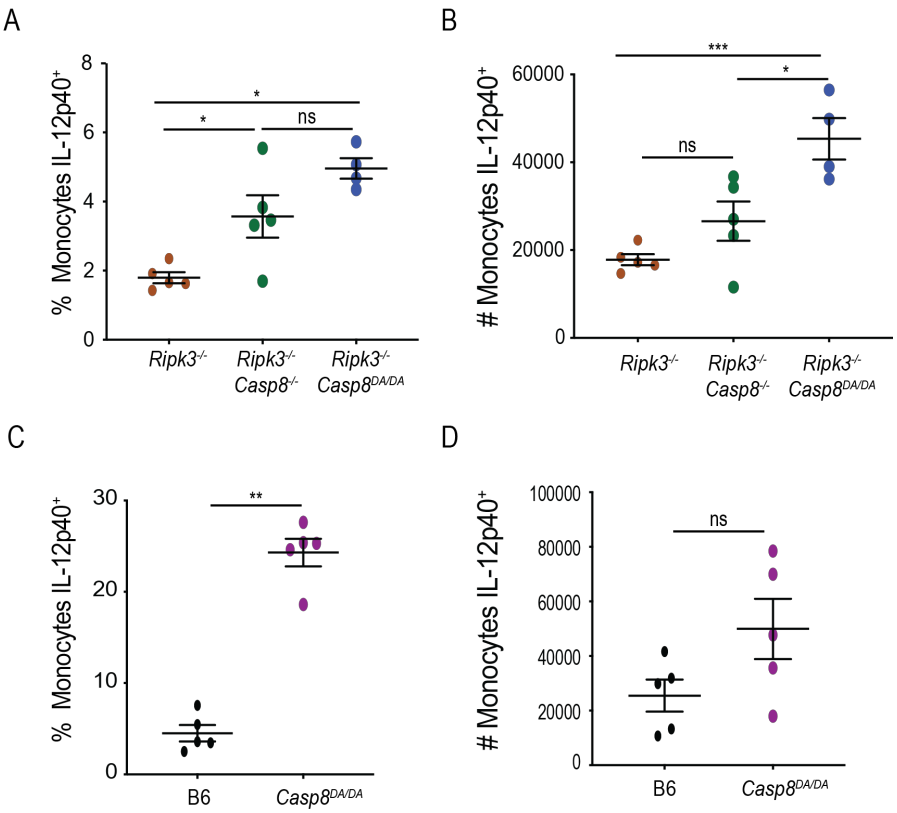

Fig 6.5 Monocyte IL-12p40 expression is independent of caspase-8.

(A) Frequency and **(B)** total numbers of IL-12p40^{+} inflammatory monocytes in the mLNs of *Ripk3*$^{-/-}$, *Ripk3*$^{-/-}$*Casp8*$^{-/-}$, and *Ripk3*$^{-/-}$*Casp8*$^{DA/DA}$ mice infected o.g. (3x10^8 CFU/mouse) with *Yersinia pseudotuberculosis* (IP2777) 2 days post-infection. Each circle represents a mouse.

(C) Frequency and **(D)** total numbers of IL-12p40^{+} inflammatory monocytes in the mLNs of B6 and *Casp8*$^{DA/DA}$ mice infected o.g. (3x10^8 CFU/mouse) with *Yersinia pseudotuberculosis* (IP2777) 2 days post-infection. Each circle represents a mouse.

Student's two-tailed unpaired t-test (n.s. not significant, * $p<0.05$, **<0.01, *** $p<0.001$). Error bars indicate ± SEM. Data representative of two independent experiments.

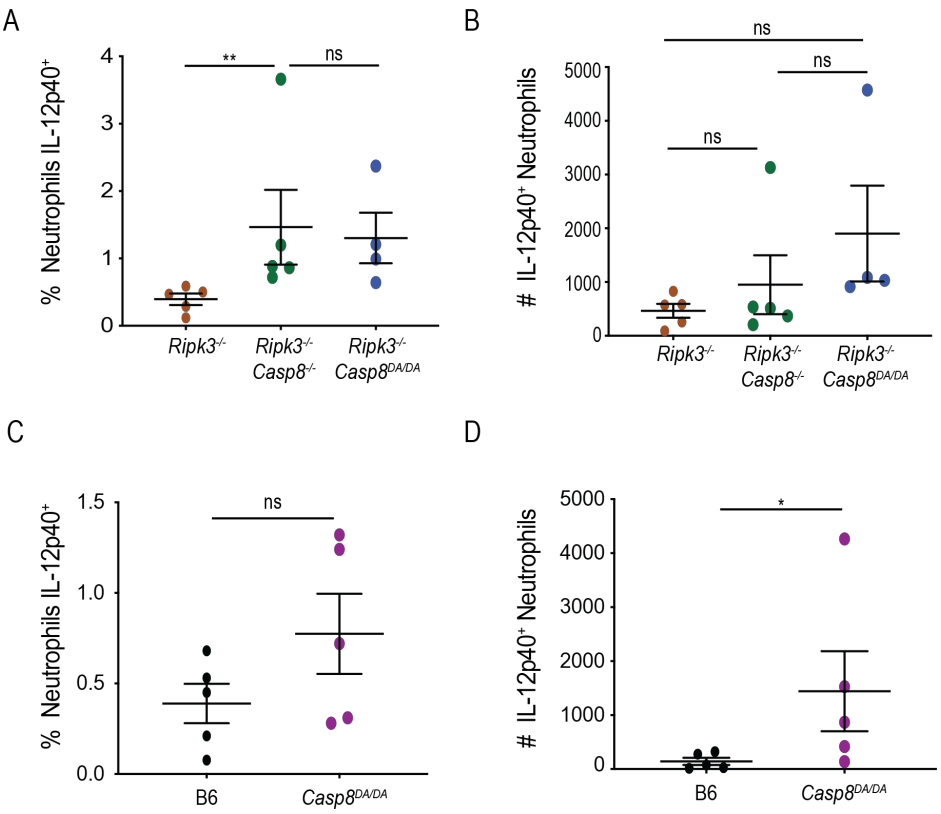

Fig 6.6. Neutrophil IL-12p40 expression is independent of caspase-8.

(A) Frequency and **(B)** total numbers of IL-12p40^{+} neutrophils in the mLNs of *Ripk3*$^{-/-}$, *Ripk3*$^{-/-}$*Casp8*$^{-/-}$, and *Ripk3*$^{-/-}$*Casp8*$^{DA/DA}$ mice infected o.g. (3x10^8 CFU/mouse) with *Yersinia pseudotuberculosis* (IP2777) 2 days post-infection. Each circle represents a mouse.

(C) Frequency and **(D)** total numbers of IL-12p40^{+} neutrophils in the mLNs of B6 and *Casp8*$^{DA/DA}$ mice infected o.g. (3x10^8 CFU/mouse) with *Yersinia pseudotuberculosis* (IP2777) 2 days post-infection. Each circle represents a mouse.

Student's two-tailed unpaired t-test (n.s. not significant, * $p<0.05$, **<0.01, *** $p<0.001$). Error bars indicate ± SEM. Data representative of two independent experiments.

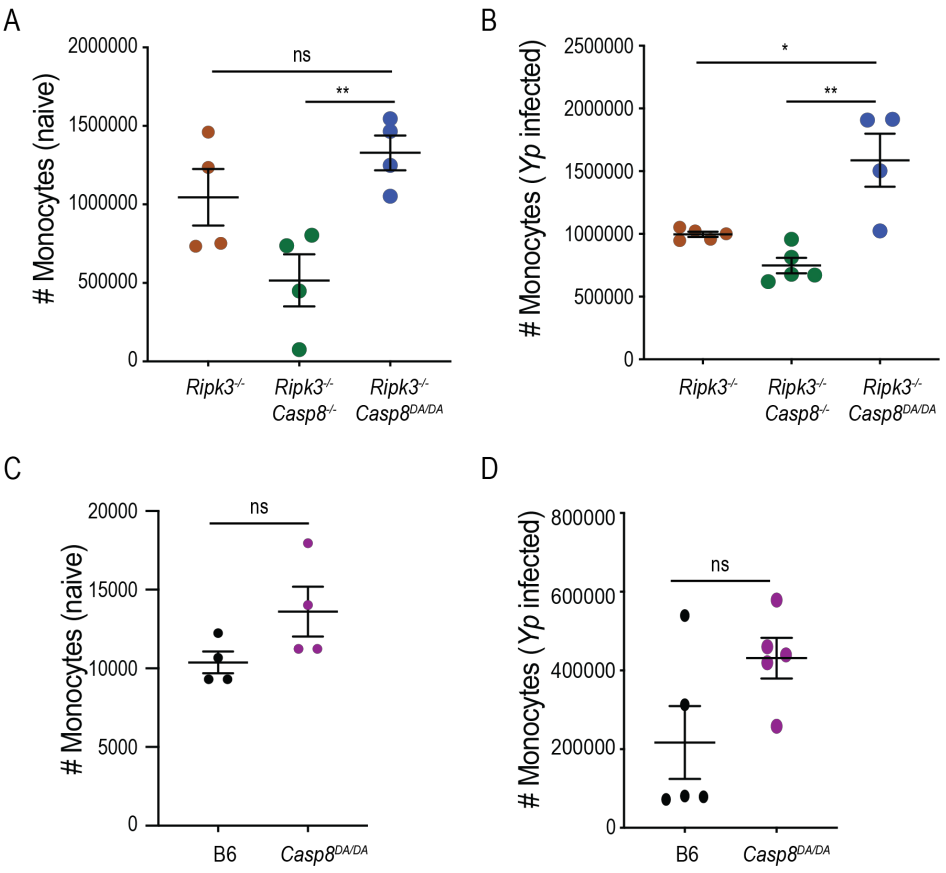

Fig 6.7 RIPK3-null mice expressing non-cleavable caspase-8 have higher levels of monocyte infiltration during *Yersinia pseudotuberculosis* infection.

(A) Total numbers of monocytes in the mLNs of naïve *Ripk3*$^{-/-}$, *Ripk3*$^{-/-}$*Casp8*$^{-/-}$, and *Ripk3*$^{-/-}$*Casp8*$^{DA/DA}$ mice. Each circle represents a mouse.

(B) Total numbers of monocytes in the mLNs of *Ripk3*$^{-/-}$, *Ripk3*$^{-/-}$*Casp8*$^{-/-}$, and *Ripk3*$^{-/-}$*Casp8*$^{DA/DA}$ mice infected o.g. (3x10^8 CFU/mouse) with *Yersinia pseudotuberculosis* (IP2777) 2 days post-infection. Each circle represents a mouse.

(C) Total numbers of monocytes in the mLNs of naïve B6 and *Casp8*$^{DA/DA}$ mice. Each circle represents a mouse.

Fig 6.7 Continued: (D) Total numbers of monocytes in the mLNs of B6 and *Casp8*$^{DA/DA}$ mice infected o.g. (3x10^8 CFU/mouse) with *Yersinia pseudotuberculosis* (IP2777) 2 days post-infection. Each circle represents a mouse.

Student's two-tailed unpaired t-test (n.s. not significant, * $p<0.05$, **<0.01). Error bars indicate ± SEM. Panels (**A**) and (**C**) are each pooled from two independent experiments. Panels (**B**) and (**D**) are each representative of two independent experiments.

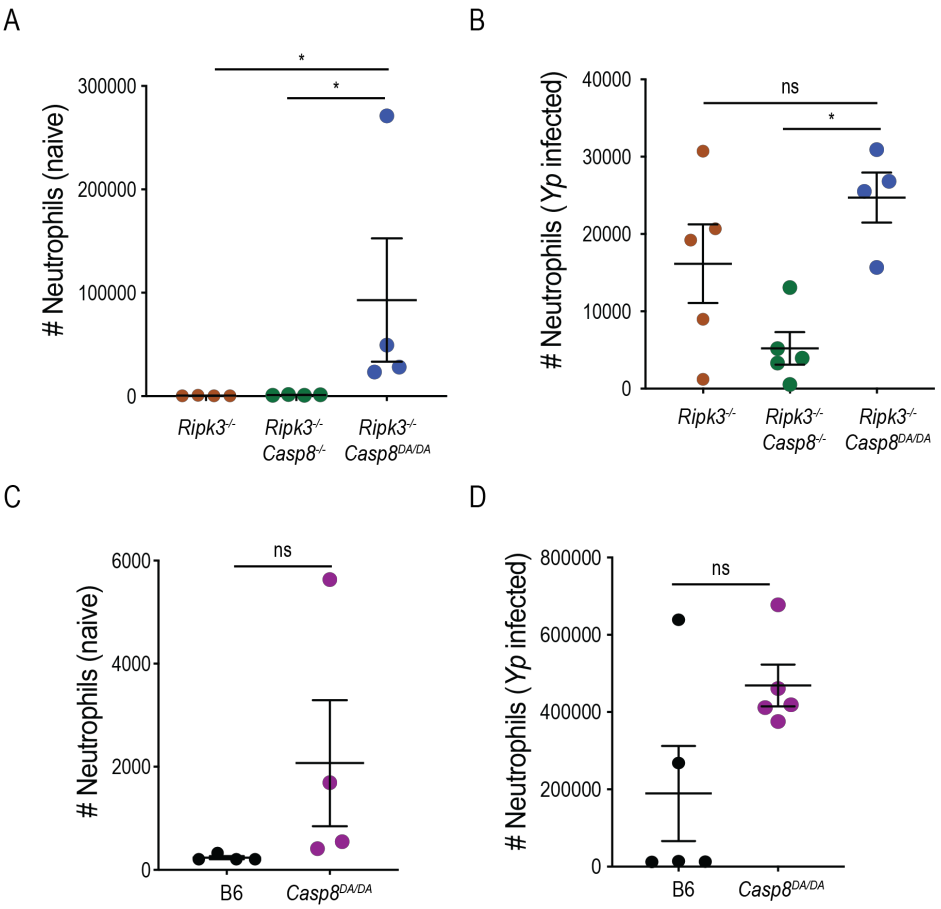

Fig 6.8 RIPK3-null mice expressing non-cleavable caspase-8 have higher neutrophil numbers at steady-state.

(A) Total numbers of neutrophils in the mLNs of naïve *Ripk3*$^{-/-}$, *Ripk3*$^{-/-}$*Casp8*$^{-/-}$, and *Ripk3*$^{-/-}$*Casp8*$^{DA/DA}$ mice. Each circle represents a mouse.

(B) Total numbers of neutrophils in the mLNs of *Ripk3*$^{-/-}$, *Ripk3*$^{-/-}$*Casp8*$^{-/-}$, and *Ripk3*$^{-/-}$ *Casp8*$^{DA/DA}$ mice infected o.g. (3x10^8 CFU/mouse) with *Yersinia pseudotuberculosis* (IP2777) 2 days post-infection. Each circle represents a mouse.

(C) Total numbers of neutrophils in the mLNs of naïve B6 and *Casp8*$^{DA/DA}$ mice. Each circle represents a mouse.

Fig 6.8 Continued: (D) Total numbers of neutrophils in the mLNs of B6 and *Casp8*$^{DA/DA}$ mice infected o.g. (3x10^8 CFU/mouse) with *Yersinia pseudotuberculosis* (IP2777) 2 days post-infection. Each circle represents a mouse.

Student's two-tailed unpaired t-test (n.s. not significant, * $p<0.05$). Error bars indicate ± SEM. Panels (**A**) and (**C**) are each pooled from two independent experiments. Panels (**B**) and (**D**) are each representative of two independent experiments.

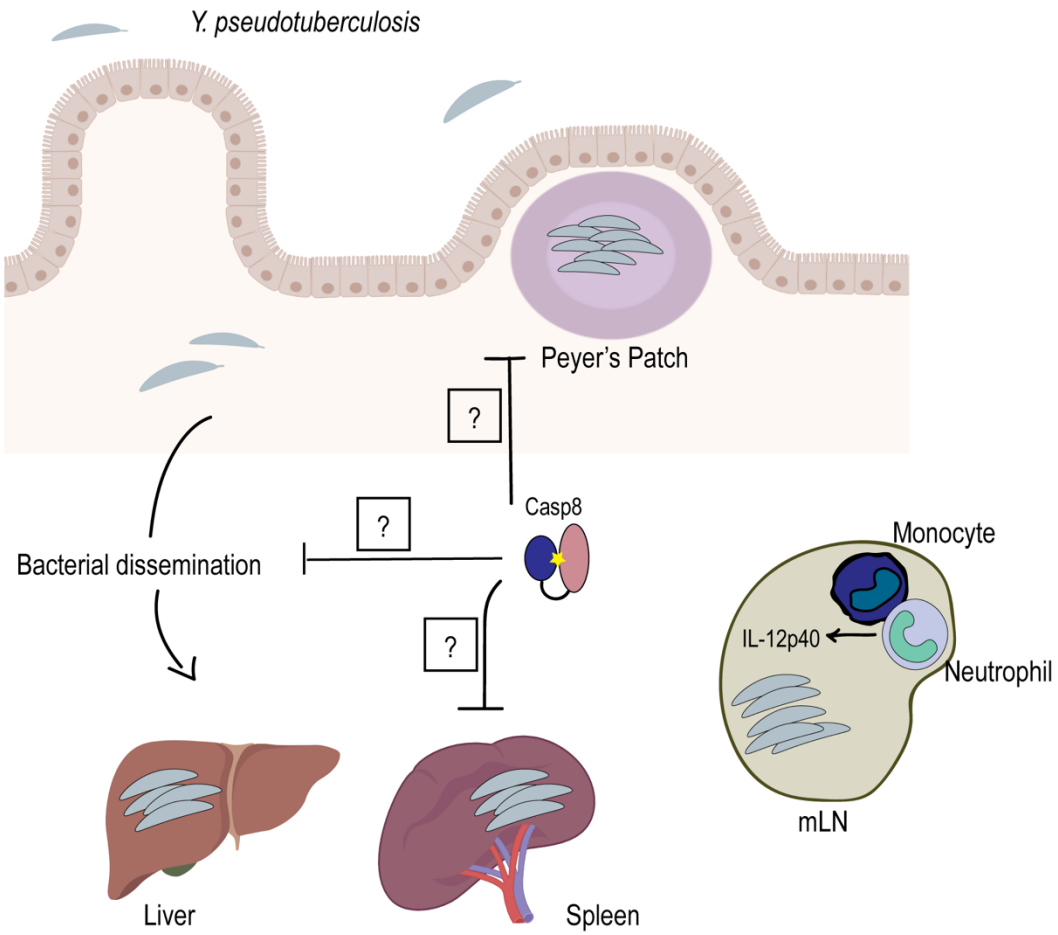

Fig 6.9. Graphical abstract and future directions: Caspase-8 promotes host survival during oral infection with *Yersinia pseudotuberculosis* independently if its cytokine regulatory or apoptotic functions.

CHAPTER 7: Discussion and future directions.

7.1 Summary of findings

In this study we hypothesized that caspase-8 enzymatic activity would play a role in inflammatory gene expression independently of its apoptotic function, and that caspase-8-mediated inflammatory gene regulation would be required for host defense against a variety of pathogens *in vivo*. In **Chapter 2** we identified the mechanism by which caspase-8 regulates the inflammatory cytokines IL-12 and IL-1β through the NF-κB family member c-Rel. We also showed that expression of c-Rel in caspase-8-deficient macrophages is sufficient to restore production of both IL-12 and IL-1β. In **Chapter 3** we tested the role for caspase-8 enzymatic activity in c-Rel translocation and inflammatory gene expression. We found that both the enzymatic and non-enzymatic functions of caspase-8 mediate c-Rel translocation and expression of caspase-8-dependent inflammatory genes. These results help address a long-standing conflict in the field regarding the relative contributions of caspase-8 enzymatic and non-enzymatic activity to gene expression.

In **Chapter 4** we defined a role for caspase-8 apoptotic activity and RIPK3-mediated programed necrosis in steady-state levels of myeloid cell populations in secondary lymphoid organs. These data implicate caspase-8 in innate immune cell turnover for the first time. In **Chapter 5** we identified a role for caspase-8-mediated cytokine secretion in host defense during acute infection with the eukaryotic pathogen *Toxoplasma gondii*. To our knowledge this is the first report of caspase-8 mediating host survival against a eukaryotic pathogen *in vivo*. In **Chapter 6** we identified a role for caspase-8 in host survival during infection with the gram-negative enteric pathogen *Yersinia pseudotuberculosis.* We found that survival during *Yersinia* infection was mediated

independently of caspase-8-dependent apoptosis and caspase-8-dependent pro-inflammatory cytokine production. These data potentially implicate caspase-8 in maintenance of intestinal barrier integrity for the first time. Collectively, these studies highlight the broad role for caspase-8 in immune homeostasis as well as host defense. Moreover, they suggest that many functions of caspase-8 are independent of caspase-8-mediated apoptosis.

7.2 Key findings of this work

7.2.1 Distinct regulation of the NF-κB family members p65 and c-Rel is mediated, in part, through caspase-8.

Our data implicate caspase-8 in the distinct regulation of c-Rel and p65 in response to TLR stimulation. Early work described a restricted role for c-Rel in *Il12b* expression in macrophages [71]. However, our data identified many caspase-8-dependent genes that were also dependent on the expression of c-Rel, potentially implicating c-Rel in the regulation of other genes in response to TLR activation. The mechanisms by which c-Rel and p65 are distinctly regulated in macrophages has yet to be elucidated; however, it is possible that caspase-8 represents one mechanism to orchestrate their distinct activation. NF-κB family-member regulation can be categorized as either canonical and non-canonical NF-κB signaling pathways that mediate differential regulation of p65 and RelB respectively [206-209]. The classification of canonical and non-canonical NF-κB signaling is largely based on the differential utilization of NEMO and IKKα respectively [210, 211]. While entirely speculative, it is possible that in macrophages differential activation of c-Rel and p65 can be characterized based on the utilization of caspase-8.

We also observed a selective effect of caspase-8-dependent IKKα/β phosphorylation on the degradation of IκBε. IκBε is thought to preferentially associate with both p65 and c-Rel, and recent evidence describes a role for IκBε/c-Rel specific interactions in certain cell-types [176, 212]. Like other IκB proteins, IκBε is degraded by the ubiquitin-26S proteasome pathway [57, 58]. However, IκBε can also be degraded by the REG*γ* proteasome in non-hematopoietic cells *in vivo* [213]. These data suggest there may be other mechanisms of IκBε regulation that are independent of IKK-mediated

degradation. Previously uncharacterized mechanisms of proteasomal degradation may provide an explanation for the distinct regulation of IκBε and IκBα in a caspase-8-deficient setting. Further experiments to test the hypothesis that there is preferential association between c-Rel and IκBε in macrophages will help elucidate how p65 and c-Rel are distinctly regulated in this context. Testing the biochemical sensitivities of the IκB proteins to differing levels of IKK phosphorylation may also provide insight into the seemingly increased sensitivity of IκBε to perturbations in IKKα/β phosphorylation. Other studies have primarily focused on the temporal regulation of IκB protein expression [59], but these do not address the threshold of IKKα/β activation required to mediate the degradation of IκB proteins.

One looming question from these studies is how exactly caspase-8 regulates IKK activation. We could find no role for caspase-8 in the activation of the upstream kinases TAK1 or TBK1 that are classically thought to promote IKK activation [211, 214, 215]. One possible explanation may be the specific requirement for NIK (Mitogen-activated protein kinase kinase kinase kinase 4) in this signaling pathway. NIK is activated in response to both CD40 and TNF to promote IKK phosphorylation [207, 209]. One caveat to this hypothesis is that NIK is constitutively degraded by TRAF3 at steady state, and the kinetics of TRAF3 degradation and NIK activation may not be concordant with the role of caspase-8 in the rapid response to TLR stimulation. However, it is still possible that NIK plays a role in our system; therefore, we will test the impact of caspase-8 on NIK activation specifically, which may help elucidate the mechanism by which caspase-8 mediates IKK activation.

7.2.2 Caspase-8 regulates inflammatory gene expression through both its enzymatic and non-enzymatic activity.

In **Chapter 3** we demonstrated a role for caspase-8 enzymatic activity in the expression of pro-inflammatory cytokines in response to both TLR4 and TLR9 activation. These data provoke the hypothesis that caspase-8 regulates inflammatory gene expression through its cleavage activity. A candidate substrate for caspase-8 would need to meet two key requirements: (1) the substrate would need to be cytoplasmic, as caspase-8 has no NLS and is not known to localize to the nucleus; additionally, (2) the caspase-8 substrate is likely a negative regulator of IKK activation based on the finding that inhibition of caspase-8 enzymatic activity reduced IKK phosphorylation to the same magnitude observed in caspase-8-deficient cells. Earlier in this project we tested several potential caspase-8 targets, including HDAC7 and EHMT1, which have both cytoplasmic and nuclear localization as well as putative caspase-8-cleavage sites. However, these proteins are much more distal to TLR stimulation than IKK phosphorylation [216-218], and—perhaps not surprisingly—inhibition of HDAC7 or EHMT1 was not sufficient to restore inflammatory cytokine transcription in caspase-8-deficient cells (data not shown). Another logical candidate for caspase-8 cleavage is the linear deubiquitinase CYLD which cleaves K63 ubiquitin on RIPK1 [133]. Ubiquitination of RIPK1 is known to mediate expression of pro-survival genes during TNFR activation through the recruitment of NEMO, IKKα, and IKKβ [106, 107]. However, siRNA knock down of CYLD was not sufficient to restore cytokine secretion in caspase-8-deficient cells (data not shown).

Although these data are not conclusive, they suggest there is a cytoplasmic target of caspase-8 that has yet to be identified. Recently caspase-8 has been implicated in

maintenance of chromosome stability through the cleavage of Polo-like kinase 1 (PLK1) a mediator of centrosome assembly and spindle maturation during the M-phase of cell division [219]. Given our findings regarding the role of caspase-8 in cell cycle gene regulation (**Chapter 2**), it is tempting to speculate that PLK1 may play a previously uncharacterized role in TLR-induced inflammation in macrophages. We are interested in testing the impact of PLK1 inhibition during TLR stimulation in caspase-8-deficient macrophages. We hypothesize that if PLK1 is a target of caspase-8 in response to TLR stimulation then inhibition of PLK1 should be sufficient to restore inflammatory cytokine transcription in caspase-8-deficient cells. It is also possible that caspase-8 cleaves PLK1 in macrophages, but this cleavage does not mediate inflammatory gene expression. However, PLK1 cleavage may be the primary mechanism of caspase-8-mediated cell cycle gene regulation during TLR stimulation. Regardless of the outcome of these experiments we will gain further insight into the diverse array of caspase-8 cleavage targets during TLR stimulation.

Another set of experiments we are interested in performing are unbiased proteomics to identify novel caspase-8 cleavage targets. This approach would utilize a method known as TAILS (Terminal amine isotopic labeling of substrates) which identifies novel N-termini through TMT labeling [220]. We hypothesize that caspase-8-sufficent macrophages will have specific N-termini that are absent in caspase-8-deficient cells upon TLR stimulation. This approach would allow us to identify a variety of caspase-8 substrates, and combine this data with our knowledge regarding caspase-8 and IKK activation to identify potential candidates for further analysis.

7.2.3 Caspase-8 regulates cell cycle gene expression in response to multiple TLRs.

The most surprising result to emerge from these studies was the finding that caspase-8 deficiency leads to a defect in cell cycle gene expression during TLR stimulation (**Chapter 2**). Expression of cell cycle-related genes was impaired in caspase-8-deficient cells during both TLR4 and TLR9 stimulation (**Fig 2.2B** and **Fig 2.2D**). These data were particularly interesting in light of recent evidence that caspase-8 cleaves PLK1 a mediator of centrosome assembly and spindle maturation during the M-phase of cell division [219]. The study describing caspase-8-mediate cleavage of PLK1 was conducted in tumor-derived cell lines as well as mouse embryonic fibroblasts (MEFs); therefore, these data may not be generalizable to all cell types. However, there is evidence that c-Rel regulates cell cycle progression in B cells [221, 222], potentially implicating c-Rel, PLK1, and caspase-8 in cell cycle gene regulation. Collectively, these studies lead us to hypothesize that PLK1 may play a role in cell cycle gene expression in macrophages. To test this hypothesis we plan to inhibit and transiently ablate PLK1 in caspase-8-deficient macrophages. Our expectation is that loss of PLK1 function will be sufficient to restore cell cycle gene expression in caspase-8-deficient cells. We will further test the ability of caspase-8 to cleave PLK1 directly to determine if PLK1 is a substrate of caspase-8 during TLR activation.

Another potential area of investigation is the impact of caspase-8 on cell cycle progression myeloid in cell populations such as monocytes. We hypothesize that caspase-8 cleavage of PLK1 would promote differentiation of monocytes in response to TLR stimulation. TLR activation is known to induce monocyte differentiation into macrophages [223], and caspase-8 may be one mechanism that promotes this rapid differentiation. Our

future investigations will focus on elucidating the mechanism by which caspase-8 regulates cell cycle gene expression in a TLR-dependent manner.

7.2.4 Caspase-8-dependent apoptosis, and RIPK3-mediated programmed necrosis may regulate steady-state numbers of myeloid cells.

In an effort to elucidate the contribution of caspase-8-mediated cytokine production *in vivo,* we generated a mouse in which the apoptotic conformation of caspase-8 is rendered unstable while preserving its cytokine regulatory function (*Casp8*$^{DA/DA}$) [75]. Caspase-8 is also known to negatively regulate another cell death pathway known as RIPK3-mediated programed necrosis [104, 105]. Mice deficient in caspase-8 do not survive embryonic development because of the de-repression of programed necrosis. Dual ablation of caspase-8 and RIPK3 rescues mice from embryonic lethality. We further crossed *Casp8*$^{DA/DA}$ mice onto a RIPK3-null background to facilitate direct comparison between mice completely lacking caspase-8, and mice lacking caspase-8 apoptotic activity specifically. *Ripk3*$^{-/-}$*Casp8*$^{-/-}$ mice display a lymphoproliferative disease that is similar to that observed in mice lacking Fas or FasL, and this phenotype is attributed the inability of *Ripk3*$^{-/-}$*Casp8*$^{-/-}$ mice to undergo caspase-8-mediated apoptosis [104, 105]. Therefore, we hypothesized that mice expressing non-cleavable caspase-8 on a RIPK3-null background would also display a similar lymphoproliferative disease.

We were surprised to find that *Ripk3*$^{-/-}$*Casp8*$^{DA/DA}$ mice had a distinct phenotype from *Ripk3*$^{-/-}$*Casp8*$^{-/-}$ mice. *Ripk3*$^{-/-}$*Casp8*$^{DA/DA}$ mice had morphological defects in splenic architecture, and an accumulation of myeloid cells in secondary lymphoid organs (**Chapter 4**). At steady-state we could not observe an increase in total myeloid cell numbers in *Ripk3*$^{-/-}$*Casp8*$^{-/-}$ mice (**Chapter 6**), suggesting that the accumulation of myeloid cells is a unique feature of mice expressing non-cleavable caspase-8. Furthermore, we did not detect a statistical difference in myeloid populations in the mLNs of B6 and *Casp8*$^{DA/DA}$ mice.

(**Chapter 6**). We interpret these data to mean that the phenotype of *Ripk3*$^{-/-}$*Casp8*$^{DA/DA}$ mice is dependent on both the expression of non-cleavable caspase-8 and RIPK3-deficiency. These data implicate caspase-8 in another mechanism of immune cell homeostasis that is entirely dependent on its apoptotic activity. Further studies that identify the time of onset of myeloid accumulation in *Ripk3*$^{-/-}$*Casp8*$^{DA/DA}$ mice, as well as the origin of this myeloid cell population, will provide insight into the role caspase-8-mediated apoptosis plays in myeloid circulation at steady-state.

These data provoke the hypothesis that caspase-8-mediated apoptosis plays a cell-intrinsic role in turnover of myeloid cell populations in the periphery. An approach that utilizes reciprocal bone marrow chimeras in which we transfer *Ripk3*$^{-/-}$*Casp8*$^{DA/DA}$ hematopoietic cells into *Ripk3*$^{-/-}$*Casp8*$^{-/-}$ mice will help us determine if cell-intrinsic expression of non-cleavable caspase-8 in hematopoietic cells is sufficient to mediate this phenotype. Moreover, we should observe no accumulation of these cell populations in *Ripk3*$^{-/-}$*Casp8*$^{DA/DA}$ reconstituted with *Ripk3*$^{-/-}$*Casp8*$^{-/-}$ bone marrow as complete caspase-8 ablation appears sufficient to protect mice from the accumulation of myeloid cells. It is also possible the observed phenotype in *Ripk3*$^{-/-}$*Casp8*$^{DA/DA}$ mice is due to non-cleavable caspase-8-mediated expression of chemokines that promote myeloid cell egress from the bone marrow. We have shown a role for caspase-8 in the expression of *Cxcl2* in macrophages in response to TLR stimulation (**Chapter 2**). The chemokine CXCL2 mediates myeloid cell egress from the bone marrow via CCR2 [224]. Therefore, it is possible that caspase-8-dependent CXCL2 promotes myeloid cell egress, but there is no cell turnover in the periphery due to a defect in caspase-8-dependent apoptosis. To test the contribution of caspase-8-mediated CXCL2 secretion we would generate mixed bone

marrow chimeras in which *Ripk3*$^{-/-}$*Casp8*$^{DA/DA}$ mice are reconstituted with *Ccr2*$^{-/-}$ bone marrow, with the expectation that this will abrogate myeloid accumulation in the periphery. These proposed experiments will help to elucidate the mechanism of myeloid cell accumulation in *Ripk3*$^{-/-}$*Casp8*$^{DA/DA}$ mice at steady-state.

7.2.5. Caspase-8 mediates host survival during infection with *Toxoplasma gondii*.

Others have described a role for caspase-8-mediated cytokine production in response to fungal and bacterial pathogens *in vitro* as well bacterial pathogens *in vivo* [75, 77, 100, 110, 147]. To our knowledge, our studies are the first to implicate caspase-8 in host defense during infection with *Toxoplasma gondii* (**Chapter 5**). The mechanism of caspase-8-mediated resistance to *T. gondii* is likely through its cytokine regulatory function. Caspase-8-deficient DCs had impaired intracellular IL-12 production, and caspase-8-deficient animals had impaired recruitment of inflammatory monocytes into the site of infection. Moreover, caspase-8-deficient mice could be completely rescued through endogenous injection of IL-12. These data, while correlative, suggest a cell-intrinsic role for caspase-8-mediated cytokine production *in vivo* in response to *T. gondii*. To directly test the contribution of caspase-8-mediated IL-12 production in DCs we plan to generate mixed bone marrow chimeras with congenically labeled bone marrow from *Ripk3*$^{-/-}$*Casp8*$^{-/-}$ and Zbtb46-cre IRF8-floxed mice—in which conventional type 1 dendritic cells are selectively ablated [197]. Transferring this mixed bone barrow into a sublethally irradiated *Ripk3*$^{-/-}$*Casp8*$^{-/-}$ host will allow us to determine if intracellular production of IL-12 in *Ripk3*$^{-/-}$*Casp8*$^{-/-}$ DCs is rescued by caspase-8-sufficient bone marrow via bystander effects, or if caspase-8-deficient DCs still have impaired IL-12 production. The later result would suggest a cell-intrinsic defect in cytokine production.

Another area of investigation is the role of caspase-8 in host defense during infection with another Apicomplexan parasite: *Cryptosporidium. parvum*. Infection with *Cryptosporidium spp.* causes severe developmental delays in infected children with the highest prevalence rate in developing countries [225, 226]. It has only recently become

possible to passage these parasite in tissue culture to facilitate infection of different strains of immunocompromised mice [198]. Little is known about the mechanism of host defense against *C. parvum* or the mechanism of *C. parvum* antagonism of the immune system. Given the role of caspase-8 in protecting mice against the related pathogen *T. gondii* it is plausible that caspase-8 plays a similar role during *C. parvum* infection. Caspase-8 likely plays a much more extensive role in defense against bacterial, fungal, and protozoan pathogens through both its apoptotic and cytokine regulatory functions, and we hope the studies described in **Chapter 5** serve as a basis for further investigation into caspase-8-mediated host defense.

7.2.6 Caspase-8 may play a role in intestinal epithelial cell homeostasis at steady-state and during infection.

In **Chapter 6** we show that global ablation of caspase-8 and hematopoietic-specific ablation of caspase-8 have distinct impacts on the inflammatory response to the gram-negative bacterial pathogen *Yersinia pseudotuberculosis* (*Yp*). Hematopoietic-specific ablation of caspase-8 leads to acute host mortality, increased bacterial burdens, and impaired inflammatory response during oral infection with *Yp*. Global ablation of caspase-8 results in acute host mortality, and higher systemic bacterial burdens, but no impairment in inflammatory cytokine production. Moreover, caspase-8 apoptotic activity seems to be dispensable for *Yp*-protection in this context. Expression of non-cleavable caspase-8 was sufficient to reduce bacterial burdens and limit host mortality. These data suggest that caspase-8 may play a role in non-hematopoietic cells that is independent of both its cytokine regulatory function and apoptotic function. These results led us to hypothesize that caspase-8 plays a role in epithelial cell turnover in the small intestine.

The systemic dissemination we observed two days post infection in caspase-8-deficient animals may be mediated by a disruption in barrier integrity in the small intestine. Previous groups have shown that colonization of livers and spleens in *Yp*-infected animals is mediated by bacterial translocation directly from the small intestine. It is tempting to speculate that the role of caspase-8 in cell cycle gene expression may be a common function of caspase-8 in other cell types, including intestinal epithelial cells. Recent data has shown that mouse embryos lacking caspase-8 have defects in mitotic alignment in their colons, skin, and livers [219]. Immunohistochemical analysis of the small intestine of caspase-8-deficient and caspase-8-sufficient animals at steady-state, and

during *Yp* infection, will help us test the hypothesis that caspase-8 mediates barrier integrity. We would also like to perform live imaging of 3D organoid cultures derived from *Ripk3*$^{-/-}$, *Ripk3*$^{-/-}$*Casp8*$^{-/-}$, and *Ripk3*$^{-/-}$*Casp8*$^{DA/DA}$ mice to test the hypothesis that caspase-8 regulates cell division in this context [227]. Caspase-8 expression is dysregulated in tumorigenic tissue [182], and previous work has largely focused on the impact that this disruption has on apoptosis of tumorigenic cells [228, 229]. However, recent data that demonstrate a role for caspase-8 in cell cycle progression [219] suggest that caspase-8 has multiple roles in the prevention of tumor development, potentially expanding the viable caspase-8 targets during tumor therapy.

7.3 Concluding remarks

The mechanisms that govern the spectrum of immune activation have far reaching implications for human disease. Chronic inflammation leads to diseases that have become globally pervasive: inflammatory bowel disease, diabetes, and heart disease among others. And prolonged immune suppression leads to the outgrowth of tumorigenic cells and chronic infection. In these studies we have implicated caspase-8 as a protein that regulates the magnitude of immune activation during infection. We have shown that caspase-8 enzymatic activity contributes to both cell death and cell-intrinsic cytokine production. Moreover, it is likely that in a heterogenous environment *in vivo* caspase-8 promotes both cell death and cytokine secretion in distinct cells to ultimately facilitate pathogen clearance while dictating the appropriate level of immune activation. We propose that caspase-8 serves as a regulatory node to integrate both cell-death-inducing and pro-inflammatory stimuli, in turn mediating a rapid intracellular response that is dependent on the extracellular environment. In this way, a given cell is rapidly poised to undergo either cell death or secrete inflammatory mediators, but ultimately the *context* of the environment dictates the final outcome. It is clear from the studies described here as well as emerging literature that cell death and inflammation are intrinsically linked. We hope that the data described in this thesis begin the process of supplanting models in which inflammation and cell death are easily separable pathways with a new model in which there is an appreciation for the integration between these two essential biological processes.

CHAPTER 8: Materials and Methods

8.1 Experimental Model and Subject Details

8.1.1 Mice

C57BL/6 mice were obtained from Jackson Laboratories. The *Ripk3*$^{-/-}$*Casp8*$^{-/-}$ mice and *Mlkl*$^{-/-}$*Fadd*$^{-/-}$ mice used in these studies have been described previously [105, 127], and were provided by Doug Green (St. Jude Children's Research Hospital). *Ripk3*$^{-/-}$ mice were provided by Vishva Dixit (Genentech). *Il12b*$^{-/-}$ mice were previously described and provided by the Hunter lab [230]. *Rel*$^{-/-}$ mice were generated and provided by Hsiou-chi Liou [231]. *Casp8*$^{DA/DA}$ mice were previously described [75]. These mice were further crossed onto *Ripk3*$^{-/-}$ mice for 8 generations. For animal experiments, age- and sex-matched 8-12-week old mice were used.

All animal studies were performed in compliance with the federal regulations set forth in the Animal Welfare Act (AWA), the recommendations in the Guide for the Care and Use of Laboratory Animals of the National Institutes of Health, and the guidelines of the University of Pennsylvania Institutional Animal Use and Care Committee. All protocols used in this study were approved by the Institutional Animal Care and Use Committee at the University of Pennsylvania (Multiple Project Assurance # A3709-01, Protocol #804523, Protocol #805045).

8.1.2. *Toxoplasma gondii*

Transgenic Pru-tdTomato parasites were generated as previously described [232]. Parasites were maintained *in vitro* in a 37°C 5% CO2 humidified incubator by serial passage through human foreskin fibroblasts in DMEM supplemented with 20% M199, 10% fetal bovine serum, 1% pencillin-streptomycin, and 25 μg/ml gentamicin.

Tachyzoites were prepared for infection by serial needle passage and filtered through a 5-μm pore-size filter. Mice were infected i.p. with 10^4 live, invasion-competent parasites.

8.1.3. *Yersinia pseudotuberculosis*

Mice were fasted for 12–16 hours and infected orally with 2–4 x 10^8 *Yersinia* (32777) or ΔYopJ (32777) as indicated. Mice were monitored for survival or sacrificed and tissues were harvested 2 days post-infection, as indicated. Bacterial load was determined by plating dilutions of tissue homogenates on LB+irgasan plates, serum cytokines were measured using ELISA, and single-cell analysis was performed by flow cytometry.

8.2 Method Details

8.2.1 Bone marrow chimeras

6-week-old female B6.SJL mice were sublethally irradiated with 1100 rads. Mice were injected with 2-5x10^6 cells from bone marrow isolated from B6, *Il12b*$^{-/-}$, *Ripk3*$^{-/-}$, *Ripk3*$^{-/-}$*Casp8*$^{-/-}$ mice 6hrs post irradiation. Mice were given Sulfatrim in their water for 3 weeks. Infections were performed 10-12 weeks after irradiation and reconstitution.

8.2.2 BMDM electoporation and hc-Rel plasmid

Bone marrow derived macrophages (BMDMs) were grown as described in section 8.2.4. Cells were harvested from petri-dishes in 4°C PBS without calcium and magnesium. Cells were electroporated using the Amaxa's nucleofection procedure using 9 million BMDMs and 12ug of plasmid per condition. hc-Rel IRES-GFP containing plasmid and empty vector controls were made on a modified pBent2 plasmid. The plasmid cloning method has been previously described [50], and plasmids were purified prior to electroporation using the Qiagen Plasmid Maxi Kit.

8.2.3 Caspase-8 activity assay

BMDMs were pre-treated for 1hr with zVAD-fmk (100 μM SM Biochemicals) and stimulated with LPS (*E.coli* O55: B5 LPS Sigma, 100 ng/mL) or 1 μM CpG (IDT) for 30min or staurosporine (10 μM Sigma) for 3.5hrs. Caspase-8 activity was measured using the Caspase-8 fluorometric assay kit (Enzo, #ALX-850-222-K101). Fluorescence was read 30 minutes after substrate incubation per kit instructions.

8.2.4 Cell culture

BMDMs were grown as previously described [202] in a 37°C 5% CO_2 humidified incubator in DMEM supplemented with 10% FBS, HEPES, sodium pyruvate (complete-DMEM) and 30% L929 supernatant for 7–9 days. 16–20 hrs prior to treatment cells were re-plated into 96-, 48-, 24-, 12- or 6-well dishes in complete-DMEM containing 10% L929 supernatant. Cells were incubated at 37°C post-stimulation. zVAD-fmk (100 μM) or IETD-fmk (500 μM SM Biochemicals) was added 1 hr prior to treatment with LPS (100 ng/mL) or CpG (1μM). The generation of immortalized cells and retroviral transduction were previously described [114].

8.2.5 ChIP-qPCR

BMDMs were stimulated with LPS (100ng/mL) for indicated time points. Cells were cross linked with disuccinimidyl glutarate (Thermo Fisher) and formaldehyde (Sigma). Nuclear lysis was performed with the truChIP Chromatin Shearing Reagent KIT (Covaris) and nuclei were sonicated using the Covaris S220 sonicator. Chromatin was immunoprecipitated using anti-p65 antibody (sc-372X Santa Cruz) and anti-c-Rel antibody (sc-71X Santa Cruz) and protein G agarose beads (Millipore). All samples were column purified with the QIAquick PCR purification Kit (Qiagen). qPCR was performed using SYBER Green PCR Master Mix (Thermo Fisher) with 45 cycles of 95˚C(15s), 60˚C(30s) and 72˚C(30s). Primer pairs were designed to amplify 80-250 bp fragments of the promoter region of each gene and melt curve analysis was used to confirm the amplification of unique products. Primer sequences used are listed in the **Appendix**.

8.2.6 Confocal Microscopy

BMDMs were seeded on round, glass coverslips in 24-well plates and allowed to adhere overnight. BMDMs were pre-treated for 1hr zVAD-fmk (100 μM) where indicated and stimulated with LPS (100 ng/mL) or CpG 1 μM CpG for 2hrs. BMDMs were fixed with 4% PFA, permeabilized with 0.2% Triton, and blocked in 10% BSA. BMDMs were incubated with p65 (CST #8242, 1:200) and c-Rel(Santa Cruz #365720, clone G-7, 1:25) primary antibodies for 2 hours at 37°C, 5% CO_2 in 4% BSA. BMDMs were washed in PBS and incubated with Alexa Fluor rabbit 488 (Thermo Fisher, 1:5000) and Alexa Fluor mouse 488 (Thermo Fisher, 1:5000) at room temperature for 1 hour in 4% BSA. BMDMs were washed in PBS and stained with Hoechst (Fisher Scientific, 1:2500) and Alexa Fluor 647 Phalloidin (Thermo Fisher, 1:50) for 30 min in PBS at RT. Coverslips were washed, mounted on glass slides with Fluoromount-G (Thermo Fisher) and dried overnight at RT. Slides were imaged on a Leica SP5-II Confocal/FLIM Microscope at 63x. Three single image slices each containing 20-50 cells were taken for each genotype and condition. Cells imaged for display were imaged at an additional 2.5x. The brightness and contrast of display images were enhanced equally across genotypes using ImageJ, with each channel enhanced separately using secondary only, *Rel*$^{-/-}$ BMDMs, and unstained controls. Images used for quantification were not altered. Nuclear and cytoplasmic intensity of c-Rel and p65 was analyzed with the Multi Wavelength Cell Scoring application within MetaMorph version 7.8 (Molecular Devices Corporation, San Jose, CA). 60-150 cells were analyzed per genotype and condition.

8.2.7 Cytospins

150,000 peritoneal exudate cells were centrifuged at 1000 rpm onto glass microscope slides for 5 min. Slides were dried for 1hr in the dark. Slides were stained with Giemsa May-Grünwald reagents (Sigma). Slides were dried overnight and sealed. 500 cells were counted per slide.

8.2.8 ELISA (*in vitro*)

BMDMs were pre-treated for 1hr with IETD-fmk (500 μM) or zVAD-fmk (100 μM) where indicated and stimulated with 100 ng/mL *E. coli* LPS (Sigma) or 1 μM CpG (IDT) for 5 hours unless otherwise indicated. Release of proinflammatory cytokines was measured by enzyme-linked immunosorbent assay (ELISA) using capture and detection antibodies against IL-6 (BD), IL-12p40 (BD) or TNFα (BioLegend).

8.2.9 ELISA (*in vivo*)

Whole blood was isolated via cardiac puncture, incubated at 4C for 3hrs and spun at 15,000 g for 13 min at 4C. Serum was isolated and cytokines was measured by enzyme-linked immunosorbent assay (ELISA) using capture and detection antibodies against IL-12p40 (BD) or TNFα (BioLegend).

8.2.10 FasL stimulation of thymocytes and thymocyte characterization

$1.5x10^5$ thymocytes were plated in a 96-well flat bottom plate, and treated with cycloheximide (25μg/mL) and anti-CD95 (Jo2, BD) at the indicated concentrations for 24hrs. Cells were treated with staurosporine (10μM) where indicated for 8hrs. Cells were harvested and washed once in 4C sterile PBS. Cells were stained in Annexin V (Thermo

Fisher) for 15 min, washed with Annexin binding buffer. Cells were stained with 7AAD (Thermo Fisher), placed on ice and run immediately after staining.

Thymi were isolated from mice and processed into a single cell suspensions. $2x10^6$ thymocytes were plated in 96-well U-bottom plates in sterile PBS and stained for viability (Zombie Aqua, BioLegend) and then for CD4 (Bio Legend Clone-RM4-5), CD11b (BioLegend Clone-M1/70), CD11c (BioLegend Clone-3.9), CD19 (BioLegend Clone-1D3), CD49 (BioLegend Clone-9C10 (MFR4.B)), Gr-1 (BioLegend Clone-RB6-8C5), CD25 (BioLegend Clone-PC61), TCRβ (BioLegend Clone-H57-597), CD8 (BioLegend Clone-RPA-T8), CD44 (BioLegend Clone-BJ18), c-Kit (BioLegend Clone-2B8), CD5 (BioLegend Clone-53-7.3), and CD69 (BioLegend Clone-H1.2F3).

8.2.11 Flow cytometry (*in vitro*)

BMDMs were plated in 96 well-u-bottom plates and pre-treated with zVAD-fmk (100 μM) for 1 hr prior to PAMP stimulation, where indicated. BFA and monensin were added 1 hr later and samples were harvested for analysis 4–5 hrs later. Cells were washed with PBS, stained for viability (Zombie Yellow, BioLegend), Il-12p40 (BD Clone-C15.6) and pro-IL-1β(Thermo Fisher Clone NJTEN3). BMDMs were gated on live singlets. For hc- experiments involving hc-Rel transfection, BMDMs were plated in 6-well suspension dishes after electroporation. Electroporated BMDMs were stimulated with PAMPs 2 hrs after electroporation, and brefeldin A/monensin (Sigma, BD) were added 1hr after PAMP stimulation. Cells were harvested 3 hours later into PBS containing 2mM EDTA. Cells were washed with PBS, stained for viability (Zombie Yellow, BioLegend), Il-12p40 (BD Clone-C15.6), and pro-IL-1β(Thermo Fisher Clone NJTEN3).

8.2.12 Flow cytometry (*in vivo*)

mLNs and PECs were isolated in 4C sterile PBS. RBCs were lysed in 1x ACK buffer for 3min at room temperature. 1-2x10^6 PECs were plated in 96-well U-bottom T/C treated plates in cDMEM with β-mercaptoethanol, Pen-Strep, and brefeldin A/monensin (Sigma, BD) for 6hrs. 4-5x10^6 mLN cells were plated in 96-well U-bottom T/C treated plates in cDMEM with β-mercaptoethanol, Pen-Strep, and brefeldin A/monensin (Sigma, BD) for 6hrs. Cells were washed with PBS, stained for viability (Zombie Aqua or Zombie Yellow, BioLegend) and stained for CD45.1 (BioLegend Clone-A20), CD45.2 (BioLegend Clone-104), B220 (BioLegend Clone-RA3-6B2), CD3 (BioLegend Clone-17A2), CD19 (BioLegend Clone-1D3), NK1.1 (BioLegend Clone-PK136), MHCII (BioLegend Clone-M5), Ly6G (BioLegend Clone-1A8), Ly6C (BioLegend Clone-HK1.4), CD11b (BioLegend Clone-M1/70), CD11c (BioLegend Clone-3.9), CD64 (BioLegend Clone-10.1), Il-12p40 (BD Clone-C15.6). Cells were gated on live singlets.

8.2.13 RNA-seq

1x10^6 BMDMs per well were plated in 6-well T/C-treated dishes and placed in a 5% CO2 37°C incubator for 16 hours. BMDMs were stimulated with LPS (100 ng/mL) or CpG (1μM) for 0, 2, or 6 hrs. RNA was isolated using the RNeasy Mini Kit (Qiagen) and processed per the manufacturer's instructions. RNA-seq libraries were prepared using the TruSeq Stranded Total RNA LT Kit with Ribo-Zero Gold, according to the manufacturer's instructions. Samples were run on Illumina NextSeq 500 to generate 75-base pair, single-

end reads with a Q30 score of ~80%, resulting in 25–50 million fragments/sample. Bioinformatic analyses were carried out as previously described[233]. Briefly, data analyses were performed using the statistical computing environment R (v3.5.1), RStudio (v1.1.456), and the Bioconductor suite of packages for R (*http://www.bioconductor.org*) [234]. Fastq files were mapped to the mouse transcriptome (Ensembl, mouse cDNA GRCh38) using Kallisto [235]. Reads were annotated with EnsemblDB [236] and EnsDb.Mmusculus.v79 [237], and Tximport [238] was used to summarize transcripts to genes. Data were log2 transformed and scaled using weighted trimmed mean of M-values with (edgeR [239]). The prcomp function was used to perform principal component analyses (PCA) on normalized data. Unsupervised hierarchical clustering and PCA plots were visualized using ggplot2 [240]. For differential gene expression analysis, data were filtered to remove unexpressed and lowly expressed (>1 count per million (cpm) across 2 or more samples. Differentially expressed genes (false discovery rate < 0.05 and absolute log2 fold change >= 0.59), were identified using limma [241]. Heatmaps were created and visualized using gplots [242]. Gene Ontology (GO) was performed using the Database for Annotation, Visualization and Integration of Data (DAVID) [243]. HOMER transcription factor motif analysis [61]was performed on a set of genes that were identified to be caspase-8-dependent by the analysis described above. Raw data is available on the Gene Expression Omnibus (GEO) (accession number pending).

8.2.14 RT-qPCR

1x106 BMDMs/well were plated in 6-well T/C-treated dishes 16 hrs before the experiment. Cells were pre-treated with with IETD-fmk (500 μM) or zVAD-fmk (100 μM)

prior to LPS (100 ng/mL) or CpG(1 μM) stimulation. Cells were harvested 2 hours post stimulation and lysed in Trizol Reagent (Invitrogen/Thermo Fisher) and RNA was extracted using the phenol/chloroform extraction method. RNA was resuspended in RNAse-free water and cDNA synthesis was performed using High Capacity RNA to cDNA kit (Thermo Fisher) as per the manufacturer's instructions. qPCR was run using Power Sybr Green Master Mix (Thermo Fisher) on a QuantStudio Flex6000 (Thermo Fisher). Primer sequences used are listed in the Appendix.

8.2.15 Western Blots

BMDMs were seeded in TC-treated 48, 24 or 12 well plates. Where indicated IETD-fmk (500 μM) or zVAD-fmk (100 μM) was used to inhibit caspase-8 activity for 1 hr before LPS (100ng/mL) or CpG(1 μM) stimulation. Cells were lysed at the indicated times in lysis buffer (20 mM HEPES, 150 mM NaCl, 10% glycerol, 1% Triton X-100, 1mM EDTA, pH7.5) plus 1x complete protease inhibitor cocktail (Roche) and 1x sample buffer (25 mM Tris, 2% SDS, 10% glycerol, 0.012% bromophenol blue, 0.2% β-mercaptoethanol). Lysates were boiled at 110°C, spun at full speed for 5 minutes, run on 4-12% polyacrylamide gels (Invitrogen), and transferred to PVDF (Millipore). Membranes were immunoblotted using the following primary antibodies: β-Actin (Sigma #A228, 1:5000), cRel (Santa Cruz sc-71X, 1:100), p65 (CST #8242 1:1000), IκBα (CST #9242, 1:1000), IκBε (Novus Biologics #AF4637, 1ug/mL) IκBβ (Novus Biologics #AF5225, 1ug/mL), pIKKα/β (CST #2697, 1:1000), IKKβ (CST #8943, 1:1000), p-p38 (CST #9215,1:1000), p38 (CST #9212, 1:1000), GFP (Abcam ab6556, 1:1000), CYLD (Thermo #43-700, 1:100), CNBP (Santa Cruz sc-515387, 1:100), HDAC1 (CST #34589S, 1:1000),

Tubulin (Thermo #A11126, 1:5000), TAK1 (CST 1:1000), pTAK1 (Abcam pS439 1:1000), TBK1 (CST 1:000), pTBK1 (CST pS172 1:1000). Species specific HRP-conjugated secondary antibodies were used for each antibody (1:5000). Membranes were developed using Pierce ECL Plus and SuperSignal West Femto Maximum Sensitivity Substrate (Fisher Scientific) according to the manufacturer's instructions.

8.3 Quantification and statistical analysis

Statistical significance for experiments with two groups was calculated using Student's two-tailed unpaired t-test. In the case of paired replicate experiments statistical significance was calculated using Student's two-tailed paired t-test. Adjusted p-values were calculated using Prism 5.0 from GraphPad. n.s. denotes not significant; *, **, ***, and **** illustrate p-values of 0.05, 0.01, 0.001, and 0.0001 respectively. Error bars indicate ± SEM of at least three replicates. Investigators were not blinded to experimental groups.

8.4 Appendix

Table S1. Primer list for ChIP qPCR and cDNA amplification.

Gene Target	Type	Forward	Reverse
Csf2	cDNA	GGCCTTGGAAGCATGTAGAGG	GAGAACTCGTTAGAGACGACTT
Gapdh	cDNA	CTCCCACTCTTCCACCTTCG	CCACCACCCTGTTGCTGTAG
Il12b	cDNA	TTGAAAGGCTGGGTATCGGT	GAATTTCTGTGTGGCACTGG
Il1b	cDNA	CCTCTGATGGGCAACCACTT	TTCATCCCCCACACGTTGAC
Il1a	cDNA	CGAAGACTACAGTTCTGCCATT	GACGTTTCAGAGGTTCTCAGAG
Il4i1	cDNA	TCCAGCTTGAACCCTATTGAGA	GTCCTGCATCACTGAGCATCT
Il6	cDNA	TCACTGGAGCCTCGAATGTC	GTGAGGAAGGCTGTGCATTG
Tnfsf9	cDNA	CGGCGCTCCTCAGAGATAC	ATCCCGAACATTAACCGCAGG
Gapdh	ChIP	GGTCCAAAGAGAGGGAGGAG	GCCCTGCTTATCCAGTCCTA
Hbb-bs	ChIP	GCATGGAAGACAGGACAATC	GTGGGAGGAGTGTACAAGGA
Il12b	ChIP	GGGGAGGGAGGAACTTCTTA	CTTTCTGATGGAAACCCAAAG
Il1b	ChIP	CCCACCCTTCAGTTTTGTTG	CTTGTTTTCCCTCCCTTGTTT
Il6	ChIP	AATGTGGGATTTTCCCATGA	GCTCCAGAGCAGAATGAGCTA
Tnf	ChIP	GATTCCTTGATGCCTGGGTGTC	GAGCTTCTGCTGGCTGGCTGT

REFERENCES

1. Janeway, C.A., Jr., *Approaching the asymptote? Evolution and revolution in immunology.* Cold Spring Harb Symp Quant Biol, 1989. **54 Pt 1**: p. 1-13.
2. Hashimoto, C., K.L. Hudson, and K.V. Anderson, *The Toll gene of Drosophila, required for dorsal-ventral embryonic polarity, appears to encode a transmembrane protein.* Cell, 1988. **52**(2): p. 269-79.
3. Lemaitre, B., et al., *The dorsoventral regulatory gene cassette spatzle/Toll/cactus controls the potent antifungal response in Drosophila adults.* Cell, 1996. **86**(6): p. 973-83.
4. Medzhitov, R., P. Preston-Hurlburt, and C.A. Janeway, Jr., *A human homologue of the Drosophila Toll protein signals activation of adaptive immunity.* Nature, 1997. **388**(6640): p. 394-7.
5. Chaudhary, P.M., et al., *Cloning and characterization of two Toll/Interleukin-1 receptor-like genes TIL3 and TIL4: evidence for a multi-gene receptor family in humans.* Blood, 1998. **91**(11): p. 4020-7.
6. Rock, F.L., et al., *A family of human receptors structurally related to Drosophila Toll.* Proc Natl Acad Sci U S A, 1998. **95**(2): p. 588-93.
7. Takeda, K., T. Kaisho, and S. Akira, *Toll-like receptors.* Annu Rev Immunol, 2003. **21**: p. 335-76.
8. Inohara, et al., *NOD-LRR proteins: role in host-microbial interactions and inflammatory disease.* Annu Rev Biochem, 2005. **74**: p. 355-83.
9. Bourke, E., et al., *The toll-like receptor repertoire of human B lymphocytes: inducible and selective expression of TLR9 and TLR10 in normal and transformed cells.* Blood, 2003. **102**(3): p. 956-63.
10. Wang, J., et al., *Toll-like receptors expressed by dermal fibroblasts contribute to hypertrophic scarring.* J Cell Physiol, 2011. **226**(5): p. 1265-73.
11. Abreu, M.T., et al., *TLR signaling at the intestinal epithelial interface.* J Endotoxin Res, 2003. **9**(5): p. 322-30.
12. Melmed, G., et al., *Human intestinal epithelial cells are broadly unresponsive to Toll-like receptor 2-dependent bacterial ligands: implications for host-microbial interactions in the gut.* J Immunol, 2003. **170**(3): p. 1406-15.
13. Price, A.E., et al., *A Map of Toll-like Receptor Expression in the Intestinal Epithelium Reveals Distinct Spatial, Cell Type-Specific, and Temporal Patterns.* Immunity, 2018. **49**(3): p. 560-575 e6.
14. Hammond, T., et al., *Toll-like receptor (TLR) expression on CD4+ and CD8+ T-cells in patients chronically infected with hepatitis C virus.* Cell Immunol, 2010. **264**(2): p. 150-5.
15. Rakoff-Nahoum, S., et al., *Recognition of commensal microflora by toll-like receptors is required for intestinal homeostasis.* Cell, 2004. **118**(2): p. 229-41.
16. Uematsu, S., et al., *Detection of pathogenic intestinal bacteria by Toll-like receptor 5 on intestinal CD11c+ lamina propria cells.* Nat Immunol, 2006. **7**(8): p. 868-74.
17. Leser, T.D. and L. Molbak, *Better living through microbial action: the benefits of the mammalian gastrointestinal microbiota on the host.* Environ Microbiol, 2009. **11**(9): p. 2194-206.
18. McKernan, D.P., et al., *Altered peripheral toll-like receptor responses in the irritable bowel syndrome.* Aliment Pharmacol Ther, 2011. **33**(9): p. 1045-52.

19. Davenport, E.R., et al., *The human microbiome in evolution.* BMC Biol, 2017. **15**(1): p. 127.
20. Swain Ewald, H.A. and P.W. Ewald, *Natural Selection, The Microbiome, and Public Health.* Yale J Biol Med, 2018. **91**(4): p. 445-455.
21. Yamada, C., et al., *Molecular Insight into Evolution of Symbiosis between Breast-Fed Infants and a Member of the Human Gut Microbiome Bifidobacterium longum.* Cell Chem Biol, 2017. **24**(4): p. 515-524 e5.
22. Han, C., et al., *Integrin CD11b negatively regulates TLR-triggered inflammatory responses by activating Syk and promoting degradation of MyD88 and TRIF via Cbl-b.* Nat Immunol, 2010. **11**(8): p. 734-42.
23. Palsson-McDermott, E.M., et al., *TAG, a splice variant of the adaptor TRAM, negatively regulates the adaptor MyD88-independent TLR4 pathway.* Nat Immunol, 2009. **10**(6): p. 579-86.
24. Chen, Y., et al., *CNBP controls IL-12 gene transcription and Th1 immunity.* J Exp Med, 2018.
25. Luo, C. and L. Zheng, *Independent evolution of Toll and related genes in insects and mammals.* Immunogenetics, 2000. **51**(2): p. 92-8.
26. Xi, Z., J.L. Ramirez, and G. Dimopoulos, *The Aedes aegypti toll pathway controls dengue virus infection.* PLoS Pathog, 2008. **4**(7): p. e1000098.
27. Hayashi, F., et al., *The innate immune response to bacterial flagellin is mediated by Toll-like receptor 5.* Nature, 2001. **410**(6832): p. 1099-103.
28. Alexopoulou, L., et al., *Recognition of double-stranded RNA and activation of NF-kappaB by Toll-like receptor 3.* Nature, 2001. **413**(6857): p. 732-8.
29. Hemmi, H., et al., *Small anti-viral compounds activate immune cells via the TLR7 MyD88-dependent signaling pathway.* Nat Immunol, 2002. **3**(2): p. 196-200.
30. Hemmi, H., et al., *A Toll-like receptor recognizes bacterial DNA.* Nature, 2000. **408**(6813): p. 740-5.
31. Yarovinsky, F., et al., *TLR11 activation of dendritic cells by a protozoan profilin-like protein.* Science, 2005. **308**(5728): p. 1626-9.
32. Kawasaki, T. and T. Kawai, *Toll-like receptor signaling pathways.* Front Immunol, 2014. **5**: p. 461.
33. McGettrick, A.F. and L.A. O'Neill, *Localisation and trafficking of Toll-like receptors: an important mode of regulation.* Curr Opin Immunol, 2010. **22**(1): p. 20-7.
34. Lee, B.L. and G.M. Barton, *Trafficking of endosomal Toll-like receptors.* Trends Cell Biol, 2014. **24**(6): p. 360-9.
35. Hoebe, K., et al., *Identification of Lps2 as a key transducer of MyD88-independent TIR signalling.* Nature, 2003. **424**(6950): p. 743-8.
36. Hultmark, D., *Macrophage differentiation marker MyD88 is a member of the Toll/IL-1 receptor family.* Biochem Biophys Res Commun, 1994. **199**(1): p. 144-6.
37. Yamamoto, M., et al., *Role of adaptor TRIF in the MyD88-independent toll-like receptor signaling pathway.* Science, 2003. **301**(5633): p. 640-3.
38. Liu, S., et al., *Phosphorylation of innate immune adaptor proteins MAVS, STING, and TRIF induces IRF3 activation.* Science, 2015. **347**(6227): p. aaa2630.
39. Takeuchi, O., et al., *Cutting edge: preferentially the R-stereoisomer of the mycoplasmal lipopeptide macrophage-activating lipopeptide-2 activates immune*

cells through a toll-like receptor 2- and MyD88-dependent signaling pathway. J Immunol, 2000. **164**(2): p. 554-7.
40. Kawai, T., et al., *Lipopolysaccharide stimulates the MyD88-independent pathway and results in activation of IFN-regulatory factor 3 and the expression of a subset of lipopolysaccharide-inducible genes.* J Immunol, 2001. **167**(10): p. 5887-94.
41. Halonen, S.K. and L.M. Weiss, *Investigation into the mechanism of gamma interferon-mediated inhibition of Toxoplasma gondii in murine astrocytes.* Infect Immun, 2000. **68**(6): p. 3426-30.
42. Kyei, S.K., et al., *Mechanisms by Which Interleukin-12 Corrects Defective NK Cell Anticryptococcal Activity in HIV-Infected Patients.* MBio, 2016. **7**(4).
43. Staeheli, P., et al., *Influenza virus-susceptible mice carry Mx genes with a large deletion or a nonsense mutation.* Mol Cell Biol, 1988. **8**(10): p. 4518-23.
44. Fontana, M.F., et al., *Myeloid expression of the AP-1 transcription factor JUNB modulates outcomes of type 1 and type 2 parasitic infections.* Parasite Immunol, 2015. **37**(9): p. 470-8.
45. Laroux, F.S., et al., *Cutting edge: MyD88 controls phagocyte NADPH oxidase function and killing of gram-negative bacteria.* J Immunol, 2005. **175**(9): p. 5596-600.
46. Scanga, C.A., et al., *MyD88-deficient mice display a profound loss in resistance to Mycobacterium tuberculosis associated with partially impaired Th1 cytokine and nitric oxide synthase 2 expression.* Infect Immun, 2004. **72**(4): p. 2400-4.
47. Kagan, J.C., et al., *TRAM couples endocytosis of Toll-like receptor 4 to the induction of interferon-beta.* Nat Immunol, 2008. **9**(4): p. 361-8.
48. Rajaiah, R., et al., *CD14 dependence of TLR4 endocytosis and TRIF signaling displays ligand specificity and is dissociable in endotoxin tolerance.* Proc Natl Acad Sci U S A, 2015. **112**(27): p. 8391-6.
49. Xue, J., et al., *Transcriptome-based network analysis reveals a spectrum model of human macrophage activation.* Immunity, 2014. **40**(2): p. 274-88.
50. Siggers, T., et al., *Principles of dimer-specific gene regulation revealed by a comprehensive characterization of NF-kappaB family DNA binding.* Nat Immunol, 2011. **13**(1): p. 95-102.
51. Sakai, J., et al., *Lipopolysaccharide-induced NF-kappaB nuclear translocation is primarily dependent on MyD88, but TNFalpha expression requires TRIF and MyD88.* Sci Rep, 2017. **7**(1): p. 1428.
52. Lee, T.K., et al., *A noisy paracrine signal determines the cellular NF-kappaB response to lipopolysaccharide.* Sci Signal, 2009. **2**(93): p. ra65.
53. Raupach, B., et al., *Caspase-1-mediated activation of interleukin-1beta (IL-1beta) and IL-18 contributes to innate immune defenses against Salmonella enterica serovar Typhimurium infection.* Infect Immun, 2006. **74**(8): p. 4922-6.
54. Sun, K., et al., *Interleukin-12 promotes gamma interferon-dependent neutrophil recruitment in the lung and improves protection against respiratory Streptococcus pneumoniae infection.* Infect Immun, 2007. **75**(3): p. 1196-202.
55. Dann, S.M., et al., *IL-6-dependent mucosal protection prevents establishment of a microbial niche for attaching/effacing lesion-forming enteric bacterial pathogens.* J Immunol, 2008. **180**(10): p. 6816-26.

56. Hayden, M.S. and S. Ghosh, *NF-kappaB, the first quarter-century: remarkable progress and outstanding questions.* Genes Dev, 2012. **26**(3): p. 203-34.
57. Alkalay, I., et al., *Stimulation-dependent I kappa B alpha phosphorylation marks the NF-kappa B inhibitor for degradation via the ubiquitin-proteasome pathway.* Proc Natl Acad Sci U S A, 1995. **92**(23): p. 10599-603.
58. Alkalay, I., et al., *In vivo stimulation of I kappa B phosphorylation is not sufficient to activate NF-kappa B.* Mol Cell Biol, 1995. **15**(3): p. 1294-301.
59. Hoffmann, A., et al., *The IkappaB-NF-kappaB signaling module: temporal control and selective gene activation.* Science, 2002. **298**(5596): p. 1241-5.
60. Hargreaves, D.C., T. Horng, and R. Medzhitov, *Control of inducible gene expression by signal-dependent transcriptional elongation.* Cell, 2009. **138**(1): p. 129-45.
61. Heinz, S., et al., *Simple combinations of lineage-determining transcription factors prime cis-regulatory elements required for macrophage and B cell identities.* Mol Cell, 2010. **38**(4): p. 576-89.
62. Ghisletti, S., et al., *Identification and characterization of enhancers controlling the inflammatory gene expression program in macrophages.* Immunity, 2010. **32**(3): p. 317-28.
63. Foster, S.L., D.C. Hargreaves, and R. Medzhitov, *Gene-specific control of inflammation by TLR-induced chromatin modifications.* Nature, 2007. **447**(7147): p. 972-8.
64. Ramirez-Carrozzi, V.R., et al., *A unifying model for the selective regulation of inducible transcription by CpG islands and nucleosome remodeling.* Cell, 2009. **138**(1): p. 114-28.
65. Ramirez-Carrozzi, V.R., et al., *Selective and antagonistic functions of SWI/SNF and Mi-2beta nucleosome remodeling complexes during an inflammatory response.* Genes Dev, 2006. **20**(3): p. 282-96.
66. Weinmann, A.S., et al., *Nucleosome remodeling at the IL-12 p40 promoter is a TLR-dependent, Rel-independent event.* Nat Immunol, 2001. **2**(1): p. 51-7.
67. Huang, W., et al., *Transcriptional integration of TLR2 and TLR4 signaling at the NCoR derepression checkpoint.* Mol Cell, 2009. **35**(1): p. 48-57.
68. Goh, F.G., et al., *Beyond the enhanceosome: cluster of novel kappaB sites downstream of the human IFN-beta gene is essential for lipopolysaccharide-induced gene activation.* Blood, 2010. **116**(25): p. 5580-8.
69. Saccani, S., S. Pantano, and G. Natoli, *Modulation of NF-kappaB activity by exchange of dimers.* Mol Cell, 2003. **11**(6): p. 1563-74.
70. Saliba, D.G., et al., *IRF5:RelA interaction targets inflammatory genes in macrophages.* Cell Rep, 2014. **8**(5): p. 1308-17.
71. Sanjabi, S., et al., *Selective requirement for c-Rel during IL-12 P40 gene induction in macrophages.* Proc Natl Acad Sci U S A, 2000. **97**(23): p. 12705-10.
72. Zafra, G., et al., *Polymorphism in the 3' UTR of the IL12B gene is associated with Chagas' disease cardiomyopathy.* Microbes Infect, 2007. **9**(9): p. 1049-52.
73. Tso, H.W., et al., *Associations between IL12B polymorphisms and tuberculosis in the Hong Kong Chinese population.* J Infect Dis, 2004. **190**(5): p. 913-9.

74. Morahan, G., et al., *A promoter polymorphism in the gene encoding interleukin-12 p40 (IL12B) is associated with mortality from cerebral malaria and with reduced nitric oxide production.* Genes Immun, 2002. **3**(7): p. 414-8.
75. Philip, N.H., et al., *Activity of Uncleaved Caspase-8 Controls Anti-bacterial Immune Defense and TLR-Induced Cytokine Production Independent of Cell Death.* PLoS Pathog, 2016. **12**(10): p. e1005910.
76. Gurung, P. and T.D. Kanneganti, *Novel roles for caspase-8 in IL-1beta and inflammasome regulation.* Am J Pathol, 2015. **185**(1): p. 17-25.
77. Man, S.M., et al., *Salmonella infection induces recruitment of Caspase-8 to the inflammasome to modulate IL-1beta production.* J Immunol, 2013. **191**(10): p. 5239-46.
78. Shikama, Y., M. Yamada, and T. Miyashita, *Caspase-8 and caspase-10 activate NF-kappaB through RIP, NIK and IKKalpha kinases.* Eur J Immunol, 2003. **33**(7): p. 1998-2006.
79. Salvesen, G.S. and V.M. Dixit, *Caspase activation: the induced-proximity model.* Proc Natl Acad Sci U S A, 1999. **96**(20): p. 10964-7.
80. Oberst, A., et al., *Inducible dimerization and inducible cleavage reveal a requirement for both processes in caspase-8 activation.* J Biol Chem, 2010. **285**(22): p. 16632-42.
81. Boucher, D., et al., *Caspase-1 self-cleavage is an intrinsic mechanism to terminate inflammasome activity.* J Exp Med, 2018. **215**(3): p. 827-840.
82. Shen, C., et al., *Crystal structure of the death effector domains of caspase-8.* Biochem Biophys Res Commun, 2015. **463**(3): p. 297-302.
83. Tsao, D.H., et al., *Solution structure of N-TRADD and characterization of the interaction of N-TRADD and C-TRAF2, a key step in the TNFR1 signaling pathway.* Mol Cell, 2000. **5**(6): p. 1051-7.
84. Hsu, H., et al., *TRADD-TRAF2 and TRADD-FADD interactions define two distinct TNF receptor 1 signal transduction pathways.* Cell, 1996. **84**(2): p. 299-308.
85. Dickens, L.S., et al., *A death effector domain chain DISC model reveals a crucial role for caspase-8 chain assembly in mediating apoptotic cell death.* Mol Cell, 2012. **47**(2): p. 291-305.
86. Schleich, K., et al., *Stoichiometry of the CD95 death-inducing signaling complex: experimental and modeling evidence for a death effector domain chain model.* Mol Cell, 2012. **47**(2): p. 306-19.
87. Lavrik, I.N., et al., *CD95 stimulation results in the formation of a novel death effector domain protein-containing complex.* J Biol Chem, 2008. **283**(39): p. 26401-8.
88. Jang, T.H., et al., *Structural study of the RIPoptosome core reveals a helical assembly for kinase recruitment.* Biochemistry, 2014. **53**(33): p. 5424-31.
89. Grunert, M., et al., *The adaptor protein FADD and the initiator caspase-8 mediate activation of NF-kappaB by TRAIL.* Cell Death Dis, 2012. **3**: p. e414.
90. Bertrand, M.J., et al., *Cellular inhibitors of apoptosis cIAP1 and cIAP2 are required for innate immunity signaling by the pattern recognition receptors NOD1 and NOD2.* Immunity, 2009. **30**(6): p. 789-801.
91. Irmler, M., et al., *Inhibition of death receptor signals by cellular FLIP.* Nature, 1997. **388**(6638): p. 190-5.

92. Dillon, C.P., et al., *Survival function of the FADD-CASPASE-8-cFLIP(L) complex.* Cell Rep, 2012. **1**(5): p. 401-7.
93. Feoktistova, M., et al., *cIAPs block Ripoptosome formation, a RIP1/caspase-8 containing intracellular cell death complex differentially regulated by cFLIP isoforms.* Mol Cell, 2011. **43**(3): p. 449-63.
94. Geserick, P., et al., *Cellular IAPs inhibit a cryptic CD95-induced cell death by limiting RIP1 kinase recruitment.* J Cell Biol, 2009. **187**(7): p. 1037-54.
95. Majkut, J., et al., *Differential affinity of FLIP and procaspase 8 for FADD's DED binding surfaces regulates DISC assembly.* Nat Commun, 2014. **5**: p. 3350.
96. Yeh, W.C., et al., *Requirement for Casper (c-FLIP) in regulation of death receptor-induced apoptosis and embryonic development.* Immunity, 2000. **12**(6): p. 633-42.
97. Orning, P., et al., *Pathogen blockade of TAK1 triggers caspase-8-dependent cleavage of gasdermin D and cell death.* Science, 2018. **362**(6418): p. 1064-1069.
98. Peterson, L.W., et al., *Cell-Extrinsic TNF Collaborates with TRIF Signaling To Promote Yersinia-Induced Apoptosis.* J Immunol, 2016. **197**(10): p. 4110-4117.
99. Dondelinger, Y., et al., *NF-kappaB-Independent Role of IKKalpha/IKKbeta in Preventing RIPK1 Kinase-Dependent Apoptotic and Necroptotic Cell Death during TNF Signaling.* Mol Cell, 2015. **60**(1): p. 63-76.
100. Weng, D., et al., *Caspase-8 and RIP kinases regulate bacteria-induced innate immune responses and cell death.* Proc Natl Acad Sci U S A, 2014. **111**(20): p. 7391-6.
101. Kaiser, W.J. and M.K. Offermann, *Apoptosis induced by the toll-like receptor adaptor TRIF is dependent on its receptor interacting protein homotypic interaction motif.* J Immunol, 2005. **174**(8): p. 4942-52.
102. Li, H., et al., *Cleavage of BID by caspase 8 mediates the mitochondrial damage in the Fas pathway of apoptosis.* Cell, 1998. **94**(4): p. 491-501.
103. Tenev, T., et al., *The Ripoptosome, a signaling platform that assembles in response to genotoxic stress and loss of IAPs.* Mol Cell, 2011. **43**(3): p. 432-48.
104. Kaiser, W.J., et al., *RIP3 mediates the embryonic lethality of caspase-8-deficient mice.* Nature, 2011. **471**(7338): p. 368-72.
105. Oberst, A., et al., *Catalytic activity of the caspase-8-FLIP(L) complex inhibits RIPK3-dependent necrosis.* Nature, 2011. **471**(7338): p. 363-7.
106. Moquin, D.M., T. McQuade, and F.K. Chan, *CYLD deubiquitinates RIP1 in the TNFalpha-induced necrosome to facilitate kinase activation and programmed necrosis.* PLoS One, 2013. **8**(10): p. e76841.
107. Legarda, D., et al., *CYLD Proteolysis Protects Macrophages from TNF-Mediated Auto-necroptosis Induced by LPS and Licensed by Type I IFN.* Cell Rep, 2016. **15**(11): p. 2449-61.
108. Mompean, M., et al., *The Structure of the Necrosome RIPK1-RIPK3 Core, a Human Hetero-Amyloid Signaling Complex.* Cell, 2018. **173**(5): p. 1244-1253 e10.
109. Huang, D., et al., *The MLKL Channel in Necroptosis Is an Octamer Formed by Tetramers in a Dyadic Process.* Mol Cell Biol, 2017. **37**(5).
110. Gurung, P., et al., *FADD and caspase-8 mediate priming and activation of the canonical and noncanonical Nlrp3 inflammasomes.* J Immunol, 2014. **192**(4): p. 1835-46.

111. Kang, S., et al., *Caspase-8 scaffolding function and MLKL regulate NLRP3 inflammasome activation downstream of TLR3.* Nat Commun, 2015. **6**: p. 7515.
112. Henry, C.M. and S.J. Martin, *Caspase-8 Acts in a Non-enzymatic Role as a Scaffold for Assembly of a Pro-inflammatory "FADDosome" Complex upon TRAIL Stimulation.* Mol Cell, 2017. **65**(4): p. 715-729 e5.
113. Kang, T.B., et al., *Mutation of a self-processing site in caspase-8 compromises its apoptotic but not its nonapoptotic functions in bacterial artificial chromosome-transgenic mice.* J Immunol, 2008. **181**(4): p. 2522-32.
114. Philip, N.H., et al., *Caspase-8 mediates caspase-1 processing and innate immune defense in response to bacterial blockade of NF-kappaB and MAPK signaling.* Proc Natl Acad Sci U S A, 2014. **111**(20): p. 7385-90.
115. Medzhitov, R., *Inflammation 2010: new adventures of an old flame.* Cell, 2010. **140**(6): p. 771-6.
116. Carswell, E.A., et al., *An endotoxin-induced serum factor that causes necrosis of tumors.* Proc Natl Acad Sci U S A, 1975. **72**(9): p. 3666-70.
117. Rubinstein, M., et al., *Human leukocyte interferon purified to homogeneity.* Science, 1978. **202**(4374): p. 1289-90.
118. Levy, W.P., et al., *Amino acid sequence of a human leukocyte interferon.* Proc Natl Acad Sci U S A, 1981. **78**(10): p. 6186-90.
119. Dinarello, C.A., *Historical insights into cytokines.* Eur J Immunol, 2007. **37 Suppl 1**: p. S34-45.
120. Cantell, K., et al., *Production of interferon in human leukocytes from normal donors with the use of Sendai virus.* Methods Enzymol, 1981. **78**(Pt A): p. 29-38.
121. Brennan, F.M., et al., *Detection of interleukin 8 biological activity in synovial fluids from patients with rheumatoid arthritis and production of interleukin 8 mRNA by isolated synovial cells.* Eur J Immunol, 1990. **20**(9): p. 2141-4.
122. Reimund, J.M., et al., *Mucosal inflammatory cytokine production by intestinal biopsies in patients with ulcerative colitis and Crohn's disease.* J Clin Immunol, 1996. **16**(3): p. 144-50.
123. Su, D., et al., *FoxO1 links insulin resistance to proinflammatory cytokine IL-1beta production in macrophages.* Diabetes, 2009. **58**(11): p. 2624-33.
124. Bai, F., et al., *Serum levels of adipokines and cytokines in psoriasis patients: a systematic review and meta-analysis.* Oncotarget, 2018. **9**(1): p. 1266-1278.
125. Pierini, R., et al., *AIM2/ASC triggers caspase-8-dependent apoptosis in Francisella-infected caspase-1-deficient macrophages.* Cell Death Differ, 2012. **19**(10): p. 1709-21.
126. Kang, T.B., et al., *Caspase-8 blocks kinase RIPK3-mediated activation of the NLRP3 inflammasome.* Immunity, 2013. **38**(1): p. 27-40.
127. Nogusa, S., et al., *RIPK3 Activates Parallel Pathways of MLKL-Driven Necroptosis and FADD-Mediated Apoptosis to Protect against Influenza A Virus.* Cell Host Microbe, 2016. **20**(1): p. 13-24.
128. Bitzer, M., et al., *Sendai virus infection induces apoptosis through activation of caspase-8 (FLICE) and caspase-3 (CPP32).* J Virol, 1999. **73**(1): p. 702-8.
129. Green, D.R., et al., *Immunogenic and tolerogenic cell death.* Nat Rev Immunol, 2009. **9**(5): p. 353-63.

130. Faouzi, S., et al., *Anti-Fas induces hepatic chemokines and promotes inflammation by an NF-kappa B-independent, caspase-3-dependent pathway.* J Biol Chem, 2001. **276**(52): p. 49077-82.
131. Zhu, M., et al., *Mitochondria Released by Apoptotic Cell Death Initiate Innate Immune Responses.* Immunohorizons, 2018. **2**(11): p. 384-397.
132. Peterson, L.W., et al., *RIPK1-dependent apoptosis bypasses pathogen blockade of innate signaling to promote immune defense.* J Exp Med, 2017. **214**(11): p. 3171-3182.
133. O'Donnell, M.A., et al., *Caspase 8 inhibits programmed necrosis by processing CYLD.* Nat Cell Biol, 2011. **13**(12): p. 1437-42.
134. Ch'en, I.L., et al., *Mechanisms of necroptosis in T cells.* J Exp Med, 2011. **208**(4): p. 633-41.
135. Montoya, J.G. and O. Liesenfeld, *Toxoplasmosis.* Lancet, 2004. **363**(9425): p. 1965-76.
136. *Parasites Toxoplasmosis (Toxoplasma Infection)*. [Web] 2018 August 29 2019 [cited 2019 1/20/2019]; 1]. Available from: https://www.cdc.gov/parasites/toxoplasmosis/index.html.
137. Hunter, C.A., et al., *Studies on the role of interleukin-12 in acute murine toxoplasmosis.* Immunology, 1995. **84**(1): p. 16-20.
138. Yap, G., M. Pesin, and A. Sher, *Cutting edge: IL-12 is required for the maintenance of IFN-gamma production in T cells mediating chronic resistance to the intracellular pathogen, Toxoplasma gondii.* J Immunol, 2000. **165**(2): p. 628-31.
139. Christian, D.A., et al., *Use of transgenic parasites and host reporters to dissect events that promote interleukin-12 production during toxoplasmosis.* Infect Immun, 2014. **82**(10): p. 4056-67.
140. Hunter, C.A., et al., *Production of gamma interferon by natural killer cells from Toxoplasma gondii-infected SCID mice: regulation by interleukin-10, interleukin-12, and tumor necrosis factor alpha.* Infect Immun, 1994. **62**(7): p. 2818-24.
141. Khan, I.A., et al., *Immune CD8(+) T cells prevent reactivation of Toxoplasma gondii infection in the immunocompromised host.* Infect Immun, 1999. **67**(11): p. 5869-76.
142. Correa, G., et al., *Activation of the P2X(7) receptor triggers the elimination of Toxoplasma gondii tachyzoites from infected macrophages.* Microbes Infect, 2010. **12**(6): p. 497-504.
143. Grover, H.S., et al., *The Toxoplasma gondii peptide AS15 elicits CD4 T cells that can control parasite burden.* Infect Immun, 2012. **80**(9): p. 3279-88.
144. Goebel, S., U. Gross, and C.G. Luder, *Inhibition of host cell apoptosis by Toxoplasma gondii is accompanied by reduced activation of the caspase cascade and alterations of poly(ADP-ribose) polymerase expression.* J Cell Sci, 2001. **114**(Pt 19): p. 3495-505.
145. Nash, P.B., et al., *Toxoplasma gondii-infected cells are resistant to multiple inducers of apoptosis.* J Immunol, 1998. **160**(4): p. 1824-30.
146. Allam, R., et al., *Mitochondrial apoptosis is dispensable for NLRP3 inflammasome activation but non-apoptotic caspase-8 is required for inflammasome priming.* EMBO Rep, 2014. **15**(9): p. 982-90.

147. Ganesan, S., et al., *Caspase-8 modulates dectin-1 and complement receptor 3-driven IL-1beta production in response to beta-glucans and the fungal pathogen, Candida albicans.* J Immunol, 2014. **193**(5): p. 2519-2530.
148. Paff, J.R., D.A. Triplett, and T.N. Saari, *Clinical and laboratory aspects of Yersinia pseudotuberculosis infections, with a report of two cases.* Am J Clin Pathol, 1976. **66**(1): p. 101-10.
149. Galindo, C.L., et al., *Pathogenesis of Y. enterocolitica and Y. pseudotuberculosis in Human Yersiniosis.* J Pathog, 2011. **2011**: p. 182051.
150. Achtman, M., et al., *Yersinia pestis, the cause of plague, is a recently emerged clone of Yersinia pseudotuberculosis.* Proc Natl Acad Sci U S A, 1999. **96**(24): p. 14043-8.
151. Mecsas, J., I. Bilis, and S. Falkow, *Identification of attenuated Yersinia pseudotuberculosis strains and characterization of an orogastric infection in BALB/c mice on day 5 postinfection by signature-tagged mutagenesis.* Infect Immun, 2001. **69**(5): p. 2779-87.
152. Barnes, P.D., et al., *Yersinia pseudotuberculosis disseminates directly from a replicating bacterial pool in the intestine.* J Exp Med, 2006. **203**(6): p. 1591-601.
153. Kugeler, K.J., et al., *Epidemiology of human plague in the United States, 1900-2012.* Emerg Infect Dis, 2015. **21**(1): p. 16-22.
154. Monack, D.M., et al., *Yersinia signals macrophages to undergo apoptosis and YopJ is necessary for this cell death.* Proc Natl Acad Sci U S A, 1997. **94**(19): p. 10385-90.
155. Cornelis, G.R., *Molecular and cell biology aspects of plague.* Proc Natl Acad Sci U S A, 2000. **97**(16): p. 8778-83.
156. Denecker, G., et al., *Yersinia enterocolitica YopP-induced apoptosis of macrophages involves the apoptotic signaling cascade upstream of bid.* J Biol Chem, 2001. **276**(23): p. 19706-14.
157. Chun, H.J., et al., *Pleiotropic defects in lymphocyte activation caused by caspase-8 mutations lead to human immunodeficiency.* Nature, 2002. **419**(6905): p. 395-9.
158. Lemmers, B., et al., *Essential role for caspase-8 in Toll-like receptors and NFkappaB signaling.* J Biol Chem, 2007. **282**(10): p. 7416-23.
159. Su, H., et al., *Requirement for caspase-8 in NF-kappaB activation by antigen receptor.* Science, 2005. **307**(5714): p. 1465-8.
160. Lu, J.V., et al., *Complementary roles of Fas-associated death domain (FADD) and receptor interacting protein kinase-3 (RIPK3) in T-cell homeostasis and antiviral immunity.* Proc Natl Acad Sci U S A, 2011. **108**(37): p. 15312-7.
161. Eckhart, L., et al., *Identification of novel mammalian caspases reveals an important role of gene loss in shaping the human caspase repertoire.* Mol Biol Evol, 2008. **25**(5): p. 831-41.
162. Kawai, T. and S. Akira, *Signaling to NF-kappaB by Toll-like receptors.* Trends Mol Med, 2007. **13**(11): p. 460-9.
163. Kawai, T. and S. Akira, *TLR signaling.* Semin Immunol, 2007. **19**(1): p. 24-32.
164. Stranges, P.B., et al., *Elimination of antigen-presenting cells and autoreactive T cells by Fas contributes to prevention of autoimmunity.* Immunity, 2007. **26**(5): p. 629-41.

165. Drappa, J., et al., *Fas gene mutations in the Canale-Smith syndrome, an inherited lymphoproliferative disorder associated with autoimmunity.* N Engl J Med, 1996. **335**(22): p. 1643-9.
166. Shlomchik, M.J., et al., *The role of B cells in lpr/lpr-induced autoimmunity.* J Exp Med, 1994. **180**(4): p. 1295-306.
167. Straus, S.E., et al., *The development of lymphomas in families with autoimmune lymphoproliferative syndrome with germline Fas mutations and defective lymphocyte apoptosis.* Blood, 2001. **98**(1): p. 194-200.
168. Chinnaiyan, A.M., et al., *FADD, a novel death domain-containing protein, interacts with the death domain of Fas and initiates apoptosis.* Cell, 1995. **81**(4): p. 505-12.
169. Boldin, M.P., et al., *A novel protein that interacts with the death domain of Fas/APO1 contains a sequence motif related to the death domain.* J Biol Chem, 1995. **270**(14): p. 7795-8.
170. Hsu, H., J. Xiong, and D.V. Goeddel, *The TNF receptor 1-associated protein TRADD signals cell death and NF-kappa B activation.* Cell, 1995. **81**(4): p. 495-504.
171. Machida, K., et al., *Inhibition of cytochrome c release in Fas-mediated signaling pathway in transgenic mice induced to express hepatitis C viral proteins.* J Biol Chem, 2001. **276**(15): p. 12140-6.
172. Thome, M., et al., *Viral FLICE-inhibitory proteins (FLIPs) prevent apoptosis induced by death receptors.* Nature, 1997. **386**(6624): p. 517-21.
173. Paquette, N., et al., *Serine/threonine acetylation of TGFbeta-activated kinase (TAK1) by Yersinia pestis YopJ inhibits innate immune signaling.* Proc Natl Acad Sci U S A, 2012. **109**(31): p. 12710-5.
174. Brodsky, I.E. and R. Medzhitov, *Reduced secretion of YopJ by Yersinia limits in vivo cell death but enhances bacterial virulence.* PLoS Pathog, 2008. **4**(5): p. e1000067.
175. Traenckner, E.B., et al., *Phosphorylation of human I kappa B-alpha on serines 32 and 36 controls I kappa B-alpha proteolysis and NF-kappa B activation in response to diverse stimuli.* EMBO J, 1995. **14**(12): p. 2876-83.
176. Whiteside, S.T., et al., *I kappa B epsilon, a novel member of the I kappa B family, controls RelA and cRel NF-kappa B activity.* EMBO J, 1997. **16**(6): p. 1413-26.
177. Hughes, M.A., et al., *Co-operative and Hierarchical Binding of c-FLIP and Caspase-8: A Unified Model Defines How c-FLIP Isoforms Differentially Control Cell Fate.* Mol Cell, 2016. **61**(6): p. 834-49.
178. Mukherjee, S., et al., *Yersinia YopJ acetylates and inhibits kinase activation by blocking phosphorylation.* Science, 2006. **312**(5777): p. 1211-4.
179. Zhang, Y. and J.B. Bliska, *Role of Toll-like receptor signaling in the apoptotic response of macrophages to Yersinia infection.* Infect Immun, 2003. **71**(3): p. 1513-9.
180. Kreuz, S., et al., *NF-kappaB inducers upregulate cFLIP, a cycloheximide-sensitive inhibitor of death receptor signaling.* Mol Cell Biol, 2001. **21**(12): p. 3964-73.
181. Watanabe-Fukunaga, R., et al., *Lymphoproliferation disorder in mice explained by defects in Fas antigen that mediates apoptosis.* Nature, 1992. **356**(6367): p. 314-7.

182. Teitz, T., et al., *Caspase 8 is deleted or silenced preferentially in childhood neuroblastomas with amplification of MYCN.* Nat Med, 2000. **6**(5): p. 529-35.
183. Ishikawa, T., et al., *Protective role of Fas-FasL signaling in lethal infection with herpes simplex virus type 2 in mice.* J Virol, 2009. **83**(22): p. 11777-83.
184. Boldin, M.P., et al., *Involvement of MACH, a novel MORT1/FADD-interacting protease, in Fas/APO-1- and TNF receptor-induced cell death.* Cell, 1996. **85**(6): p. 803-15.
185. Del-Rey, M., et al., *A homozygous Fas ligand gene mutation in a patient causes a new type of autoimmune lymphoproliferative syndrome.* Blood, 2006. **108**(4): p. 1306-12.
186. Cohen, P.L. and R.A. Eisenberg, *Lpr and gld: single gene models of systemic autoimmunity and lymphoproliferative disease.* Annu Rev Immunol, 1991. **9**: p. 243-69.
187. Brunner, T., et al., *Cell-autonomous Fas (CD95)/Fas-ligand interaction mediates activation-induced apoptosis in T-cell hybridomas.* Nature, 1995. **373**(6513): p. 441-4.
188. Senju, S., et al., *Functional significance of the Fas molecule in naive lymphocytes.* Int Immunol, 1996. **8**(3): p. 423-31.
189. Summers, C., et al., *Neutrophil kinetics in health and disease.* Trends Immunol, 2010. **31**(8): p. 318-24.
190. Raetz, M., et al., *Cooperation of TLR12 and TLR11 in the IRF8-dependent IL-12 response to Toxoplasma gondii profilin.* J Immunol, 2013. **191**(9): p. 4818-27.
191. Wilson, D.C., S. Matthews, and G.S. Yap, *IL-12 signaling drives CD8+ T cell IFN-gamma production and differentiation of KLRG1+ effector subpopulations during Toxoplasma gondii Infection.* J Immunol, 2008. **180**(9): p. 5935-45.
192. Curiel, T.J., et al., *Cloned human CD4+ cytotoxic T lymphocytes specific for Toxoplasma gondii lyse tachyzoite-infected target cells.* J Immunol, 1993. **151**(4): p. 2024-31.
193. Hakim, F.T., et al., *CD8+ T cells from mice vaccinated against Toxoplasma gondii are cytotoxic for parasite-infected or antigen-pulsed host cells.* J Immunol, 1991. **147**(7): p. 2310-6.
194. Cabral, G.R.A., et al., *Inhibition of Nitric Oxide Production in Activated Macrophages Caused by Toxoplasma gondii Infection Occurs by Distinct Mechanisms in Different Mouse Macrophage Cell Lines.* Front Microbiol, 2018. **9**: p. 1936.
195. Robben, P.M., et al., *Recruitment of Gr-1+ monocytes is essential for control of acute toxoplasmosis.* J Exp Med, 2005. **201**(11): p. 1761-9.
196. Jordan, K.A., et al., *Role of the NF-kappaB transcription factor c-Rel in the generation of CD8+ T-cell responses to Toxoplasma gondii.* Int Immunol, 2010. **22**(11): p. 851-61.
197. Loschko, J., et al., *Inducible targeting of cDCs and their subsets in vivo.* J Immunol Methods, 2016. **434**: p. 32-8.
198. Vinayak, S., et al., *Genetic modification of the diarrhoeal pathogen Cryptosporidium parvum.* Nature, 2015. **523**(7561): p. 477-80.

199. Karray, S., et al., *Complete loss of Fas ligand gene causes massive lymphoproliferation and early death, indicating a residual activity of gld allele.* J Immunol, 2004. **172**(4): p. 2118-25.
200. Monack, D.M., et al., *Yersinia-induced apoptosis in vivo aids in the establishment of a systemic infection of mice.* J Exp Med, 1998. **188**(11): p. 2127-37.
201. Bohn, E. and I.B. Autenrieth, *IL-12 is essential for resistance against Yersinia enterocolitica by triggering IFN-gamma production in NK cells and CD4+ T cells.* J Immunol, 1996. **156**(4): p. 1458-68.
202. Brodsky, I.E., et al., *A Yersinia effector protein promotes virulence by preventing inflammasome recognition of the type III secretion system.* Cell Host Microbe, 2010. **7**(5): p. 376-87.
203. Marchiando, A.M., et al., *The epithelial barrier is maintained by in vivo tight junction expansion during pathologic intestinal epithelial shedding.* Gastroenterology, 2011. **140**(4): p. 1208-1218 e1-2.
204. Steinbrecher, K.A., et al., *Loss of epithelial RelA results in deregulated intestinal proliferative/apoptotic homeostasis and susceptibility to inflammation.* J Immunol, 2008. **180**(4): p. 2588-99.
205. Lorenz, V.N., M.P. Schon, and C.S. Seitz, *c-Rel in Epidermal Homeostasis: A Spotlight on c-Rel in Cell Cycle Regulation.* J Invest Dermatol, 2016. **136**(6): p. 1090-1096.
206. Sun, S.C., *Non-canonical NF-kappaB signaling pathway.* Cell Res, 2011. **21**(1): p. 71-85.
207. Derudder, E., et al., *RelB/p50 dimers are differentially regulated by tumor necrosis factor-alpha and lymphotoxin-beta receptor activation: critical roles for p100.* J Biol Chem, 2003. **278**(26): p. 23278-84.
208. Dejardin, E., et al., *The lymphotoxin-beta receptor induces different patterns of gene expression via two NF-kappaB pathways.* Immunity, 2002. **17**(4): p. 525-35.
209. Coope, H.J., et al., *CD40 regulates the processing of NF-kappaB2 p100 to p52.* EMBO J, 2002. **21**(20): p. 5375-85.
210. Solt, L.A., et al., *Interleukin-1-induced NF-kappaB activation is NEMO-dependent but does not require IKKbeta.* J Biol Chem, 2007. **282**(12): p. 8724-33.
211. Takaesu, G., et al., *TAK1 is critical for IkappaB kinase-mediated activation of the NF-kappaB pathway.* J Mol Biol, 2003. **326**(1): p. 105-15.
212. Clark, J.M., et al., *Inhibitor of kappa B epsilon (IkappaBepsilon) is a non-redundant regulator of c-Rel-dependent gene expression in murine T and B cells.* PLoS One, 2011. **6**(9): p. e24504.
213. Xu, J., et al., *The REGgamma-proteasome forms a regulatory circuit with IkappaBvarepsilon and NFkappaB in experimental colitis.* Nat Commun, 2016. **7**: p. 10761.
214. Wang, C., et al., *TAK1 is a ubiquitin-dependent kinase of MKK and IKK.* Nature, 2001. **412**(6844): p. 346-51.
215. Pomerantz, J.L. and D. Baltimore, *NF-kappaB activation by a signaling complex containing TRAF2, TANK and TBK1, a novel IKK-related kinase.* EMBO J, 1999. **18**(23): p. 6694-704.
216. Fang, T.C., et al., *Histone H3 lysine 9 di-methylation as an epigenetic signature of the interferon response.* J Exp Med, 2012. **209**(4): p. 661-9.

217. Ea, C.K., et al., *EHMT1 protein binds to nuclear factor-kappaB p50 and represses gene expression.* J Biol Chem, 2012. **287**(37): p. 31207-17.
218. Scott, F.L., et al., *Caspase-8 cleaves histone deacetylase 7 and abolishes its transcription repressor function.* J Biol Chem, 2008. **283**(28): p. 19499-510.
219. Liccardi, G., et al., *RIPK1 and Caspase-8 Ensure Chromosome Stability Independently of Their Role in Cell Death and Inflammation.* Mol Cell, 2019. **73**(3): p. 413-428 e7.
220. Rauniyar, N. and J.R. Yates, 3rd, *Isobaric labeling-based relative quantification in shotgun proteomics.* J Proteome Res, 2014. **13**(12): p. 5293-309.
221. Cheng, S., et al., *Cyclin E and Bcl-xL cooperatively induce cell cycle progression in c-Rel-/- B cells.* Oncogene, 2003. **22**(52): p. 8472-86.
222. Grumont, R.J., A. Strasser, and S. Gerondakis, *B cell growth is controlled by phosphatidylinosotol 3-kinase-dependent induction of Rel/NF-kappaB regulated c-myc transcription.* Mol Cell, 2002. **10**(6): p. 1283-94.
223. Krutzik, S.R., et al., *TLR activation triggers the rapid differentiation of monocytes into macrophages and dendritic cells.* Nat Med, 2005. **11**(6): p. 653-60.
224. Kurihara, T., et al., *Defects in macrophage recruitment and host defense in mice lacking the CCR2 chemokine receptor.* J Exp Med, 1997. **186**(10): p. 1757-62.
225. Putignani, L. and D. Menichella, *Global distribution, public health and clinical impact of the protozoan pathogen cryptosporidium.* Interdiscip Perspect Infect Dis, 2010. **2010**.
226. Mor, S.M. and S. Tzipori, *Cryptosporidiosis in children in Sub-Saharan Africa: a lingering challenge.* Clin Infect Dis, 2008. **47**(7): p. 915-21.
227. Bolhaqueiro, A.C.F., et al., *Live imaging of cell division in 3D stem-cell organoid cultures.* Methods Cell Biol, 2018. **145**: p. 91-106.
228. Schimmer, A.D., et al., *Small-molecule antagonists of apoptosis suppressor XIAP exhibit broad antitumor activity.* Cancer Cell, 2004. **5**(1): p. 25-35.
229. Arnt, C.R., et al., *Synthetic Smac/DIABLO peptides enhance the effects of chemotherapeutic agents by binding XIAP and cIAP1 in situ.* J Biol Chem, 2002. **277**(46): p. 44236-43.
230. Magram, J., et al., *IL-12-deficient mice are defective in IFN gamma production and type 1 cytokine responses.* Immunity, 1996. **4**(5): p. 471-81.
231. Liou, H.C., et al., *c-Rel is crucial for lymphocyte proliferation but dispensable for T cell effector function.* Int Immunol, 1999. **11**(3): p. 361-71.
232. John, B., et al., *Dynamic Imaging of CD8(+) T cells and dendritic cells during infection with Toxoplasma gondii.* PLoS Pathog, 2009. **5**(7): p. e1000505.
233. Beiting, D.P., et al., *Differential induction of TLR3-dependent innate immune signaling by closely related parasite species.* PLoS One, 2014. **9**(2): p. e88398.
234. Huber, W., et al., *Orchestrating high-throughput genomic analysis with Bioconductor.* Nat Methods, 2015. **12**(2): p. 115-21.
235. Bray, N.L., et al., *Near-optimal probabilistic RNA-seq quantification.* Nat Biotechnol, 2016. **34**(5): p. 525-7.
236. J, R., *ensembldb: Utilities to create and use Ensembl-based annotation databases. R package version 2.4.1,.* 2018.
237. J, R., *EnsDb.Mmusculus.v79: Ensembl based annotation package. R package version 2.99.0.* 2017.

238. Soneson, C., M.I. Love, and M.D. Robinson, *Differential analyses for RNA-seq: transcript-level estimates improve gene-level inferences.* F1000Res, 2015. **4**: p. 1521.
239. Robinson, M.D., D.J. McCarthy, and G.K. Smyth, *edgeR: a Bioconductor package for differential expression analysis of digital gene expression data.* Bioinformatics, 2010. **26**(1): p. 139-40.
240. H, W., *ggplot2: Elegant Graphics for Data Analysis. Springer-Verlag New York.* 2016.
241. Ritchie, M.E., et al., *limma powers differential expression analyses for RNA-sequencing and microarray studies.* Nucleic Acids Res, 2015. **43**(7): p. e47.
242. Gregory R, B.W., L Bonebakker, R Gentleman, TLW Huber, A Liaw, M Maechler, A Magnusson and M Steffen Moeller., *gplots: various R programming tools for plotting data. R package version 3.0.1.* 2016.
243. Huang da, W., B.T. Sherman, and R.A. Lempicki, *Systematic and integrative analysis of large gene lists using DAVID bioinformatics resources.* Nat Protoc, 2009. **4**(1): p. 44-57.